CHALMERS

Uncertainty in arch stability analysis

An investigation of uncertainties in arch stability analysis in hard rock conditions

Master of Science Thesis in the Master's Programme Geo and Water Engineering

ARON BODÉN

MASTER'S THESIS 2012:17

Uncertainty in arch stability analysis

An investigation of uncertainties in arch stability analysis in hard rock conditions

Master of Science Thesis in the Master's Programme Geo and Water Engineering

ARON BODÉN

Department of Civil and Environmental Engineering
Division of GeoEngineering
Engineering Geology
CHALMERS UNIVERSITY OF TECHNOLOGY
Göteborg, Sweden 2012

Uncertainty in arch stability analysis
An investigation of uncertainties in arch stability analysis in hard rock conditions
Master of Science Thesis in the Master's Programme Geo and Water Engineering
ARON BODÉN

Department of Civil and Environmental Engineering
Division of GeoEngineering
Engineering Geology
Chalmers University of Technology
SE-412 96 Göteborg
Sweden
Telephone: + 46 (0)31-772 1000

Cover:
Principles of load distribution in a pressured arch (modified from Eriksson, Nord & Stille 2005). The shape of the arch creates a structure which is moment neutral.

Uncertainty in arch stability analysis

An investigation of uncertainties in arch stability analysis in hard rock conditions

Master of Science Thesis in the Master's Programme Geo and Water Engineering
ARON BODÉN
Department of Civil and Environmental Engineering
Division of GeoEngineering
Engineering Geology
Chalmers University of Technology

ABSTRACT

Rock tunnel construction with low rock cover requires special attention. Prior to excavation there is a need to verify the stability of the tunnel roof. The analyses are made based on certain geological parameters, controlling the stability. These parameters are analysed and interpreted from the results of the geological investigation. Due to scale factors and property variations there is a risk that the construction is uncertain because of the large uncertainties from the preliminary investigation.

This study aims to see which of the parameters in the arch stability analysis that has the major impact on the overall uncertainty in the analysis. The report also gives advice about procedures that may be of interest to implement to reduce these uncertainties.

During the work with this project a great number of calculations have been made in Excel, with the add-on Crystal Ball to perform Monte-Carlo simulations. All of these calculations are based on the model for arch stability developed by Stille (1980). Sensitivity analysis is done by varying of input parameter in the calculations.

The survey was divided into three parts.

- Basic model
- Parameter study
- In-depth study of the uncertainties regarding the horizontal stress

The parameter study shows that horizontal stress is the parameter that has the greatest impact in terms of the overall uncertainty. However, for uncertainties in the safety factor against rotation, it turns out that the uncertainty in rock cover plays an even greater role than uncertainty in horizontal stress. When it comes to the uncertainties regarding the safety factor against sliding the fracture dip and angle of friction is crucial.

This study recommends studying and examining the horizontal stress condition, and to make an effort to determine the state of stress locally. It is also recommended to conduct studies to see what happens with the uncertainty for the factor of safety against rotation if the uncertainty in the decision of the rock surface is changed. At last it is of interest to further study the uncertainties surrounding the fracture dip and friction angle to further understand their effects on the uncertainty in safety factor against sliding. In general, sensitivity analysis should be performed, as shown by the result in this report.

Key words: Arch stability, Tunneling, Varberg tunnel, Horizontal stress

Osäkerheter i valvstabilitetsanalys

En undersökning av osäkerheter i valvstabilitetsanalys vid hårda bergförhållanden

Examensarbete inom Geo and Water Engineering

ARON BODÉN

Institutionen för bygg- och miljöteknik

Avdelningen för Geologi och Geoteknik

Teknisk Geologi

Chalmers tekniska högskola

SAMMANFATTNING

Bergtunnelbyggande med liten bergtäckning kräver särskild uppmärksamhet. Innan utgrävningen börjar är det viktigt att verifiera tunneltakets stabilitet. Analyserna är baserade på vissa geologiska parametrar, som styr stabiliteten. Dessa parametrar kommer från analysen och tolkningen av resultaten från den geologiska förundersökningen. På grund av skalfaktorer och variationer i egenskaperna finns en risk för att konstruktionen är osäker på grund av de stora osäkerheterna från förundersökningen.

Undersökningen syftar till att se vilken av parametrarna i valvstabilitetsanalysen som har störst inverkan på den övergripande osäkerheten i analysen. Rapporten ger även tips om förfaranden som kan vara av intresse att genomföra för att minska dessa osäkerheter.

Under arbetets gång har en stor mängd beräkningar gjorts i Excel, med tillägget Crystal Ball för att genomföra Monte-Carlo simuleringar. Alla beräkningar är baserade på den modell för valvstabilitet som Stille (1980) presenterat. Känslighetsanalysen har gjorts genom att variera ingångsparametrarna i beräkningarna.

Undersökningen delades in i tre olika delar.

- Grundmodell
- Parameterstudie
- Fördjupad studie av osäkerheterna avseende horisontalspänningen

Parameterstudien visar på att horisontalspänningen är den parameter som har störst inverkan när det gäller osäkerheterna kring pilhöjden. För osäkerheterna när det gäller säkerhetsfaktorn för rotation visar det sig att osäkerheten i bergtäckning spelar en än större roll än vad osäkerheten kring horisontalspänningen gör. När det kommer till osäkerheterna kring säkerhetsfaktorn för säkerhetsfaktorn mot glidning är sprickornas stupning och friktionsvinkel helt avgörande.

Denna studie rekommenderar att studera och undersöka den horisontella spänningens tillstånd samt att efter bästa förmåga bestämma spänningstillståndet lokalt. Det är också rekommenderat att genomföra fördjupade studier för att se vad som händer med osäkerheten kring säkerhetsfaktorn mot rotation om osäkerheten kring bestämningen av bergytans läge förändras. Slutligen är det intressant att vidare studera osäkerheterna kring stupningen och friktionsvinkeln hos sprickorna och hur de påverkar osäkerheterna i säkerhetsfaktorn mot glidning. Generellt så bör känslighetsanalys genomföras, vilket visas av resultaten i denna rapport.

Nyckelord: Valvstabilitet, Tunneldrivning, Varbergstunneln, Horisontalspänning

Contents

Preface

This study was carried out at the Division of GeoEngineering at the Chalmers University of Technology on the initiative of Ramböll.

I would like to express my gratitude to all of those who help me to complete this thesis. My father who has read this report more times than anyone else. Bengt Ludvig at Petro Team AB for helping me with the material from the mapping of the Varberg area. Håkan Stille at the Royal Institute of Technology, KTH, for helping me to understand the basic model. The employees at the department of Geo and Rock Engineering at Ramböll Göteborg who have help me with all possible problems that arose during the project. My reference group, consisting of Behnam Shariari and Malin Odenstedt-Lindhe from the Swedish Transport Administration, for giving valuable comments on my work.

Finally I wish to thank my supervisors, Magnus Eriksson from Ramböll and Lars-Olof Dahlström from Chalmers, for letting me do this master thesis project.

Göteborg February 2012

Aron Bodén

Notations

Roman upper case letters

B — Distance between bedding planes

D_{rock} — Rock cover

D_{soil} — Soil thickness

FS_{rot} — Factor of safety against rotation

FS_{slide} — Factor of safety against sliding

H_q — Horizontal force

L — Tunnel width

Roman lower case letters

f — Arch height

g — Gravitational acceleration

q — Vertical load

q_{ext} — External vertical load

Greek lower case letters

α — Angle of pressure line at support points

β — Angle between the pressure line and the vertical line

γ — Heaviness of soil

ρ — Density of rock

σ_H — Horizontal in-situ stress (Primary)

σ_h — Horizontal in-situ stress (Secondary)

σ_v — Vertical in-situ stress

σ_x — Horizontal in-situ stress perpendicular to tunnel

σ_θ — Tangential stress

ϕ — Friction angle

ϕ' — Equivalent friction angle

φ — Fracture dip

1 Introduction

Tunnel construction with low rock cover is getting more common, especially in larger cities where older underground constructions exist and the lack of space on the surface forces new infrastructure projects to be seated sub-surface. To find practical solutions for new underground constructions it is often relevant to put the new tunnels close to the surface or close to older tunnels, which results in tunnels with low rock cover. Prior to excavation there is a need to verify the stability of the tunnel roof to ensure the safety against collapse. The analyses are made based on certain parameters from the geologic investigation and the interpretation of those parameters. Thus, it means that the design may be unsafe due to large uncertainties from the pre-investigation.

1.1 Objectives

The purpose of this master thesis is to:

- identify uncertainties of geological parameter that have most impact on the arch stability for tunnels with low rock cover

and

- propose possible additional investigations that may be cost effective or reduce risk, to implement in such excavation conditions.

1.2 Method

A literature study is undertaken to give an introduction to tunnelling, the bedrock of Sweden, how information about the bedrock is gathered and processed and to identify which uncertainties, based on knowledge about the rock mass, that have an impact on the design. Calculations to solve the rock mechanics is done with an analytical method called pressured arch theory where the blocks in the rock mass is seen as a system that can transfer the loads around the opening. The parameter sensitivity study and its effect on the rock mechanic calculations is done with Monte-Carlo simulations and gives input to what parameters that should be observed, and particularly study during the investigation program.

1.3 Delimitations

The thesis is limited to:

- One type of failure criteria, arch stability in wide tunnels with low rock cover, wide tunnels refers to tunnels with greater width than height and low rock cover means that the rock cover is lower than the height of the tunnel

- Hard crystalline rock

- Design of reinforcement during construction

As a reference project the new train tunnel through Varberg will be used.

2 Literature study

The aim with this literature study is to give a general introduction to tunnel construction and to describe how information relevant for the construction of the tunnel is gathered and processed to make sure that the stability of the tunnel is sufficient.

2.1 Tunnelling

In the production cycle of a tunnel several steps are included. This chapter shortly describes the seven main components; grouting, drilling, charging, blasting, mucking, scaling and reinforcement, see Figure 2-1. All of these activities are included in each cycle except the grouting that only is done in some of the excavation cycles.
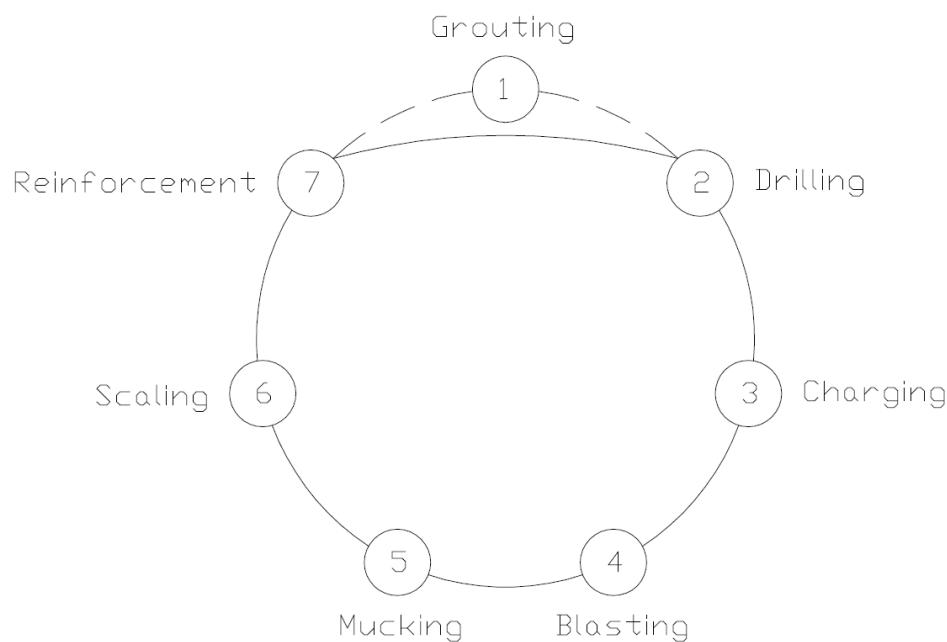
Figure 2-1 The main components in the tunnel production cycle

2.1.1 Grouting

Grouting is done to prevent water inflow from the surrounding rock mass to the tunnel. This is usually done using pre-grouting, meaning that the grouting is done ahead of the tunnel, see Figure 2-2. It can also be done as post-grouting, but this is much more difficult to reach a good result since there is no surface to press the grouting agent against and it can leak back into the tunnel. As a result post-grouting is therefore normally used if the pre-grouting has failed and water ingress to tunnel is in excess of requirements. The pre-grouting procedure starts with that a number of holes are drilled into which a grouting agent, normally cement, is injected under high pressure, this forces the cement to penetrate the fractures surrounding the tunnel. When the cement has hardened it creates a waterproof shield around the tunnel. Depending on how much water that can be allowed to leak into the tunnel different grouting classes decide how many boreholes are needed and how much grouting agent that should be used in each hole.
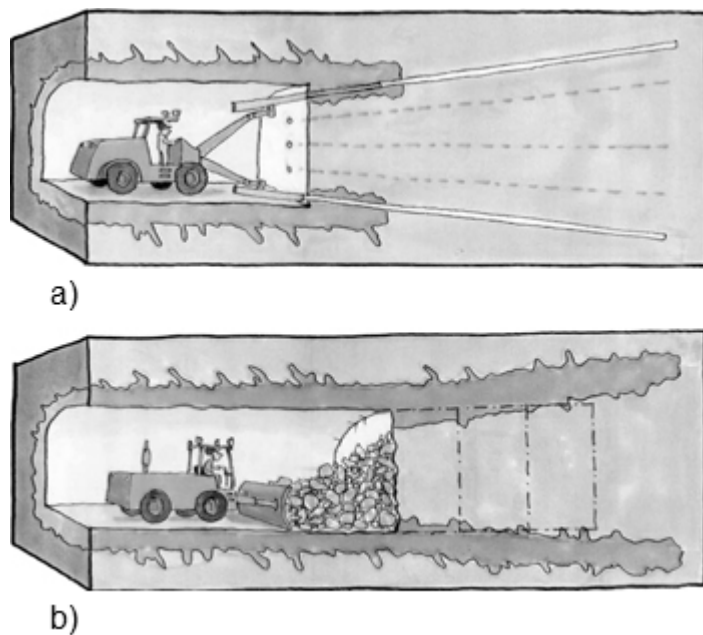
Figure 2-2 The priciple of pre-grouting a) the grouting is done ahead of excavation b) the rock is excavated in the grouted zone

Grouting is done according a predefined grouting plan in which the grouting classes are defined and which criteria that are used to decide when the grouting should be stopped. Examples of such criteria are lowest flow, maximum grouting used, lowest time grouted and maximum grouting time. During grouting the amount of grouting agent used is monitored as well as the pumping pressure. In the grouting plan it is defined at which amount of grouting agent or pumping pressure the grouting shall stop. The reason for not pumping with to high pressure is that it can damage the rock by opening up both existing and new fractures in the rock.

The most common grouting agent is cement based but it also exist different kinds of "chemical" based grouting agents that can be used. These agents are more expensive and some may have a much bigger impact on the environment and can in some cases even be harmful to humans and some agents shall therefore be avoided as much as possible, but under extra difficult circumstances it can better to use them.

When using cement based grout it is important that the cement is properly mixed to prevent forming of aggregates or lumps. Therefore a high speed mixer is normally used together with a stirrer and a pump. The most common high speed mixer used is Colloidal mixers in which the grout is rotating at high speed and mixed by shear force. The stirrer is used to prevent the cement to sediment after the mixing. The pump used is designed to work under very high pressure and are normally driven with air pressure or hydraulic. To be able to grout several holes at one time the pump can be fitted with several outlets or be in parallel with several pumps. However, normally today only one hole at the time per pump is accepted (Lindblom, Albertsson & Sjöholm 1999).

2.1.2 Drilling and charging

Drilling and charging is a critical phase in the excavation cycle, if the bore holes are drilled in wrong place, with high deviations or if they are charge with wrong amount

of explosives the tunnel contour will be different from the planned. This can lead to increased costs for unloading, reinforcement and that the tunnel face needs to be blasted again.

To be able to drill effectively it is important to have the right type of equipment for the type of drilling to be done. There are two main types of drills; air- and hydraulic powered. These exist in a variety of sizes, from handheld units to large drilling rigs. When using the drill and blast tunnelling method in hard rock, hydraulic rigs are used, serving one to four drilling machines, see Figure 2-3.
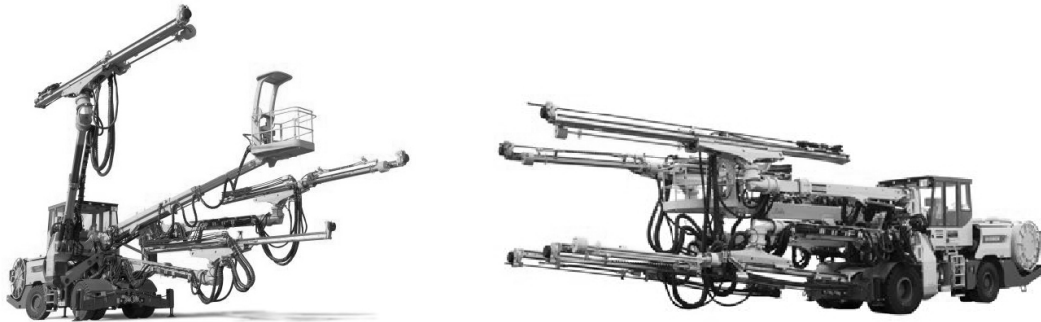
Figure 2-3 Two drill rigs from Atlas Copco (modified from Atlas Copco 2012)

Charging is when the explosive together with the detonator is placed in the boreholes. This can be done manually or with charging equipment. The charge is divided into three parts, bottom charge, column charge and stemming. It is important to measure the amount of explosives going into the hole so that the charge concentration is right, otherwise a risk for rock freeze may arise (Vägverket 1988).

2.1.3 Blasting

The most important thing to consider when blasting is the safety for people, nearby constructions and environment. It is important to notify property owners in due time before starting a project that involves blasting so it is possible to do an inspection of their property before that blasting starts.

When blasting, vibrations, air pressure waves and rock throw must be taken into consideration since they are the most common cause of damages to persons and property. For the blasting to be done in a safe way it is important to calculate and plan the blast and to make sure that the blasting follows the plan made (Vägverket 1988).

2.1.4 Mucking

Mucking is mainly done with wheel loaders and dumper trucks that transport the blasted rock to a rock heap where a rock crusher can crush the rock into smaller fragments if used in other constructions. Sometimes a conveyer belt is used to transport the rock out from the tunnel, either direct to the rock heap or to trucks that transport the rock to the heap (Vägverket 1988).

2.1.5 Scaling and reinforcement

The purpose of scaling is to ensure that no loose rock is left in the tunnel contour. Scaling is often divided into two steps. The first is mechanical scaling where a vehicle equipped with a mechanical hammer, hook or claw etc work the newly blasted surface so that loose blocks falls down. Step number two is manual scaling where a person with a scaling rod checks the tunnel contour to ensure that no loose rocks are left, if the person finds loose blocks they are removed, if large areas of loose rock are found the mechanical scaling is done once more (Vägverket 1988).

To guarantee a safe working place and to ensure that the tunnel will be standing until the final reinforcement is installed a temporary reinforcement is installed. The choice of temporary reinforcement is not just depending on the stability problem but also on the way of excavation. Stability in roof and walls is not always what sets the limit, a large uncovered face is also a stability risk. The reinforcement is used to help the rock to stabilize itself and to limit its movement towards the excavated cavity. In Scandinavia the most common way to reinforce the rock is to use rock bolts and shotcrete.

Bolting is often used as a temporary reinforcement to lock individual block close to the face. As the excavation progress the bolting is normally condensed and temporary bolts is cooperated into the permanent reinforcement system. The rock bolts increases the strength and stiffness and if the deformations in the rock does not stop after the bolts is installed the bolting pattern needs to be condensed. Two main types of different bolts exist, the pre-tensioned and the untensioned. A pre-tensioned bolt is tensioned to about half its maximum elastic deformation (Stille 1993). For an untensioned bolt the rock needs to deform the same amount for the bolt to get the same load.

Shotcrete is the most common way to reinforce rock, either alone or with rock bolts. In rock types with low adhesion problems can arise with shotcrete that becomes loose and falls down. This can be solved by installing rock bolts before applying the shotcrete. Another problem is when the deformations in the rock become too large so that the shotcrete gets fractured and loses its stiffness. This can be solved by leaving slits where no shotcrete is spray on the rock surface and letting the deformations in the rock abate before filling them.

One of the more uncommon ways to reinforce a tunnel in Sweden is to install steel arches, this due to that they are seen to be more time consuming and costly than using rock bolts and shotcrete, so that the shotcrete is anchored to the bolts. Steel arches are more commonly used in USA and parts of Europe, as well as in other parts of the world, where they are seen as a cheaper and faster to use type of reinforcement. There exists a number of different types of steel arches developed for different types of stability problems, see Figure 2-4 (Stille 1993).
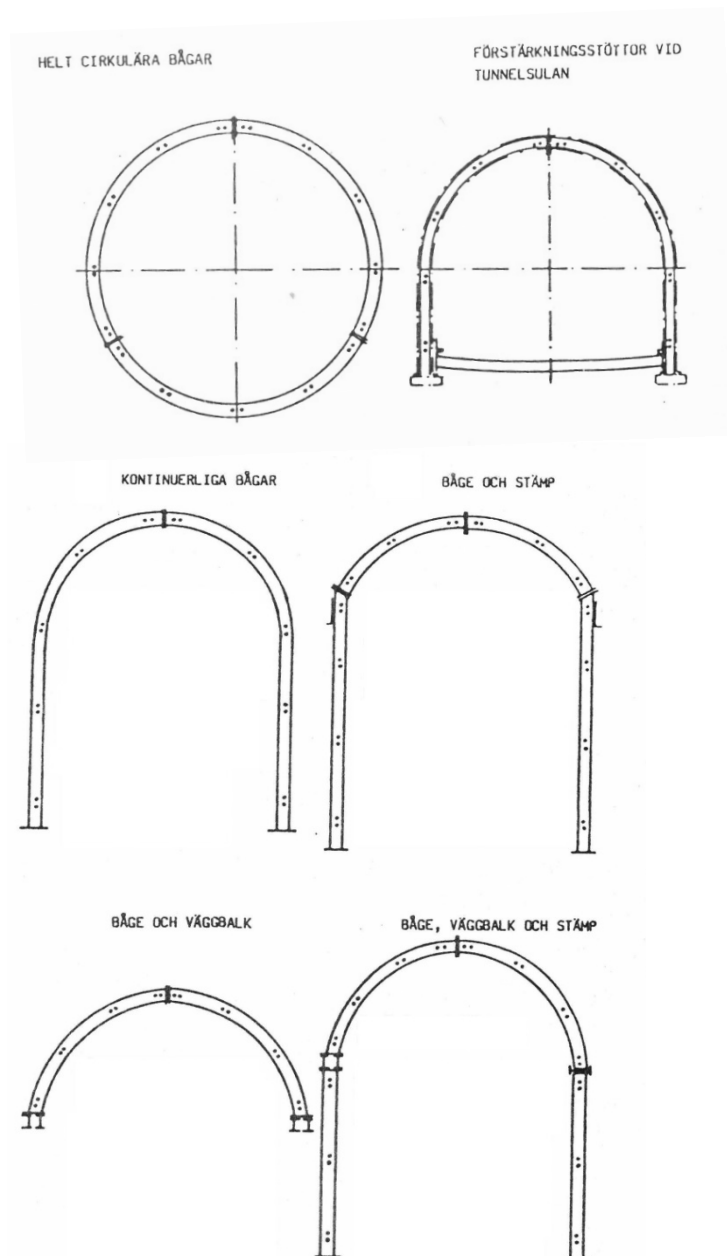
Figure 2-4 Different types of steel arches (Stille 1993)

In Scandinavia steel arches are used if it is not possible to stabilize the rock with bolt and/or shotcrete. This scenario can occur when the rock is too soft for rock bolts or if the shotcrete cannot have any adhesion to the rock surface. It can also be required to use steel arches if the rock requires instant support at the front (Stille 1993).

2.2 State of stress

In the undisturbed rock mass there exist virgin stresses, also known as in-situ stresses. These stresses consist of three main principal stresses. In a rock mass that is generally oriented one is vertical, σ_v, and two are horizontal, σ_H & σ_h, major and minor horizontal stress. The vertical stress is caused by the weight of the overlaying rock mass and can be assumed to follow a linear growth;

$$\sigma_v = \rho g z$$

Where;
$\rho =$ density of overlaying rock
$g =$ gravitational acceleration
$z =$ depth bellow surface

The horizontal stress can be derived from the burden of the overlaying rock mass, forces with tectonic origin and topographical stresses. If the rock mass is homogeneous, isotropic and linear elastic and there exist a state of one dimensional deformation, the horizontal stress that comes from the overlaying burden can be described with the theory of elasticity, see Equation 2:1. A common value for the Poisson's ratio is 0.25 this means that the horizontal stress caused by the burden of the overlaying rock mass is about one third of the vertical stress.

$$\overline{\sigma}_h = \frac{v}{1-v} \sigma_v \qquad \qquad \text{Equation 2:1}$$

Where;
$\overline{\sigma}_h =$ mean horizontal stress $(\sigma_H + \sigma_h)/2$
$v =$ Poisson's ratio

The horizontal stress derived from forces that have a tectonic origin, meaning that they originate from the movement of the tectonic plates, causes the horizontal stresses in most cases to be much higher than what they would be if they only depended on the gravitation (Nilsen & Palmström 2000).

The typical direction for the primary horizontal stress, σ_H, is northwest-southeast and is thought to be originate from the Mid-Atlantic ridge and from the collision between the African and the European plate. A normal way to describe the horizontal stress regime in Scandinavia is by using the equations formulated by Stephansson (1993), see Equation 2:2 to Equation 2:5, these equations are based on measurements with one method on a few places and should therefore only be seen as a first approximation. To understand the stress state locally it is important to do measurements locally (Nordlund, Rådberg & Sjöberg 1998).

Hydraulic fracturing

$$\sigma_H = 2.8 + 0.04 [MPa] \qquad \qquad \text{Equation 2:2}$$

$$\sigma_h = 2.2 + 0.024 [MPa] \qquad \qquad \text{Equation 2:3}$$

Over coring

$$\sigma_H = 6.7 + 0.044 [MPa] \qquad \qquad \text{Equation 2:4}$$

$$\sigma_h = 0.8 + 0.033 [MPa] \qquad \qquad \text{Equation 2:5}$$

If the topography is uneven the primary stresses will be changed from their vertical-horizontal orientation and instead they will follow a stress trajectory that

follow the topography close to the surface but as depth increases the trajectory smoothens out to become more and more horizontal. Discontinuities such as fractures and faults changes the stresses in the bedrock, if a fault exist it can be assumed that there have been a relief of stress.

During the geological history large beddings of sedimentary rock has covered today's ground surface and during the last ice age it was covered by a kilometre of ice. When the sedimentary rock was eroded away and the ice melted both vertical and horizontal stress was lowered. Even though this extra load disappeared a long time ago some of these stress still exists in the ground, the fact that most parts of Sweden still is rising from the ocean is a result of this.

In some parts of the ground the stresses are different than in the surrounding parts, even if the conditions in the ground suggest that there should be the same type of stresses. These differences in stress is called residual stress and caused by changes in the mineralogical compositions in the rock or uneven cooling of the rock when it was formed.

Horizontal stresses that are caused by the movements of the tectonic plates and the changes in topography as well as the residual stresses cannot be calculated, they have to be measured (Lindblom 2010). Some stress measurement methods are described in chapter 2.3.1.

When doing excavations stresses are introduce around the opening. These stresses are depending on the direction and the size of the virgin stresses as well as the geometry of the excavation. An easy way to calculate the tangential stress that is induced around the opening is to use Kirsch equations, see Equation 2:6 and Equation 2:7, that were develop by Gustav Kirsch in the end of the 19th century (Nilsen & Palmström 2000).

$$\sigma_\theta^{roof} = 3\sigma_x - \sigma_v \qquad \text{Equation 2:6}$$

$$\sigma_\theta^{wall} = 3\sigma_v - \sigma_x \qquad \text{Equation 2:7}$$

Where;

$\sigma_x =$ The horizontal stress acting perpendicular to the excavation

$\sigma_\theta^{roof} =$ The tangential stress in the roof

$\sigma_\theta^{wall} =$ The tangential stress in the wall

These equations are only valid for circular openings and in the middle of the roof and wall. For openings that are non-circular Hoek and Brown (1994) has modified Kirsch equations so they are valid for any shape of tunnel, see Equation 2:8 and Equation 2:9.

$$\sigma_\theta^{roof} = A\sigma_x - \sigma_v \qquad \text{Equation 2:8}$$

$$\sigma_\theta^{wall} = B\sigma_v - \sigma_x \qquad \text{Equation 2:9}$$

Where;

$A, B =$ Coefficients depending on the geometry of the opening

The coefficients A & B are decided by the shape of the opening, coefficients for some shapes are described in Figure 2-5. As can be seen the value for the coefficients are 3 when the shape is circular, which according to Kirsch equations is the case for circular openings.

	Tunnel shape								
A	5.0	4.0	3.9	3.2	3.1	3.0	2.0	1.9	1.8
B	2.0	1.5	1.8	2.3	2.7	3.0	5.0	1.9	3.9

Figure 2-5 Values for the coefficients A & B (from Nilsen & Palmström 2000)

During the use of excavated tunnel, shaft or cavern changes in air temperature or pressure induces tertiary stresses in the rock (Lindblom 2010).

2.3 Investigations

Rock investigations are made to answer the question about what the properties of the rock mass are. There are many types of investigation methods and many of them can answer the same questions, but some of them are better than others to answer specific questions (Lindblom 2010).

In Scandinavia the rock mass normally consists of intact rock, with high strength, that is divided by discontinuities, with much lower strength. This makes the strength of the entire rock mass more dependent on the strength of the discontinuities. Discontinuities are all the fields in the rock that have little or no tensile strength; this can be fractures, weak rock layers or faults (Johansson 2005).

Investigations can be divided into two categories; field- and laboratory investigations. Both of them can then be divided into subcategories.

2.3.1 Field investigations:

- *Pre investigations:* field reconnaissance and possible seismic surveys are put into this category
- *Detailed investigations:* Drilling and Coring are in this category
- *Rock stress investigations:* measurement of stress in the ground
- *Loading tests:* Large test to measure deformations in the rock mass

The pre investigations are often done in the early phase of a project and give information about the overall picture, i.e. environment conditions such as watercourse and vegetation, main fracture orientations, weakness planes etc. This information is then used to evaluate the possibility for tunnel construction, the main properties of the

rock mass, water conditions, fracture frequency and weakness zones in the rock. For more detailed studies in the field some sort of borehole is needed (Lindblom 2010).

Investigational drilling

It exist two types of drilling methods, core and percussion drilling. Core drilling is the most common type of investigational drilling, but it is expensive and as a result the number of holes drilled using this technique is limited in a project. Since the number of cores drilled is limited it is important to evaluate where to drill them, this is done based on the results from the pre investigations. From the drilled cores information about rock type, colour, weathering, orientation of irregularities, fracture geometry, fracture roughness and fracture coating can be found. The cores can also be used for mechanical testing of the rock.

A cheaper alternative to core drilling is percussion drilling. This method gives less information than core drilling but since it is cheaper more bore holes can be drilled at the same cost. The equipment used for percussion drilling is almost the same used for drilling for blasting, but instead of focusing on the shortest drilling time focus is on the information that can be gained. Parameters registered during drilling are; drill rate, pressure, torque, rpm, water pressure, water loss, drill bit wearing, drill cuttings etc. These parameters are then compared to parameters in rock with known strength that has been evaluated from core drillings. The most important parameter in percussion drilling is the drilling rate, this indicates where the different rock layers are, and where weakness zones are found. By compiling the results from the different boreholes a three dimensional model can be constructed where the different layers can be analysed.

In both core drilling and percussion drilling, two important stability parameters are lost, the width and filling of the fractures (Lindblom 2010). To get an estimation of these parameters it is possible to conduct water loss measurements and TV-inspections of the holes.

The water loss measurement gives information about the hydraulic conductivity of single fracture planes. Measuring the water pressure and the amount of water going in to the fracture it is possible to estimate the hydraulic conductivity by using Darcy's law.

TV-inspections are performed with a small camera that is lowered into the borehole and filming the inside. If the lighting is sufficient and the water is clear it is possible to evaluate rock types, fracture width and geometry, strike and dip and water movements (Lindblom 2010).

Rock stress

Several ways to measure the rock stresses exist. The most common is overcoring, hydraulic fracturing and flat-jack test. The method of overcoring is to first drill a hole down to the depth where the stress measurement shall be done (Figure 2-6a). This hole is about 76mm wide. In this hole, a smaller hole about 36mm wide is drilled. In this hole is deformation measurement equipment installed (Figure 2-6b). The rock around this core is cut off from the surrounding rock mass (Figure 2-6c), when the rock is relived from the surrounding stresses it deformes. Measuring the deformations

(Figure 2-6d) will give a value on how the state of stress has changed, from the in-situ case (with load) and the unloaded case. If this then is compared to the mechanical properties of the rock it is possible to calculate the absolute state of stress in this point.
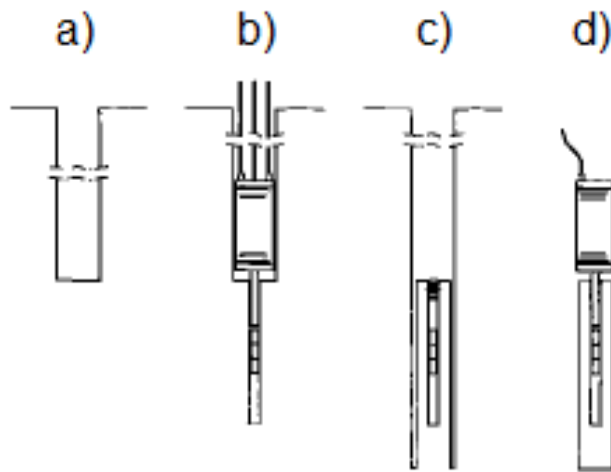
Figure 2-6 The overcoring method; a) a hole is drilled, b) a smaller hole is drilled within the first hole were measurment equipment is installed, c) the rock around the measurement equipment is cut of from the surrounding rock mass, d) the deformations in the stress relieved rock core is measured (modified from Lindblom 2010)

In the hydraulic fracturing an unfractured part of a vertical borehole sealed off. The sealed off zone is put under an increasing water pressure, see Figure 2-7a-b, that rises until a fracture is created, see Figure 2-7c-d, the pressure at this point is recorded and the water flow is stopped and the pressure is let to decrease to steady state and the fracture close completely, see Figure 2-7e. Then the pressure in the borehole is increased once again so that the fracture opens up once more at a certain water pressure, this pressure level is recorded and the difference between this pressure level and the pressure needed to create the fracture is equal to the tensile strength of the rock. By setting up an equation system the different stresses acting in this point can be calculated and by sending a video camera down or using imprint-packer, the direction of the different pressures can be determined.
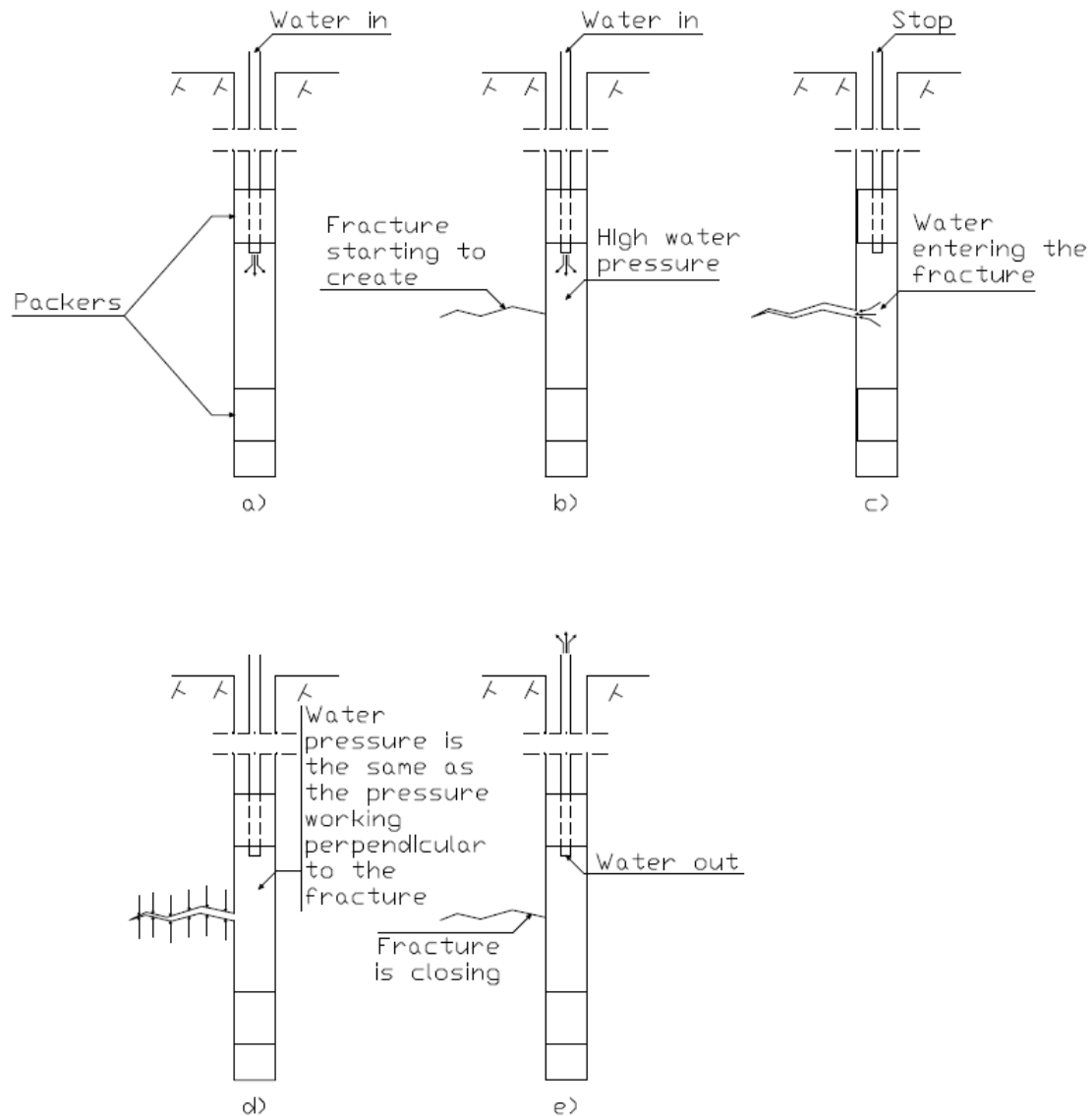
Figure 2-7 Hydraulic fracturing; a) water is pumped in, b) a fracture is starting to create, c) the fracture opens and water enters, d) the water pressure in the sealed of borehole is the same as the pressure working perpendicular to the fracture, e) water pressure is released and the fracture closes.

In the flat-jack method, two rock bolts are drilled into the rock wall of a tunnel, Figure 2-8a, with the distance y between them. A slit is made between the two rock bolts resulting in an excessive pressure in the rock walls of the slit, Figure 2-8b. The tangential stresses acting in the rock will make the slit shrink until the internal resistance against movement in the rock is the same as the tangential stress, Figure 2-8c. By inserting a flat-jack into the slit and applying an increasing pressure on the walls of the slit, Figure 2-8d, the distance between the rock bolts increase. The pressure needed to open up the slit so much so that the distance between the bolts is back to the original distance, Figure 2-8e, is the same as the tangential stress around the tunnel (Lindblom 2010).
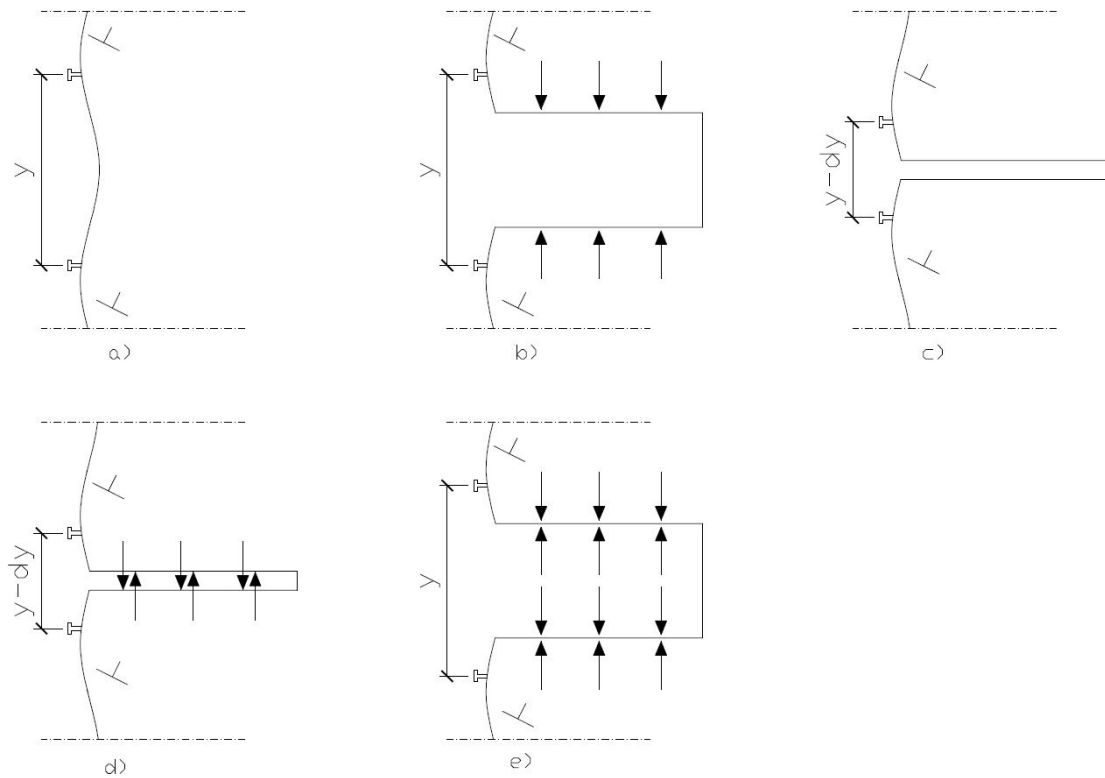
Figure 2-8 Flat-jack method; a) rock bolts drilled into the rock wall, b) a slit is made between the bolts, c) the distance between the bolts shrinks with the distance dy, d) a flat-jack is inserted in the slit and aplying an increasing pressure on the inside of the slit, e) the bolts are back at their starting position

For measurements of the rock stress close to the surface, block tests or slotting is preferred since they are considered to be easy to carry out. Both of them are carried out by installing strain gauges on a fracture free part of rock. This part of the rock is then separated from the rest of the rock and the deformations recorded by the strain gauges can then be transformed into the lost rock stress (Berg 2005).

2.3.2 Laboratory tests:

- *Physical material properties:* density, porosity, conductivity and volume changes due to moisture and temperature
- *Direct uniaxial tests:* compressive and tensile strength
- *Indirect uniaxial tests:* Brazilian test, point load test
- *Triaxial tests:* strength parameters in an 3D-environment
- *Shear tests on fractures:* direct shear test, triaxial pressure test and tilting test
- *Other tests:* specific test for special demands.

To measure the mechanical properties of the rock direct or indirect uniaxial tests as well as triaxial tests can be done. Both the direct and indirect tests measure the compressive and tensile strength of intact rock. All of these tests are made on small core samples that have been drilled from the ground using core drilling. When performing the compressive test the test specimen is put under an axial load that increases. When the load increases the length of the sample is reduced and the width is increased. Since the rock mass contains fractures, and therefore does not have any tensile strength, the tensile strength for the intact rock is rarely tested. In the triaxial test different samples of the same rock are put under different horizontal loads and

then a vertical load is slowly increased so that the samples break, but since they have different horizontal loads they will break at different vertical loads and therefore it is possible to analyse the internal friction angle and cohesion.

In the laboratory it is also possible to measure the shear strength of fractures in the rock. By isolating a fracture in a rock sample and cutting the edges of the rock so that they are perpendicular to the fracture it is possible to evaluate the shear strength of the fracture. This is possible since the shear strength of the rock is much higher than for the material in the fracture. The test method is to put a normal force on to the test sample and then increasing the shear force until the sides of the fracture slide. If multiple tests are done for the same fracture at different normal tension makes it possible to evaluate the friction angle and cohesion of the fracture. It is also possible to use triaxial testing to evaluate the friction angle and cohesion of the fracture.

If the shear strength of the fracture only depends on the friction between the sides of the fracture it is possible to use a tilt-test to evaluate the friction angle. By tilting the rock sample with a fracture that goes through the whole sample and record at which angle the top slips of gives to friction angle, however it is important not to tilt it so much that the top half of the sample starts to rotate, since this gives a tilt angle that does not represent the friction angle.

If there are special factors that are of interest for the specific construction there are many more types of tests that can be done. An example of a test can be to measure the thermal properties of the rock. These tests are usually done in the same way as other construction materials are tested (Lindblom 2010).

2.4 Models

There exist several types of analytical models that handle arch stability of tunnel roofs. Two of them are pressured arch theory and Voussoir beam theory.

2.4.1 Pressured arch theory

The main concept for the compressed arch is that the vertical loads over an opening are transferred around the roof to the side of the excavation by a system of pressured arches in the rock, see Figure 2-9. If the arch around the opening is strong enough and can distribute loads, the opening is stable. (Eriksson, Nord & Stille 2005)
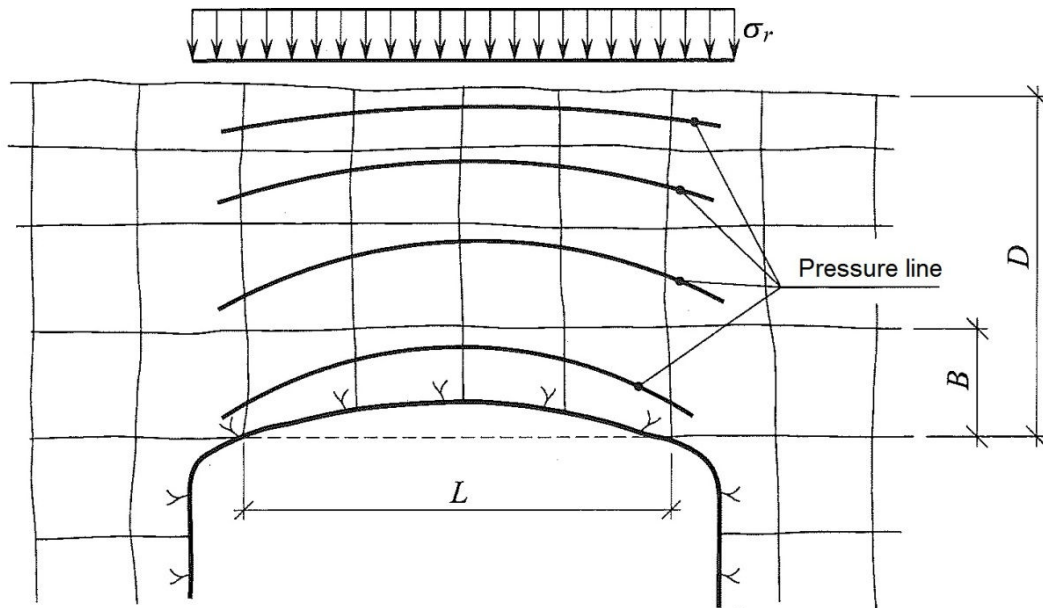
Figure 2-9 Principle of load transfer in a pressured arch (modified from Eriksson, Nord & Stille 2005)

In fractured hard rock, stability problems can arise due to the fact that a strong enough arch cannot be formed around the excavation opening. This can possibly endanger the entire stability of the tunnel. Therefore, it is important to analyse the arch stability (Eriksson, Nord & Stille 2005).

A rock mass possibility to deal with tensile forces is usually insignificant and therefore loads are transferred by the creation of a pressured arch above the excavation (Eriksson, Nord & Stille 2005). The main principle is that loads are carried by the arch and transferred as reaction forces, see Figure 2-10. The moment created by the reaction forces counteract the moment created by the load (Nelson 1998).
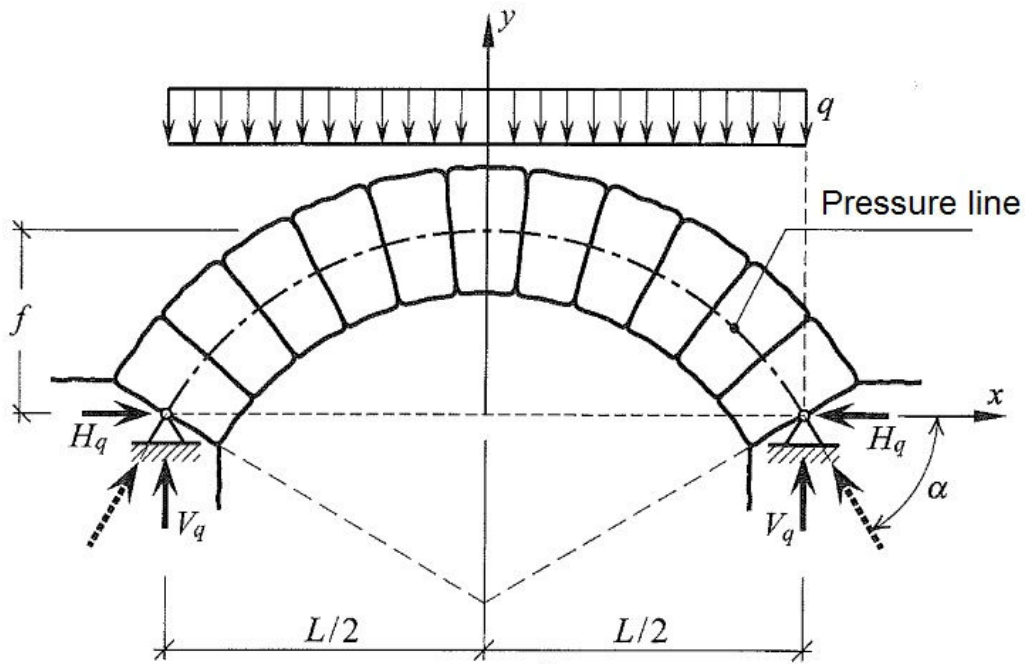
Figure 2-10 Principles of load distribution in an arch (modified from Eriksson, Nord & Stille 2005)

The easiest way to understand the stability of an arch is to compare it to a free supported beam with an evenly distributed load, see Figure 2-11. By setting up force equilibrium the forces acting on the beam can be identified. For the straight beam the vertical forces are creating a moment that is bending the beam but for the arch with its bent shape and an arch height, f, a counteracting moment is created so that the overall moment is neutralised (Nelson 1998).
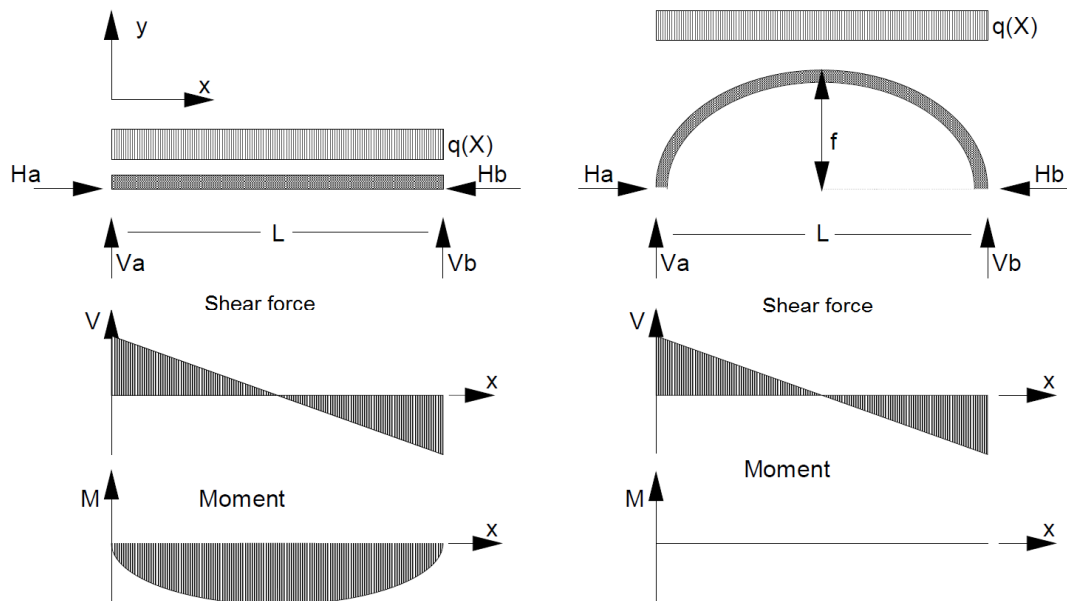
Figure 2-11 Comparison between a straight beam and an arch (modified from Nelson 1998)

There are three ways in which an arch can collapse;

- Slip in a joint
- Crushing of joint or block
- Rotation of block

The most common failure in a fractured rock mass is due to slip in joints and this therefore usually determines the bearing capacity of a pressured arch. If slip occurs, the shear force of the joint has been exceeded. If the height of the pressure line created is higher than the distance between bedding planes there exist a risk of rotating blocks (Eriksson, Nord & Stille 2005). Crushing of a joint or block occurs when the compressive strength of the rock is exceeded. This can either be caused by small contact surfaces between blocks or a weakness zone in the rock mass (Nelson 1998).
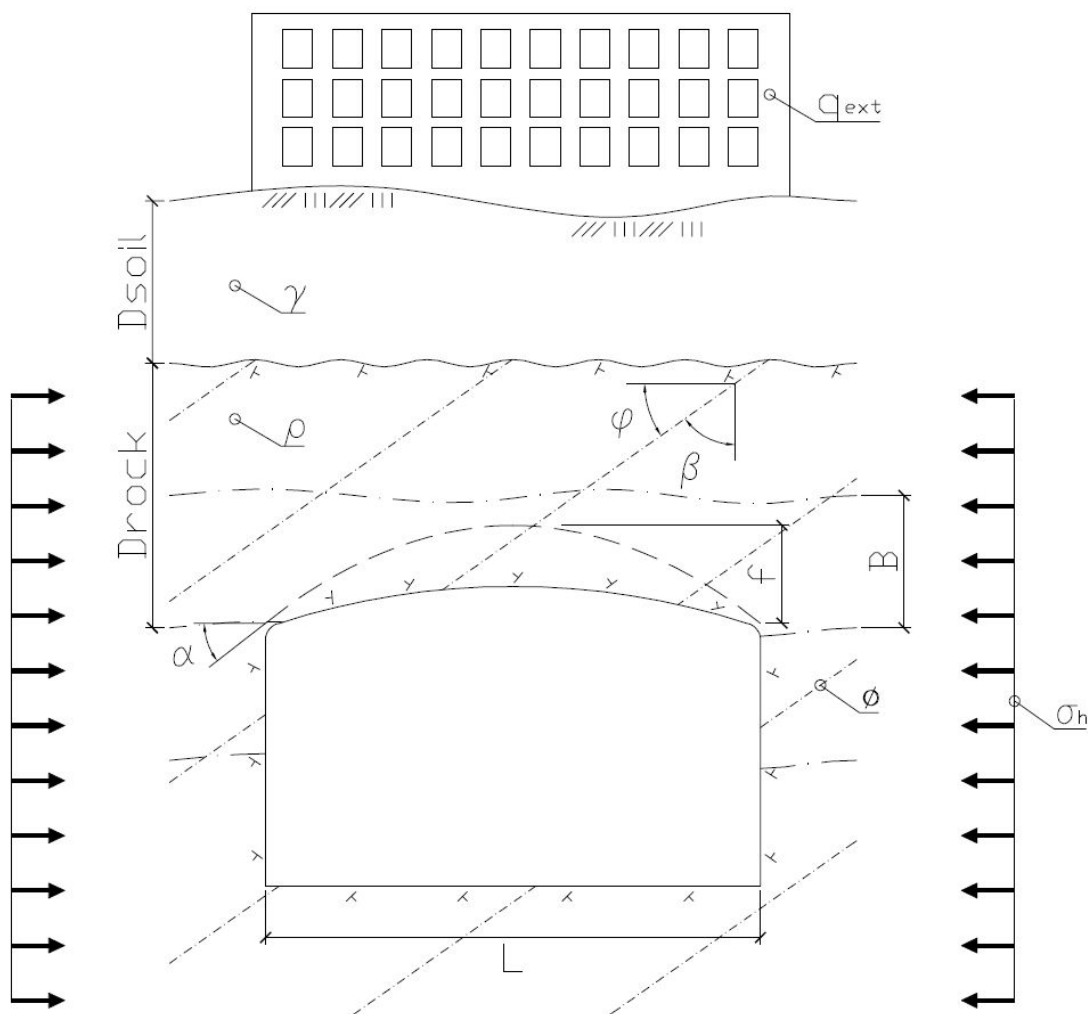
Figure 2-12 The parameters in the pressured arch theory

The different input parameters for a pressured arch stability analysis are shown in Figure 2-12. Important factors when calculating the stability is the arch height, f, and the angle of the pressure line, α, at the supporting points. The arch height can be calculated using Equation 2:10. If the arch height is higher than the bedding plane, there is a risk that rotation of the block will occur and that the block will fall down from the roof. To calculate the angle of the pressure line Equation 2:11 can be used.

This value should be smaller than the equivalent friction angle, ϕ', which is calculated by subtracting the angle between the fracture plane and the vertical plane, β, from the real friction angle, ϕ, see Equation 2:12 and Equation 2:13. If the angle of the pressure line is greater than the equivalent friction angle there is a risk of slip in the joints (Eriksson, Nord & Stille 2005).

$$f = \frac{qL^2}{8H_q}$$

Equation 2:10

$$\alpha = \arctan \frac{4f}{L}$$

Equation 2:11

$$\beta = 90 - \varphi$$

Equation 2:12

$$\phi' = \phi - \beta$$

Equation 2:13

As seen in Equation 2:10 the arch height is depending on the vertical load, q, tunnel width, L, and the horizontal force, H_q, acting on the supporting points of the arch. The horizontal force can be calculated using Equation 2:14 and is determined by multiplying the horizontal stress, σ_h, with the height of the arch, f, (Stille 1980). To calculate the vertical load the vertical forces are added together, see Equation 2:15, where ρ refers to the density of the rock, g the gravitational acceleration, D_{rock} the rock cover, γ the heaviness of the soil, D_{soil} the soil thickness and q_{ext} to the external vertical load created by constructions on the ground.

$$H_q = \sigma_h \cdot f$$

Equation 2:14

$$q = \rho g D_{rock} + \gamma D_{soil} + q_{ext}$$

Equation 2:15

It is seen from Equation 2:10 and Equation 2:14 that f is needed when calculating H_q and vice versa. By combining them, a first estimation of f can be calculated using Equation 2:16.

$$f = \frac{qL^2}{8\sigma_h f} \Rightarrow f^2 = \frac{qL^2}{8\sigma_h} \Rightarrow f = +\sqrt{\frac{qL^2}{8\sigma_h}}$$

Equation 2:16

As mentioned earlier the arch can collapse if a slip in a joint occurs or if the pressure line is higher than the distance between bedding planes. To make sure that none of these types of failures occurs it is important to check that $\alpha < \phi'$ and $f < B$, where B is the distance between bedding planes. The safety against these types of failures can be described using a safety factor, see Equation 2:17 and Equation 2:18, where FS_{rot} is the safety factor against rotation and FS_{slide} is the safety factor against sliding. If the safety factor is more than 1 it means that the design is safe.

$$FS_{rot} = \frac{B}{f}$$

Equation 2:17

$$FS_{slide} = \frac{\phi'}{\alpha}$$

2.4.2 Voussoir beam theory

In the Voussoir beam theory it is also assumed that a pressured arch is created in a heavily stratified rock mass. The stratification of a rock mass can be a result of the creation of the rock (sedimentary layering, igneous flow or metamorphic processes) or horizontal jointing created by the stresses in the ground. In this theory each stratum is replaced with a beam that is divided in two by a vertical cut, see Figure 2-13, and in this beam a pressured arch can form. This can only be assumed if there are no vertical fractures crossing the strata or if the fractures are steep. If there exists fractures that crosses the strata with a low angle the blocks needs to be bolted together to create the beam.
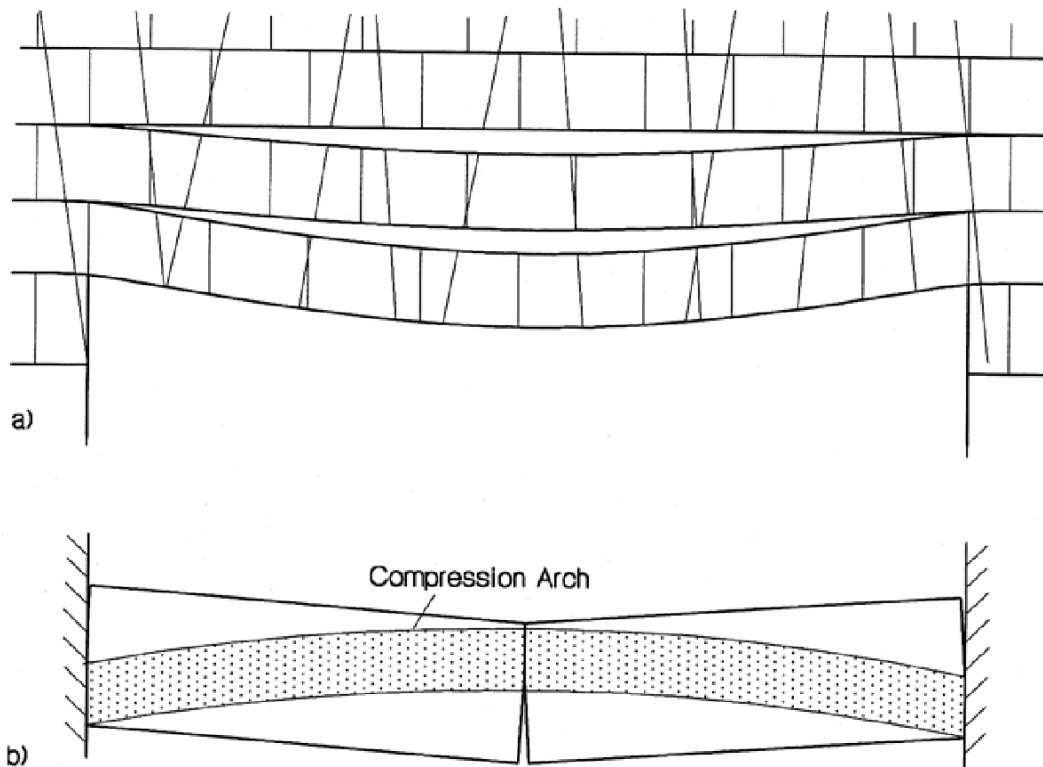
Figure 2-13 Principles of the Voussoir beam theory a) jointed rock beam b) Voussoir beam (Töyrä 2004)

There exist four types of failure modes for the Voussoir beam theory, see Figure 2-14. In thin beams, high ratio between the span and thickness of the beam, there is a risk of snap-through, meaning that there is insufficient thickness in the two pieces of the beam to create a pressured arch that can withstand the vertical load. There is also a risk of crushing in thin beams, this failure occurs when the pressure in the middle and the side of the beam becomes greater than the compressive strength of the rock. For thicker beams there is a risk of slip at the supporting points. When this occurs the vertical force caused by the self-weight of the beam has become larger than the friction forces in the supporting points. The friction is caused by the deformation of the beam, creating horizontal stress at the support points. The thicker the beam is the harder it is to deform it, which means that it is harder to create the necessary

horizontal stress. If the loads that are put on the beam are too large the risk of tensile fracturing along the arch occurs. This type of failure can occur within both thin and thick beams (Töyrä 2004).
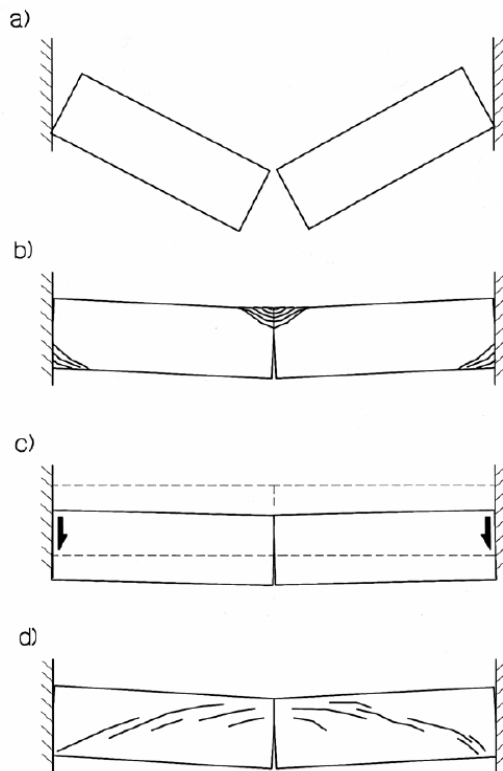
Figure 2-14 Failure modes of a Voussoir beam a) snap-through b) crushing c) slip d) tensile fracturing (Töyrä 2004)

2.4.3 Uncertainties

In stability analysis it exists three types of uncertainties; geometrical, parametrical and modelling. The geometrical uncertainties derive from the problem of estimating the size of existing blocks, their shape and where they are located. Parametrical uncertainties originate from the strength parameters in the rock mass and the strains that affect the blocks. Modelling uncertainties come from the simplifications in the models used to describe the behaviour in the rock mass (Bagheri 2009).

Block geometry

Uncertainties about the block geometry depend on the inability to completely describe the orientation and the location as well as the natural variation of the fractures in a three dimensional rock mass. The parameters used to describe the fractures in the rock mass come from observations on the surface, from boreholes or from pilot tunnels. This only gives information about the fractures in these points but not how they behave further into the rock mass.

Mechanical parameters

Analyses of mechanical parameters often result in the use of a mean value for the tested samples. The natural heterogeneity in the material, which depends on the

mineralogical composition of the rock and the strain history, makes the mechanical properties deviate from the calculated mean value. Limited information about the conditions bellow surface is also a source for uncertainty since it is only a very small part of the area of interest that it is possible to get information about. During collection of data something can have happened that have caused errors in the measurements, the tested sample could have been damaged when it was collected, the equipment used to test it could have been broken or human errors such as misprinting or misreading could have occurred.

Models

A model does not represent the truth, it is a simplification of reality and every parameter that is not considered in the model creates uncertainties in the model. To not consider every parameter that affects the result is necessary to make the model user friendly.

3 Varberg tunnel

The Swedish government has decided that Västkustbanan, a railway between Göteborg and Lund, shall be upgraded to double track for the entire stretch. Large parts have already been upgraded and on some locations construction are going on. The main reason for the whole project is to increase the capacity of the railway, both for people and for goods, as well as to strengthen the competitiveness of railway.

In the beginning of the Varberg tunnel project three alternatives was proposed; keep the alignment as today, with minor upgrade, a tunnel under the city or to construct a new railway east of the city of Varberg. Viewpoints of the project by municipality of Varberg, the county administrative board and Hallandstrafiken (the public transport company) had, were taken into account. In 2001 Banverket (the National Rail Administration) decided that the best alternative for this project was a tunnel underneath Varberg. The decision was based on the effects that the project has on the development of Varberg, technology and the environment.

The new railway through Varberg will start as a 400 meter long concrete trench from the north with the railway station in the southern part. After the station a three kilometre long tunnel will be constructed. Putting the railway in a tunnel releases a large land area that can be used for future exploitation. It also eliminates the barrier towards the ocean that the railway is today. For the new railway stretch see Figure 3-1 (Banverket 2001).
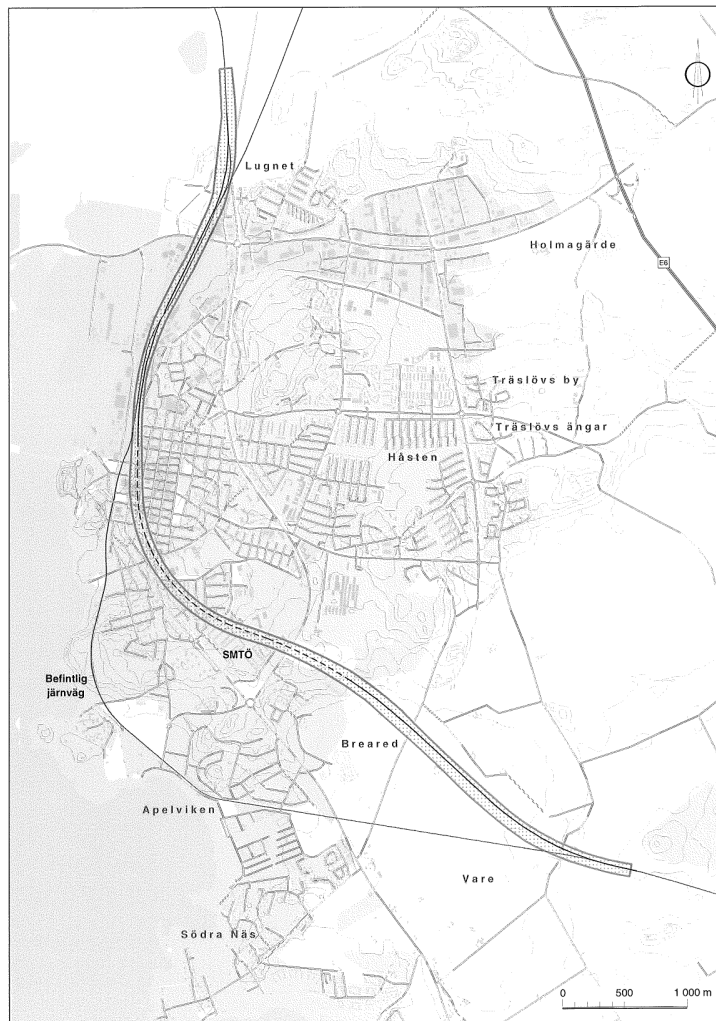
Figure 3-1 The new railway underneath Varberg (Banverket, 2002)

3.1 Geological description

The bedrock in the northern part of the proposed tunnel stretch is dominated by charnockite with elements of granite and granitic gneiss. In the more central parts of the tunnel the bedrock consists of granitic gneiss which is crossed by a small area with charnockite that changes back to granitic gneiss. For the southern part the bedrock changes back and forth between granitic gneiss and charnockite, this is interpreted as a boundary area between the two rock types (Bergström 1998).

3.1.1 Granitic gneiss

Granitic gneiss contains quartz, feldspar and garnet. The rock type has a lineation and normally also a foliation and in Varberg it has a foliation north-northwest. The fractures are mostly closed with unweathered and smooth surfaces. In some places in the granitic gneiss three to four meter long pegmatite lenses occur orientated along the foliation.

3.1.2 Granite

Only small granite bodies can be found along the proposed tunnel stretch. Normally they are found within the granitic gneiss as small lenses that have not been undergoing metamorphosis. It has the same mineral composition and foliation as the granitic gneiss.

3.1.3 Charnockite

Charnockite is an intrusive granitic rock type that contains diopside and garnet as well as quartz, feldspar and biotite. In Varberg it shows a small foliation in the north-northeastern direction. As in the granitic gneiss the fractures are mostly closed with unweathered and smooth surfaces. Due to its resistance to abrasion it is normally found exposed on high places in the terrain.

3.2 Investigations

The investigations that have been made for the Varberg tunnel project are:

- Surface fracture mapping
- Geophysics
- Soil- rock probing
- Core drilling
- Core mapping

Results from previous investigation in the area have also been used to evaluate the rock conditions underneath Varberg (Bergström 1998).

3.2.1 Surface mapping

The surface mapping results in a geological description of the rock mass condition in the area. This description contains information about the topography, major discontinuities as potential fracture zones, types of rock and the fractures mapped on outcrops in the landscapes. The most interesting information is their frequency, strike and dip as well as their surface roughness, width and length. After collecting the data fractures are group together into fracture sets that are then used to describe the irregularities in the rock mass. This is then used to estimate what can be expected in the tunnel.

3.2.2 Geophysics

There exist many types of geophysical test methods. The method used for the Varberg tunnel is refraction seismic. It is used to examine the soil and rock conditions down to a depth of 30-40 meters. It is mainly used to find the surface of the rock and to localise fracture zones in the rock mass. The theory behind refraction seismic is that different materials have different velocity for wave propagation. By inducing a shock wave into the ground the shock wave travels with a, for the material, specific velocity. When it hits a border between two materials with different seismic velocity a part of the shock wave is refracted back up to the surface. This refracted wave is then registered by a seismograph through a number of geophones that are placed on the

surface with a five meter interval. By analysing the registered shock wave arrival times to the different geophones the depth to different layers can be calculated.

3.2.3 Soil- rock probing

Soil- rock probing is used to find the rock surface level underneath the soil and to evaluate the properties of the upper part of the rock. This is done by measuring the feeding force, drilling rate, torque, rpm, flush water flow and pressure.

3.2.4 Core drilling

Two rock cores have been drilled, both of them were 45 mm in diameter and have been oriented to make it possible to determine the fractures strike and dip which has been the fracture analysis. In the bore holes water loss measurement have been conducted, with double sleeve every third meter, to estimate the hydraulic conductivity of the rock. The rock core has been used to perform core mapping.

3.2.5 Core mapping

Core mapping result in a more detailed geological description of a specific place in the rock mass. From the core information about the rock type, weathering, fracture properties, weakness zones and fracture frequency can be gained. From the core, samples for laboratory testing are taken to perform laboratory tests.

3.3   Input variables for the Varberg tunnel

The Varberg tunnel project has been chosen as a case study. In this chapter the input values for the variables and parameters in this project are given along with some assumptions made.

The input parameters for an analysis of the arch stability using the pressured arch theory are few. This makes the calculation model easy to use but at the same time information that is valuable for the analysis is lost. As seen in chapter 2.4.1 the parameters needed for an analysis are; tunnel width, fracture dip and strike, block size, fracture friction angle, horizontal stress and vertical load. The uncertainties for the tunnel width has to do with the blasting of the tunnel, how precise the drilling is done and how much explosives that are used in the contour holes. It is also depending on the natural block fall out from the tunnel contour which is caused by the properties of the fractures. Fracture dip and strike, block height, fracture friction angle, horizontal stress and vertical load uncertainties comes from the evaluation of the rock mass and how much investigations that have been done and if the samples are taken from places that are typical for the total rock mass.

3.3.1   Stresses and loads

Input values for the horizontal stresses are based on SKB (2009) giving the horizontal stress according to Equation 3:1, with a standard deviation of 12 %, this distribution is visualized in Figure 3-3. There have not been found any stress measurements in the area of Varberg that can be used as input for the calculations. The values given in SKB (2009) are considered to be used as possible values but are assumptions in lack of actual values. The reason for choosing the minor horizontal stress is that in the

Varberg area the primary stress is almost in a north-south direction according to the world stress map, see Figure 3-2, which is in the tunnel direction at the area of interest, see Appendix 2. Therefore is the minor horizontal stress perpendicular to the tunnel and the stress factor that controls the arch stability.

$$\sigma_h = 1 + 0.022 D_{rock}$$
<div style="text-align: right">**Equation 3:1**</div>
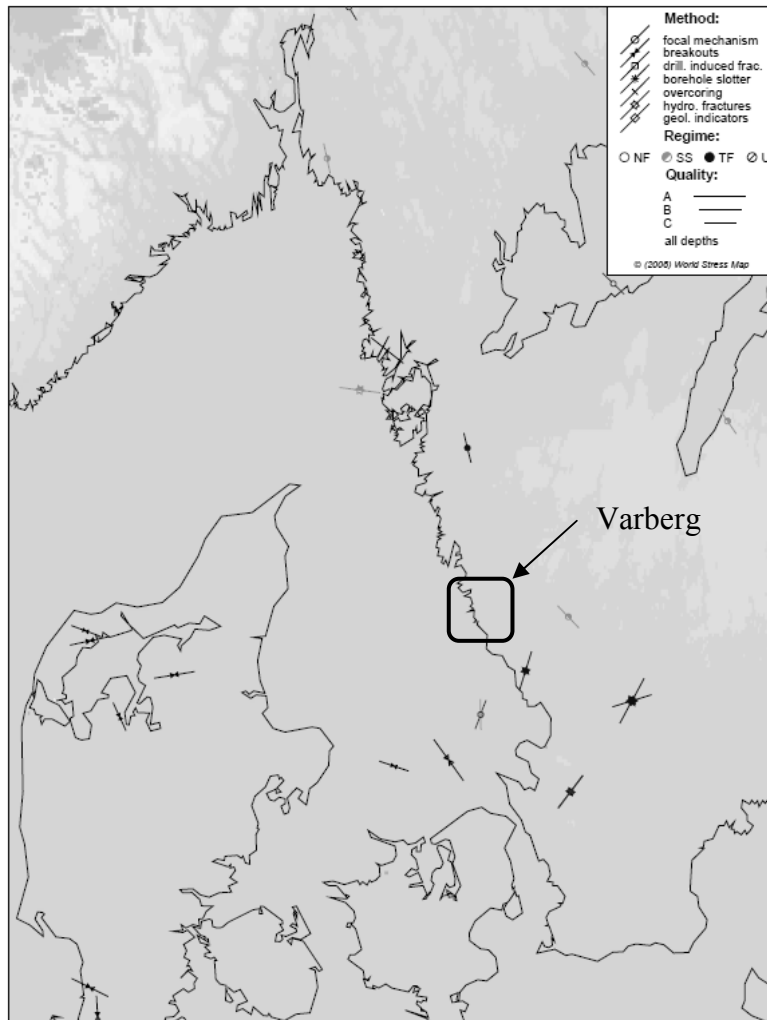
Figure 3-2 Stress map over the south-west part of Sweden, the lines represent the direction of the primary stress field (modified from Heidbach et al. 2008)
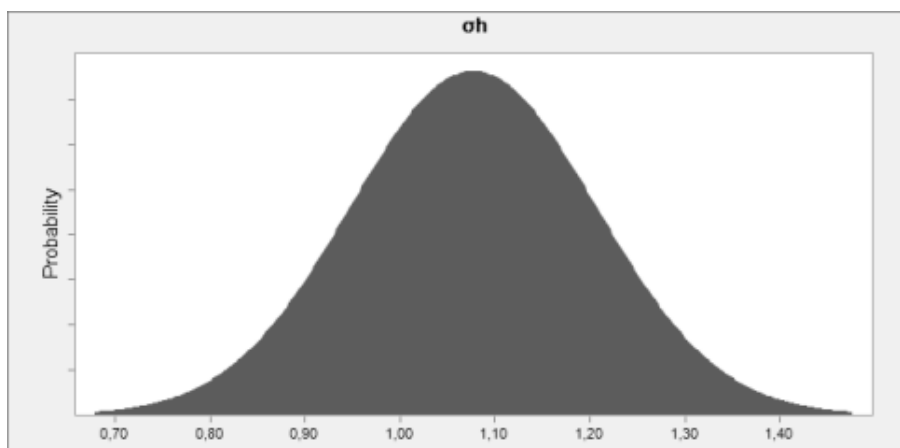
Figure 3-3 Distribution for the horizontal stress [MPa]

The external load has been put to 50 kN/m^2 due to the type of buildings on the ground. By looking on satellite pictures along the tunnel stretch the typical house type seems to be a three floor apartment house, see Appendix 3. According to Einarsson[1] the typical weight of such houses is 50 kN/m^2. The load that is working on the tunnel roof is a combination of the weight of the soil, rock mass and the external load. According to Lindblom (2010) the density of granite and gneiss is between 2600-2700 kg/m^3, see Figure 3-4. The soil is a mixture of finer and courser material which gives it a heaviness of 17-20 kN/m^3, see Figure 3-5, (Larsson 2008). The gravitational acceleration in the southern part of Sweden is about 9.82 m/s^2.
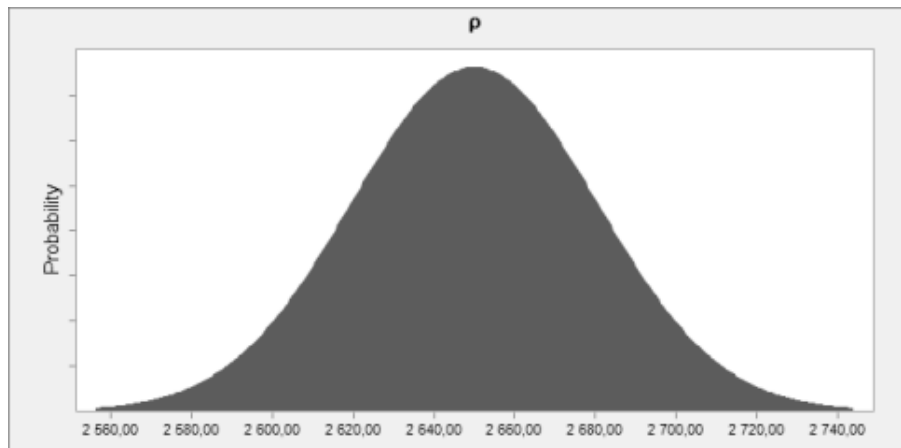
Figure 3-4 Distribution for the rock density [kg/m^3]
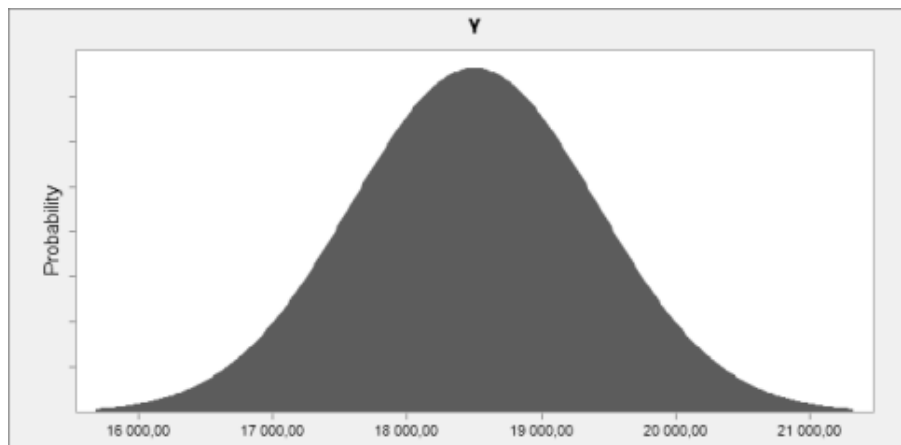
Figure 3-5 Distribution for the heaviness of the soil [kN/m^3]

3.3.2 Topography

The rock cover derives from the report VKB Varberg-Hamra Förprojektering (Bergström 1998) giving the minimum rock cover to 3.5 m. From the same report comes the soil depth and it is at the point where the rock cover is at its lowest, 10 m. The depth to the rock has been measured with refraction seismic and according to Hegardt and Meland (2011) the uncertainty of depths measured with refraction seismic is +/-0.5 m, the distributions for both the rock and soil cover is visualized in Figure 3-6 and Figure 3-7.

---

[1] Fredrik Einarsson Head of Department Construction Engineering Ramböll, E-mail on the 11th of November 2011
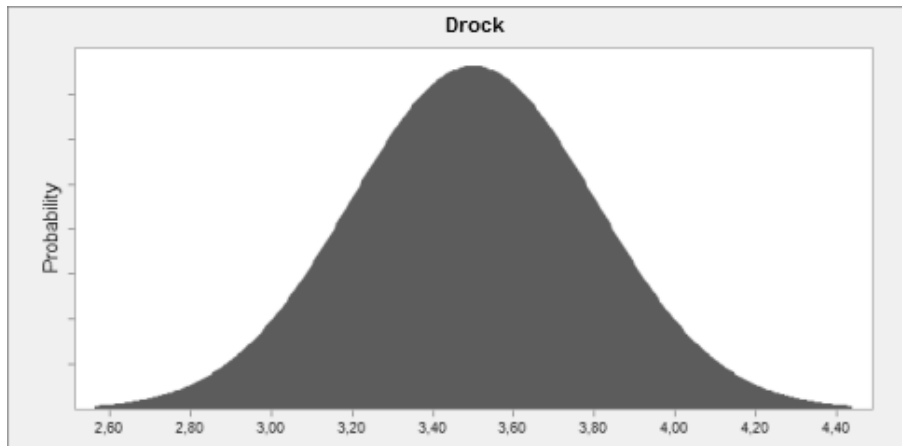
Figure 3-6 Distribution for the rock cover [m]
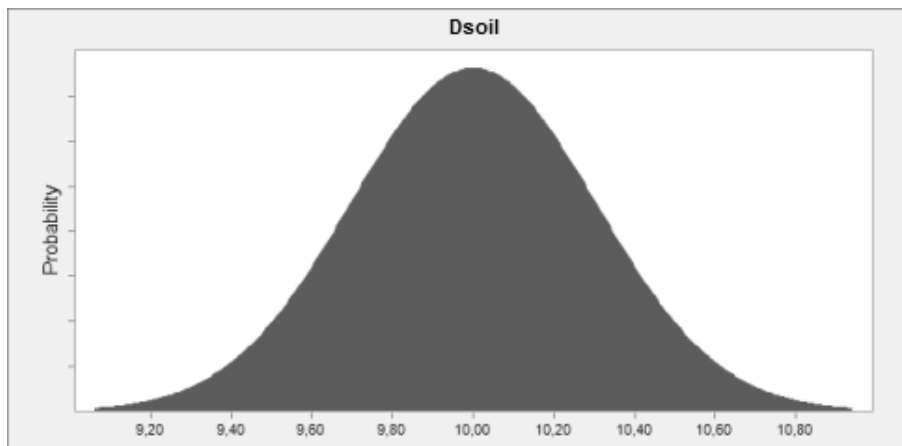
Figure 3-7 Distribution for the soil depth [m]

3.3.3 Tunnel geometry

When constructing a tunnel with the drill and blast method it is impossible to get perfect theoretical tunnel geometry. This is caused by the fact that the drill rig needs space to drill new holes for the next blast round and that lose rocks may fall out from the roof and walls. From the drawing of the tunnel, see Appendix 1, it is seen that the theoretical tunnel width is 13 m. To make sure that this width is achieved for the whole tunnel stretch the contractor normally excavates more rock. According to Dahlström[2] and Hallström[3] 20-60 cm extra on both sides with a mean value of 35 cm is excavated to create a tunnel that is wide enough.

---

[2] Richard Dahlström Project Manager Veidekke, phone call on the 11th of November 2011.
[3] Niklas Hallström Supervisor Strabag, phone call on the 11th of November 2011.
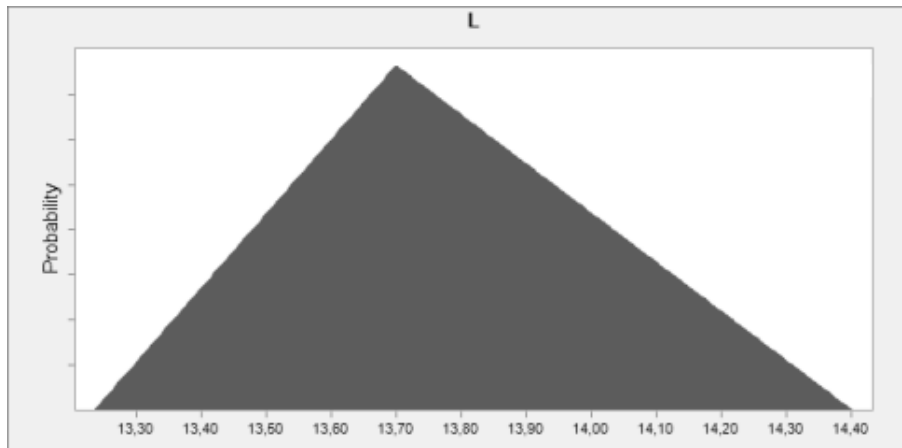
Figure 3-8 Distribution for the tunnel width [m]

3.3.4 Fractures

The fracture data used in the calculations come from the Varberg tunnel project, but not all fractures are of interest. The fractures that have been considered are the ones that deviate less than 30 degrees from the tunnel direction. According to the drawings of the tunnel at the area of interest, see Appendix 2, the tunnel is going in a north-south direction which means that the interesting fractures have a strike between 330-030 degrees and 150-210 degrees. The reason why the deviation 30 degrees have been chosen is that these fractures will follow the tunnel for a longer distance than two tunnel widths. This, according to Söder[4], means that they are going through rock that is under the full load from the vertical stresses. From the fractures that are 30 degrees from the tunnel direction only the fractures with a dip greater than 17 degrees have been chosen. Fractures with a lower dip than 17 degrees cannot cross the overlaying rock mass if the tunnel width is 13 meter, this results in a range for the dip that is between 17 and 90 degrees. The fractures with a dip of less than 17 degrees creates banking planes which specify the highest arch height that can be allowed without creating a risk of rotating blocks. It is assumed that there is no horizontal bedding plane crossing through the rock mass over the tunnel. This gives that $B = D_{rock}$ and in the following text they will both be called B. The friction angle of the fractures comes from the measured joint roughness and joint alteration that have been made for the Varberg tunnel, the range for the friction angle is between 0 and 90 degrees. After the isolation of the fractures that are of interest the fracture data has been inserted into Excel where Crystal Ball has been used to find the best fitting distribution for the values. These distributions can be seen in Figure 3-9 and Figure 3-10. For the friction angle the most probable value is 33.81 degrees and the most probable fracture dip is 63.21 degrees.

---

[4] Per-Erik Söder Consultant Ramböll, interview on the 26th of October 2011.
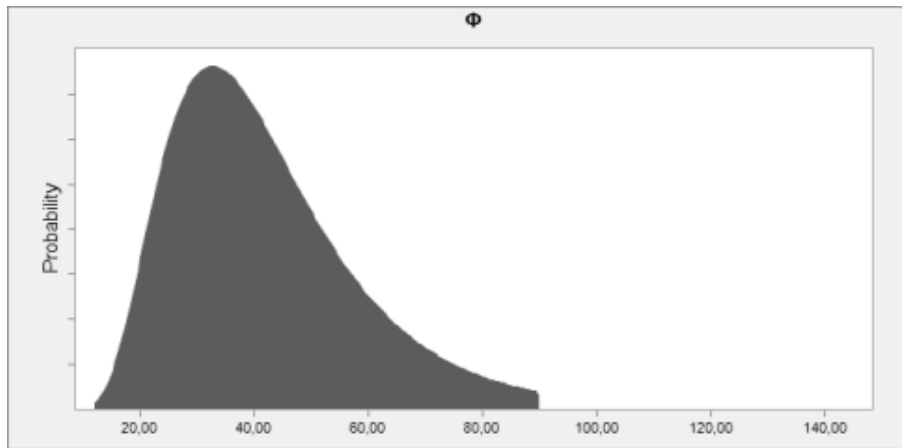
Figure 3-9 Distribution for the friction angle of the fractures
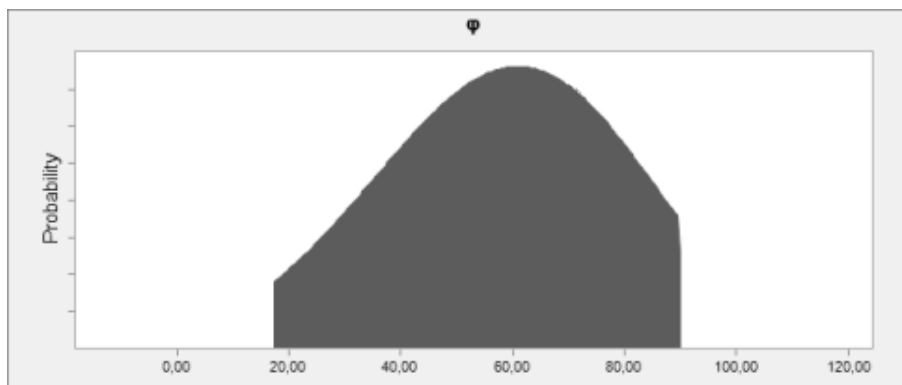
Figure 3-10 Distribution for the fracture dip

3.3.5 Strengths

Since the compressive strength of granitic rock types is between 116-343 MPa (Eriksson, Nord & Stille 2005) the risk of crushing in a shallow tunnel is very low and therefore the failure criteria of crushing will not be considered in this thesis.

3.3.6 Compilation of input variables

Table 3.1 shows a compilation of the input parameters that has been described earlier in this chapter.

Table 3.1 Compilation of input parameters for the Varberg tunnel

5%	ϕ	95%	5%	φ	95%	σh	std	5%	L	95%
	degrees			degrees		Mpa			m	
20.55	33.81	71.72	19.41	63.21	84.70	1+0.022*Drock	0.12*σh	13.4	13.7	14.2

5%	Drock	95%	5%	Dsoil	95%	5%	ρ	95%	5%	γ	95%
	m			m			kg/m3			kN/m3	
3.0	3.5	4.0	9.5	10.0	10.5	2600	2650	2700	17.0	18.5	20.0

4 Calculations

For the calculations of the arch stability the theory for a pressured arch is used. The calculations are done in Excel with the add-on Crystal Ball. The calculations have been divided into three calculation models; Model 0, Model 1 and Model 2, see Table 4.1. In this chapter the results and analysis of the different models will be presented. For a complete presentation of each calculation see Appendix 4.

Table 4.1 Variations between calculations

Parameter	ϕ	φ	σ_h	L	B	D_{soil}	ρ	γ
Model 0	Basic model							
0_0								
Model 1	Parameter study							
1_1	░	░	░	░	░	░	░	░
1_2	░							
1_3		░						
1_4			░					
1_5				░				
1_6					░			
1_7						░		
1_8							░	
1_9								░
Model 2	In-depth study of most influential parameter							
2_1	▓	▓	▓	▓	▓	▓	▓	▓
.	▓	▓	▓	▓	▓	▓	▓	▓
.	▓	▓	▓	▓	▓	▓	▓	▓
.	▓	▓	▓	▓	▓	▓	▓	▓

Legend:
- ☐ Fixed value
- ░ Varying value
- ▓ Decided after Model 1 is analysed

The theory of a pressured arch, as described in Chapter 2.4.1, consists of a number of deterministic equations. In Model 0 the values used in the equations are fixed to the most probable value for each input parameter, according to Chapter 3.3, which results in a single answer to each equation. Model 1 is a study of the uncertainties in the parameters used in the stability analysis. Calculation 1_1 is made to see what the overall uncertainty of the analysis is when all parameters have uncertainties. In Calculation 1_2 to 1_9 one of the parameters are varying, a new parameter for each calculation, and the results from these calculations is then compared to the result from Calculation 1_1. By comparing the results the most influential parameter is found. This parameter is then studied more in Model 2. The different calculations made in Model 2 are decided after the result from Model 1 is analysed.

As mentioned before the arch stability analysis is performed using the theory for a pressured arch, see Chapter 2.4.1. This theory is based on a number of equations and they are the same for every calculation model.

Equations:

$$\sigma_h = 1 + 0.022B$$

$$q = \rho g D_{rock} + \gamma D_{soil} + q_{ext}$$

$$f = \sqrt{\frac{qL^2}{8\sigma_h}}$$

$$\alpha = \arctan\left(\frac{4f}{L}\right)$$

$$\beta = 90 - \varphi$$

$$\phi' = \phi - \beta$$

$$FS_{rot} = \frac{B}{f}$$

$$FS_{slide} = \frac{\phi'}{\alpha}$$

4.1 Crystal Ball

Crystal ball is a statistical add-on to Excel and it uses Monte-Carlo simulations to calculate the possible outcomes for equations where the uncertainties for the input parameters are known. Instead of entering fixed values in the Excel spread sheet Crystal Ball allows the user to create variable cells which then can be used as input parameters in equations. The calculations are done as simulations were the user decides how many times the same equations should be solved and for each calculation Crystal Ball randomly chooses a value for each parameter according to the predefined distributions. The results from these calculations are then presented as diagrams showing how many times the result was a specific value (Oracle 2011).

4.2 Monte Carlo simulations

Monte-Carlo simulation is a mathematical method used to approximate the probability of a certain outcome. This is done by running simulations with random variables. It was primarily developed by the scientists working with the atomic bomb but has since its development been used to model a range of different types physical and conceptual systems.

The simulations are done by making lots of calculations and for every calculation a new set of random variables, from the different probability functions, is chosen. For a calculation round, several thousands of calculations are made and the result is shown as a probability distribution (Palisade 2011).

4.3 Model 0/Basic model

The normal way of calculating the arch stability is a deterministic calculation and does not take the uncertainty of the input data into consideration. Model 0 only contains one calculation and the parameters used have fixed values, see Table 3.1.

4.3.1 Model 0 results

The result of the single calculation in Model 0, see Table 4.2, shows that the rock cover is sufficient enough to be able to form a compressed arch within it, see Figure 4-1. Problems will occur due to sliding blocks since the equivalent friction angle is much lower than the angle of the pressure line at the support points.

Table 4.2 Results from Model 0

Parameter		Calculation 0_0
5%		-
f	m	2.67
95%		-
5%		-
α	degrees	37.89
95%		-
5%		-
Φ'	degrees	7.02
95%		-
p(f<B)	-	1.00
5%		-
FS_{rot}	-	1.31
95%		-
p(α<Φ')	-	0.00
5%		-
FS_{slide}	-	0.19
95%		-

Figure 4-1 The pressured arch inside the rock mass.

4.3.2 Analysis Model 0

The results from Calculation 0_0 show that the height of the arch is around 0.8 m lower than the rock cover. This is sufficient even if the rock cover, due to the uncertainties in the estimation of the position of the rock surface, would be 0.5 m lower. The results do also show that measurements need to be taken to prevent slip in joints, this is due to the fact that the equivalent friction angle is much lower than the angle of the arch at the supporting points.

4.4   Model 1/Parameter study

Model 1 is used to see which parameter with its uncertainty that has most influence on the uncertainties in the result. The uncertainties are the ones listed in chapter 3.3. The input parameters are described with their most probable value, 5 % and 95 % or the mean value and the standard deviation. For the output parameters f, α, FS_{rot} and FS_{slide} are given as the most probable value with its 5 % and 95 %, if they have any distribution, otherwise they are just given as mean values, and $p(f < B)$ and $p(\alpha < \phi')$ are given as mean values. The study is made by first including all uncertainty in the parameters, Calculation 1_1, and then study the influence of each parameter respectively, Calculation 1_2 to 1_9. By comparing these it will be shown which parameter that have the greatest influence on the overall uncertainty.

4.4.1   Results Model 1

The results from the calculations in Model 1, see Table 4.3, show that the input parameter that gives the largest uncertainties in the estimation of the height of the arch is the horizontal stress, Calculation 1_4. In Calculation 1_1 the difference between $f_{5\%}$ and $f_{95\%}$ is 0.59 m and in Calculation 1_4 where the horizontal stress is the only varying parameter the difference between $f_{5\%}$ and $f_{95\%}$ is 0.54 m. This is almost the same range between the outer parts of the uncertainty graph, see Figure 4-2, and if it is compared to the other input parameters it is seen that the uncertainties in the arch height has the highest uncertainty when the horizontal stress is varied.

Table 4.3 Results from Model 1

Parameter		Calculation								
		1_1	1_2	1_3	1_4	1_5	1_6	1_7	1_8	1_9
5%		2.42	-	-	2.44	2.61	2.63	2.63	2.66	2.60
f	m	2.65	2.67	2.67	2.64	2.66	2.67	2.67	2.67	2.67
95%		3.01	-	-	2.98	2.76	2.70	2.70	2.67	2.73
5%		35.27	-	-	35.42	-	37.47	37.49	37.82	37.24
α	degrees	37.69	37.89	37.89	37.65	37.89	37.89	37.89	37.89	37.88
95%		41.08	-	-	40.98	-	38.29	38.28	37.96	38.51
5%		1.65	1.01	1.35	-	-	-	-	-	-
Φ'	degrees	8.83	1.91	4.45	7.01	7.02	7.02	7.02	7.02	7.02
95%		48.65	45.09	32.45	-	-	-	-	-	-
p(f<B)	-	0.99	1.00	1.00	1.00	1.00	1.00	1.00	1.00	1.00
5%		1.09	-	-	1.18	1.27	1.14	1.29	1.31	1.28
FS_{rot}	-	1.30	1.31	1.31	1.32	1.31	1.32	1.31	1.31	1.31
95%		1.52	-	-	1.44	1.34	1.48	1.33	1.32	1.34
p(α<Φ')	-	0.13	0.09	0.01	0.00	0.00	0.00	0.00	0.00	0.00
5%		0.04	0.03	0.04	0.17	-	0.18	0.18	0.18	0.18
FS_{slide}	-	0.23	0.05	0.12	0.19	0.19	0.19	0.19	0.19	0.19
95%		1.28	1.19	0.86	0.20	-	0.19	0.19	0.19	0.19

Figure 4-2 Comparison between the distribution of the arch height in Calculation 1_1, line, and Calculation 1_4, column

All calculations show high probability that the arch height will be lower than the rock cover/bedding plane and this means that the risk for collapse due to rotating block is low. Looking at the safety factor for rotation the result from Calculation 1_6 is interesting. The difference between $f_{5\%}$ and $f_{95\%}$ is low, only 0.07 m but since the rock cover is varying the safety factor against rotation shows almost the same difference between the 5- and 95-percentile as Calculation 1_1, 0.34 in Calculation 1_6 and 0.43 in Calculation 1_1, see Figure 4-3. This is a little more than in Calculation 1_4, which had the largest variation in arch height, where the span between $FS_{rot,5\%}$ and $FS_{rot,95\%}$ is 0.26, see Figure 4-4.
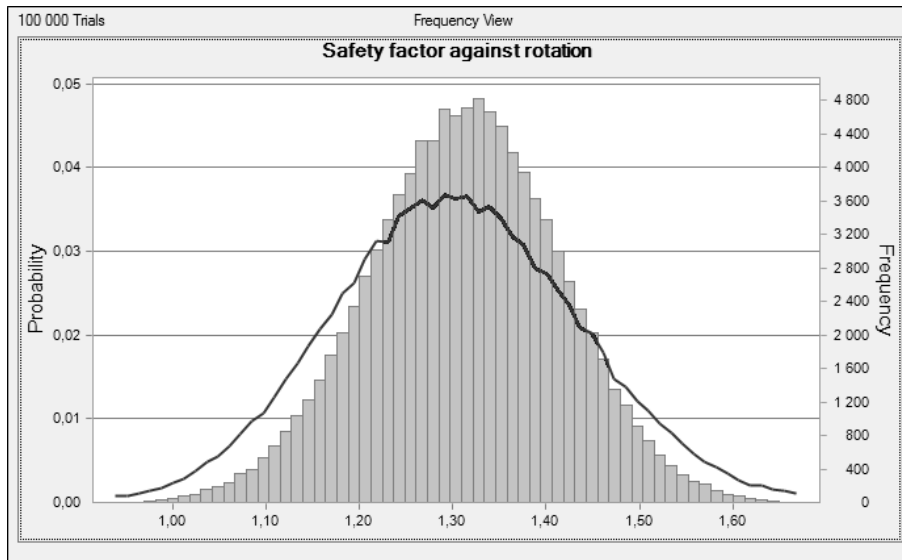
Figure 4-3 Comparison between the distribution of the safety factor against rotation in Calculation 1_1, line, and Calculation 1_6, column
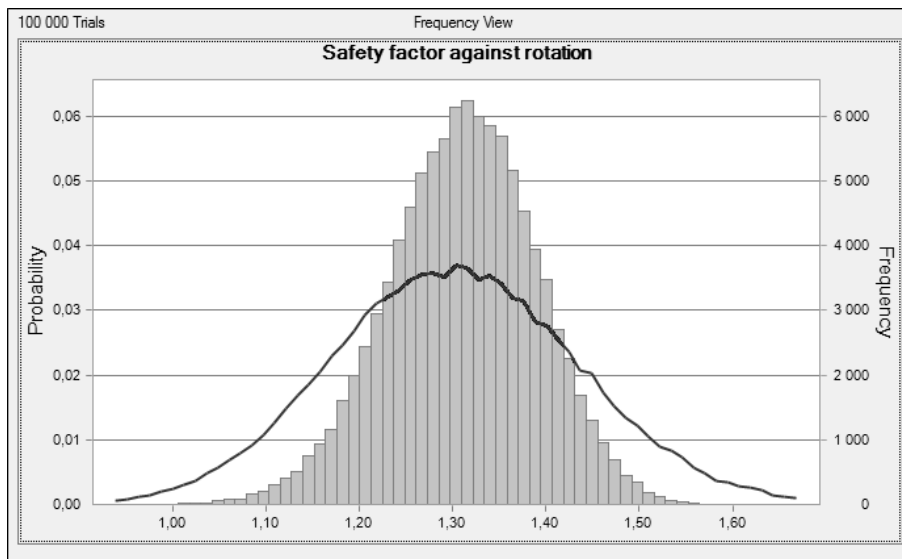
Figure 4-4 Comparison between the distribution of the safety factor against rotation in Calculation 1_1, line, and Calculation 1_4, column

The angle for the pressure line is depending on the arch height and the width of the tunnel. In Calculation 1_5 the results show that the variation in arch height created by the variation in tunnel width does not change the angle of the pressure line. So the parameter that has the largest influence in the angle of pressure line is the horizontal stress.

Only two parameters affect the equivalent friction angle, it is the friction angle and the dip of the fractures. The results from Calculation 1_2, variation in friction angle, and Calculation 1_3, variation in fracture dip, show that the variation in the friction angle has the largest influence on the uncertainties for the equivalent friction angle, see Figure 4-5 and Figure 4-6.
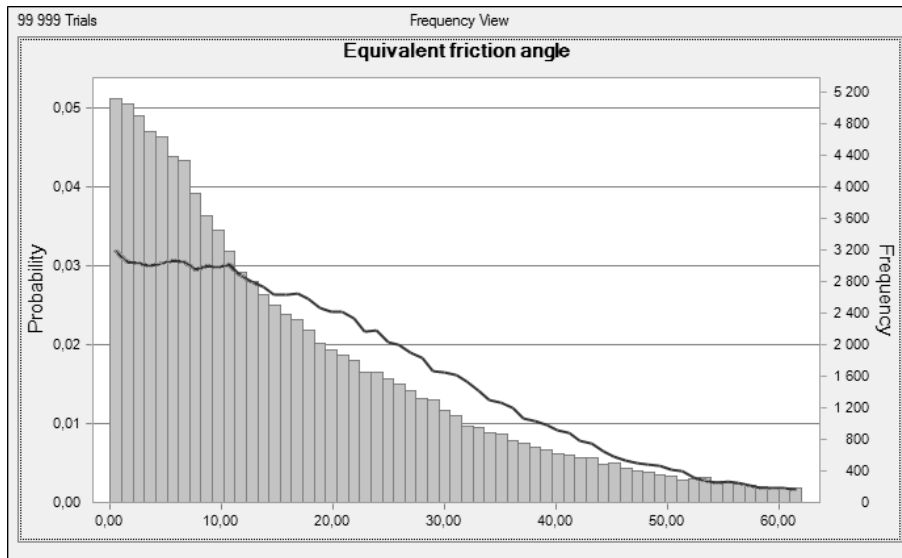
Figure 4-5 Comparison between the distribution of the equivalent friction angle in Calculation 1_1, line, and Calculation 1_2, column
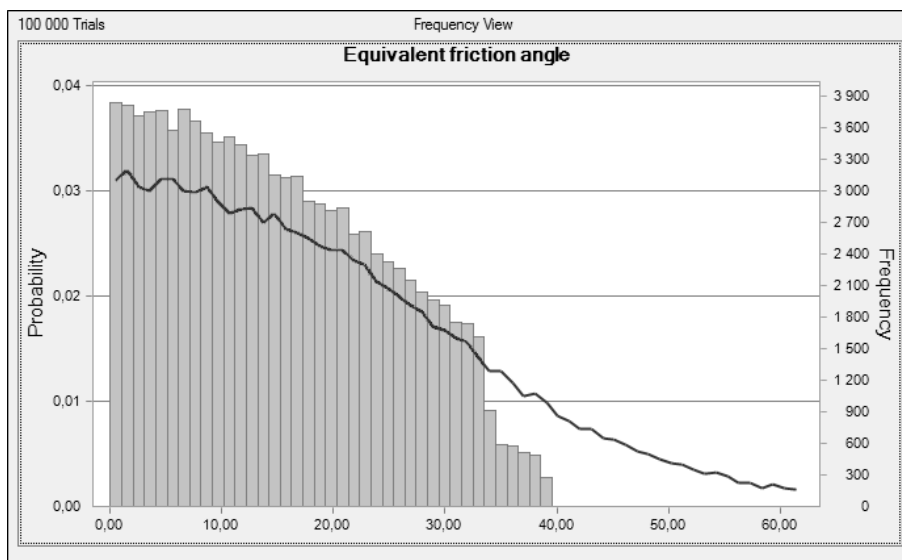
Figure 4-6 Comparison between the distribution of the equivalent friction angle in Calculation 1_1, line, and Calculation 1_3, column

For all calculations except 1_1, 1_2 and 1_3 the risk of collapse due to sliding blocks is 100 %. In Calculation 1_1 the risk is 83 %, in Calculation 1_2 it is 81 % and in Calculation 1_3 it is 99 %. The safety factor against sliding shows very low uncertainties for the calculations where the equivalent friction angle does not vary. The larger the uncertainty is in the equivalent friction angle, the larger the uncertainty is for the safety factor against sliding, see Figure 4-7.
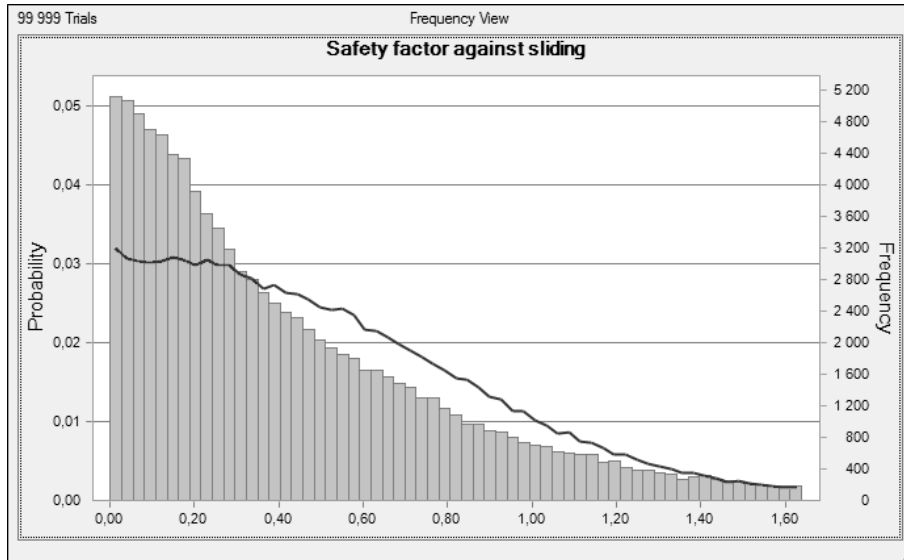
Figure 4-7 Comparison between the distribution of the safety factor against sliding in Calculation 1_1, line, and Calculation 1_2, column

4.4.2 Analysis Model 1

Model 1 show that the horizontal stress has the largest influence on the height of the compressed arch, see Table 4.4. This means that it has the largest influence on the angle at the supports for the arch. This influence is much larger than it is from the other parameters in the model. When it comes to the factor of safety against rotation, Model 1 shows that the rock cover has a major role, the changes in rock cover makes a small change in the total load on the tunnel roof but it creates a large variation in the rock mass where the arch can be formed.

Both the friction angle and the fracture dip cause large variations in the resulting equivalent friction angle. It seems that the variation in friction angle makes the model safer than the variation in fracture dip. This, since it makes the probability of the angle of the pressure line being less than the equivalent friction angle increase from 1 %, which it is when only the fracture dip is varying, to 9 %.

As a result of these findings more calculations are done in Model 2 to see what happens if more focus is put on the influence of the horizontal stress.

Table 4.4 Matrix showing a ranking of how much the uncertainties in the input parameters influence the uncertainty in the different output parameters; 1 = most influencial, 6 = least influencial, - = no influence

<table>
<tr><th></th><th></th><th colspan="8">Input parameter</th></tr>
<tr><th></th><th></th><th>ϕ</th><th>φ</th><th>σ_h</th><th>L</th><th>D_{rock}</th><th>D_{soil}</th><th>ρ</th><th>γ</th></tr>
<tr><th rowspan="5">Output parameter</th><th>f</th><td>-</td><td>-</td><td>1</td><td>2</td><td>4</td><td>4</td><td>5</td><td>3</td></tr>
<tr><th>α</th><td>-</td><td>-</td><td>1</td><td>-</td><td>3</td><td>4</td><td>5</td><td>2</td></tr>
<tr><th>Φ'</th><td>1</td><td>2</td><td>-</td><td>-</td><td>-</td><td>-</td><td>-</td><td>-</td></tr>
<tr><th>FS_{rot}</th><td>-</td><td>-</td><td>2</td><td>3</td><td>1</td><td>5</td><td>6</td><td>4</td></tr>
<tr><th>FS_{slide}</th><td>1</td><td>2</td><td>3</td><td>-</td><td>4</td><td>4</td><td>4</td><td>4</td></tr>
</table>

4.5   Model 2/Horizontal stress study

In this model, the effect of the uncertainties in the horizontal stress will be further studied. It will also be seen what happens to the overall stability if the horizontal stress regime is doubled or halved. The calculations in Model 2 is done according to Table 4.5

Table 4.5 Calculations in Model 2

Parameter	ϕ	φ	σ_h	L	B	D_{soil}	ρ	γ
Model 2	In-depth study of the horizontal stress							
2_1			-					
2_2	-	-		-	-	-	-	-
2_3			+					
2_4			-					
2_5			+					
2_6			-					
2_7			+					
2_8	+	+		+	+	+	+	+

(grey)	Varying value, same as Model 1
+	Varying value, doubled uncertainty
-	Varying value, halved uncertainty
+	Varying value, doubled value
-	Varying value, halved value
+	Varying value, doubled depth dependency
-	Varying value halved depth dependency

4.5.1   Results Model 2

Table 4.6 Results from Model 2

Parameter		Calculation							
		2_1	2_2	2_3	2_4	2_5	2_6	2_7	2_8
5%		2.51	2.44	1.72	3.43	2.34	2.47	2.26	2.38
f	m	2.66	2.65	1.88	3.75	2.56	2.70	2.58	2.67
95%		2.86	2.99	2.13	4.26	2.91	3.07	3.46	3.09
5%		36.32	35.38	26.57	44.99	34.35	35.74	33.28	34.82
α	degrees	37.85	37.89	28.63	47.55	36.71	38.19	36.99	37.72
95%		39.56	41,00	31.65	50.98	40.09	41.62	45.11	41.36
5%		1.64	0.71	1.63	1.61	1.64	1.66	1.63	0.71
Φ'	degrees	8.24	1.56	8.60	9.07	8.59	8.81	8.75	11.95
95%		49.22	25.70	49.04	48.48	48.81	48.82	48.88	57.65
p(f<B)	-	1.00	1.00	1.00	0.20	1.00	0.99	0.94	0.91
5%		1.12	1.15	1.54	0.77	1.12	1.07	0.98	0.93
FS_{rot}	-	1.31	1.31	1.84	0.92	1.34	1.27	1.30	1.28
95%		1.50	1.46	2.16	1.08	1.58	1.49	1.61	1.67
p(α<Φ')	-	0.13	0.01	0.25	0.05	0.14	0.12	0.13	0.25
5%		0.04	0.02	0.06	0.03	0.04	0.04	0.04	0.05
FS_{slide}	-	0.22	0.04	0.30	0.19	0.23	0.23	0.15	0.33
95%		1.30	0.68	1.70	1.01	1.33	1.27	1.30	1.53

The results from all calculations made in Model 2, presented in Table 4.6, show that by halving the uncertainties for the horizontal stress, Calculation 2_1, the difference between the 5-percentile and the 95-percentile for the arch height lowers with a little bit more than 40 % compared to Calculation 1_1. This is much more than if the uncertainties for all parameters except the horizontal stress are halved, Calculation 2_2, here the difference between the 5-percentile and the 95-percentile is less than 10 %, see Figure 4-8. For the safety factor against rotation the difference between the 5-percentile and the 95-percentile is lower for the case with a lowered uncertainty for the horizontal stress than it is when all parameters except the horizontal stress have their uncertainties halved. For Calculation 2_1 it is lowered

with 12 % and for Calculation 2_2 it is lowered 18 %, see Figure 4-9. Small changes in the safety factor against sliding are seen when the uncertainties in the horizontal pressure are halved, but they are so small that they can be ignored. When all other parameters have their uncertainties halved, the difference is much larger. In Calculation 2_1 the change is just a few percent and in Calculation 2_2 the change is almost 50 %, see Figure 4-10.
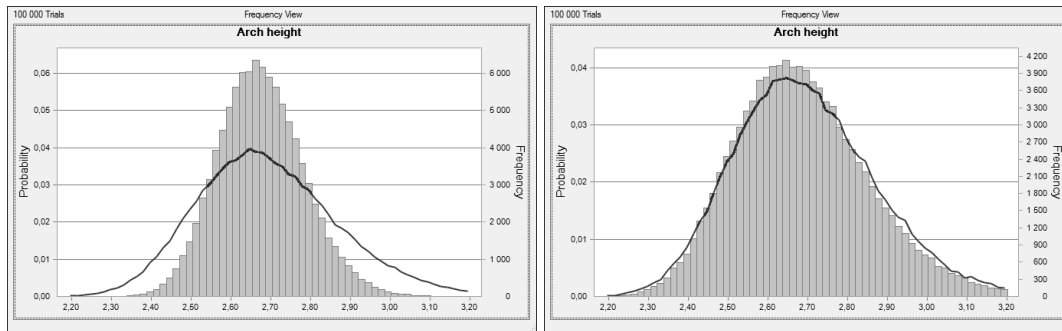
Figure 4-8 Arch height distributions; left) comparison between Calculation 1_1, line, and Calculation 2_1, column, right) comparison between Calculation 1_1, line, and Calculation 2_2, column
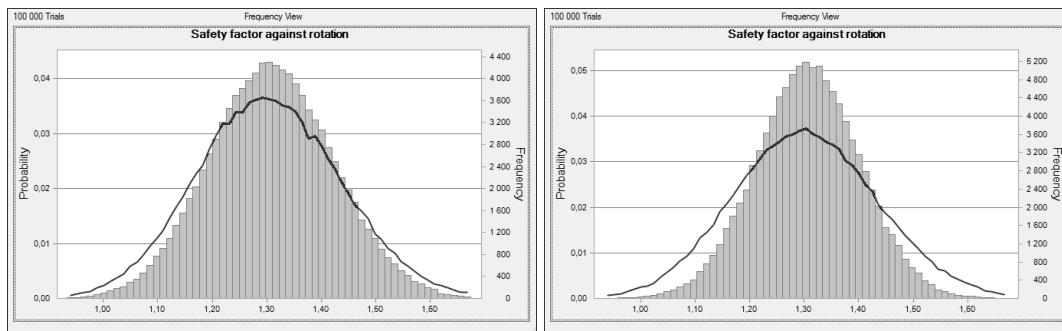
Figure 4-9 Safety factor against rotation distributions; left) comparison between Calculation 1_1, line, and Calculation 2_1, column, right) comparison between Calculation 1_1, line, and Calculation 2_2, column
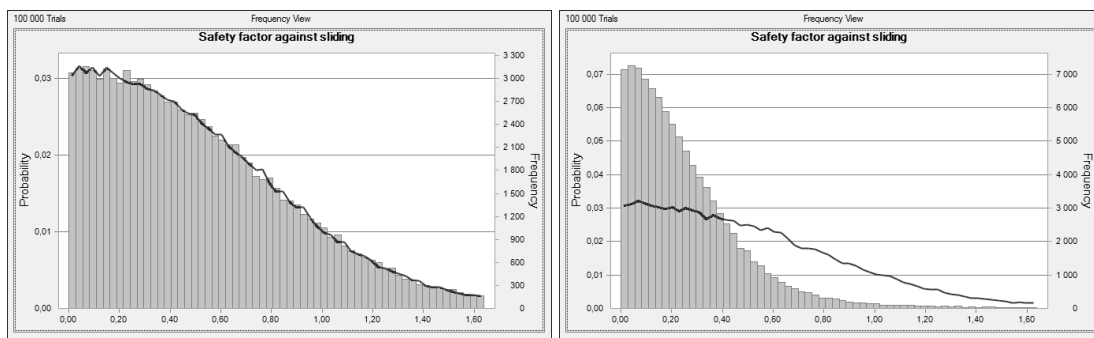
Figure 4-10 Safety factor against sliding distributions; left) comparison between Calculation 1_1, line, and Calculation 2_1, column, right) comparison between Calculation 1_1, line, and Calculation 2_2, column

If the uncertainty of the horizontal stress is doubled, Calculation 2_7, the difference between the 5-percentile and the 95-percentile for the arch height is increased a little more than 100 %. This is compared to when the uncertainty of all parameters except the horizontal stress are doubled, Calculation 2_8, where the difference is increased a little more than 20 %, see Figure 4-11. Just as when the uncertainty was halved the change in safety factor against rotation is larger when the uncertainties for all parameters except the horizontal stress are doubled than it is when the uncertainty for

the horizontal stress is doubled. In Calculation 2_7 the difference between the 5-percentile and the 95-percentile is increased with 47 % and in Calculation 2_8 it is increased with 72 %, see Figure 4-12. For the safety factor against sliding block Calculation 2_7 show an increased uncertainty of 2 %. The change in Calculation 2_8 is larger, almost 20 %, see Figure 4-13.
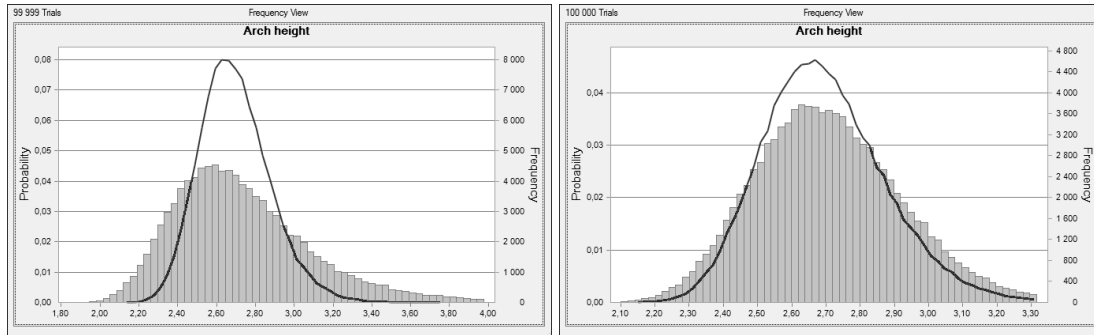
Figure 4-11 Arch height distributions; left) comparison between Calculation 1_1, line, and Calculation 2_1, column, right) comparison between Calculation 1_1, line, and Calculation 2_2, column
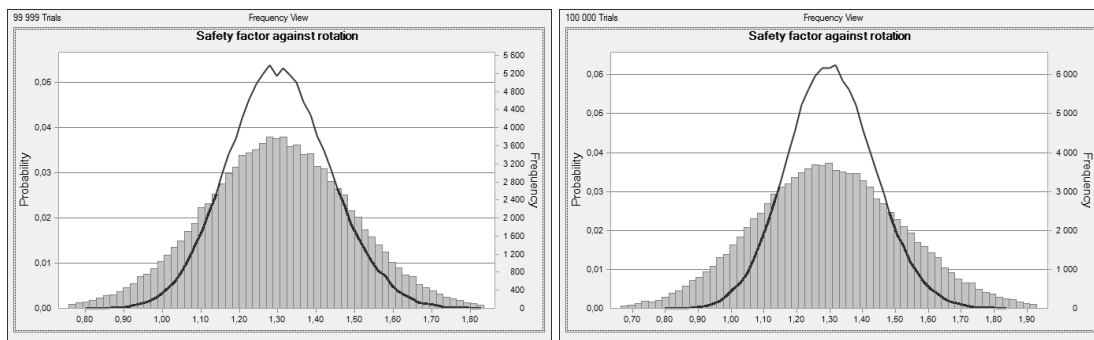
Figure 4-12 Safety factor against rotation distributions; left) comparison between Calculation 1_1, line, and Calculation 2_7, column, right) comparison between Calculation 1_1, line, and Calculation 2_8, column
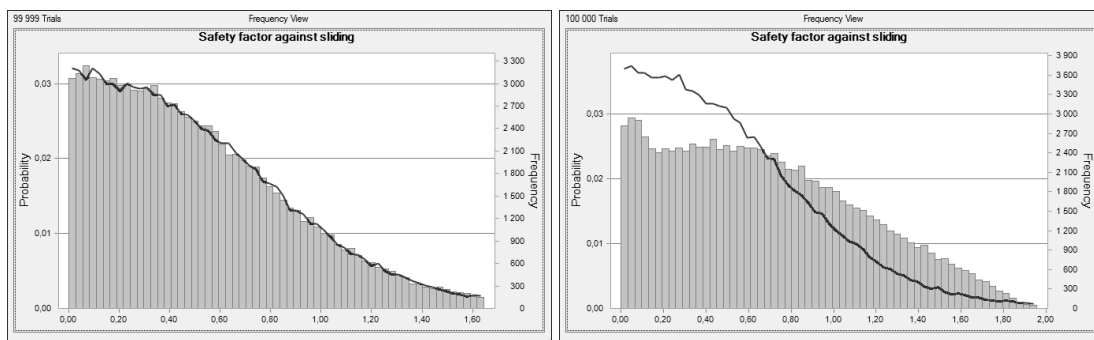
Figure 4-13 Safety factor against sliding distributions; left) comparison between Calculation 1_1, line, and Calculation 2_7, column, right) comparison between Calculation 1_1, line, and Calculation 2_8, column

In Calculation 2_3 the horizontal stress has been doubled and as a result the height of the arch has been lowered. The most probable value for the arch height is 29 % lower than in Calculation 1_1, the same change applies to the 5-percentile that also has been lowered with 29 %. The difference between the 5-percentile and the 95-percentile has decreased with 30 % which is almost the same as the decrease in the most probable value. In Calculation 2_4 where the horizontal stress has been halved the most probable arch height is increased with 42 %. Just as in Calculation 2_3 the 5-percentile has the same increase as the most probable value and the difference

between the 5-percentile and the 95-percentile has almost the same change has the most probable value. The change in the difference between the 5-percentile and the 95-percentile is 41 %, see Figure 4-14. The safety factor against rotation, most probable value, increases with 42 % in Calculation 2_3, the 5-percentile increases with 41 % and the difference between the 5-percentile and the 95-percentile increases with 44 %. In Calculation 2_4 the most probable value for the safety factor against rotation decreases with 29 % just like the 5-percentile also does and the difference between the 5-percentile and the 95-percentile decreases with 28 %, see Figure 4-15. The most probable value for the safety factor against sliding is increased with 30 % in Calculation 2_3 compared to Calculation 1_1. For Calculation 2_4 the most probable value for the safety factor against rotation has decreased with 17 % instead. The change in 5-percentile is plus 50 % and minus 25 % respectively, and the difference between the 5-percentile and the 95-percentile has changed with plus 32 % and minus 21 % respectively in Calculation 2_3 and 2_4.
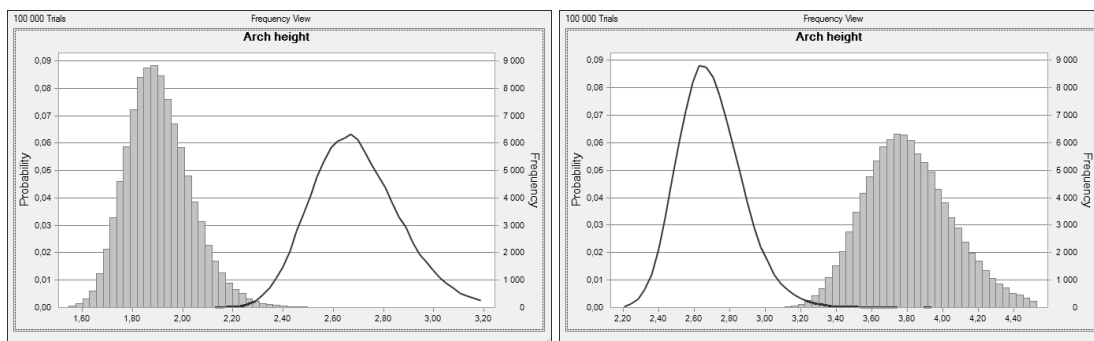
Figure 4-14 Arch height distributions; left) comparison between Calculation 1_1, line, and Calculation 2_3, column, right) comparison between Calculation 1_1, line, and Calculation 2_4, column
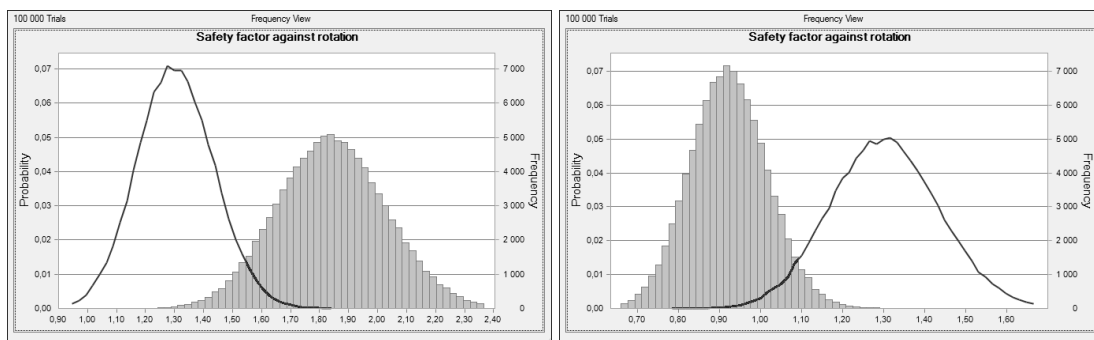
Figure 4-15 Safety factor against rotation distributions; left) comparison between Calculation 1_1, line, and Calculation 2_3, column, right) comparison between Calculation 1_1, line, and Calculation 2_4, column
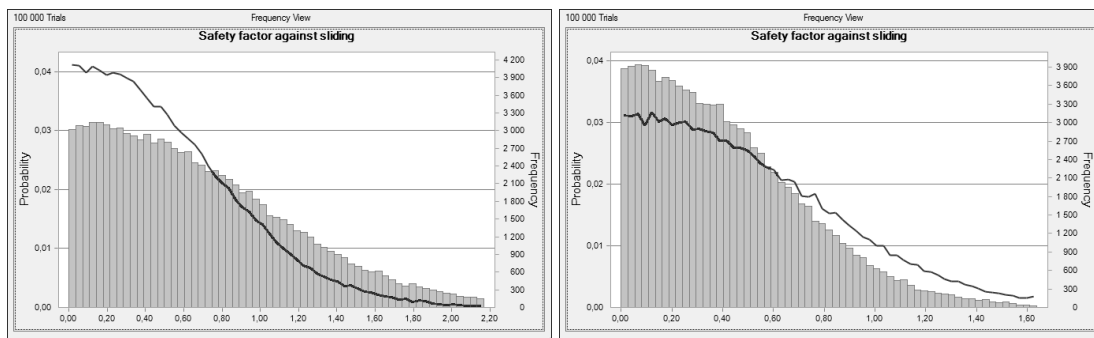
Figure 4-16 Safety factor against sliding distributions; left) comparison between Calculation 1_1, line, and Calculation 2_3, column, right) comparison between Calculation 1_1, line, and Calculation 2_4, column

Calculation 2_5 and 2_6 show the same type of behaviour as Calculation 2_3 and 2_4 but since the change in horizontal stress is smaller, in 2_5 it is increased with 7 % and in 2_6 it is decreased with 4 % compared to 1_1, the changes in arch height, safety factor against rotation and safety factor against sliding are smaller. In Calculation 2_5 the most probable value for the arch height is 3 % lower than in Calculation 1_1, the same change is seen in the 5-percentile and the difference between the 5-percentile and the 95-percentile. For Calculation 2_6 the most probable value for the arch height, the 5-percentile and the difference between the 5-percentile and the 95-percentile has increased with 2 %, see Figure 4-17. The most probable value and the 5-percentile for the safety factor against rotation are in Calculation 2_5 increased with 3 % and in Calculation 2_6 they are decreased with 2 %. The difference between the 5-percentile and the 95-percentile is in Calculation 2_5 increased with 7 % and in Calculation 2_6 it is decreased with 2 %, see Figure 4-18. In the safety factor against sliding both Calculation 2_5 and 2_6 show no change in the most probable value and 5-percentile compared to Calculation 1_1. Small changes are seen in the 95-percentile which make small change in the difference between the 5-percentile and 95-percentile. In Calculation 2_5 the difference has increased with 4 % and in Calculation 2_6 the difference has decreased with 1 %, see Figure 4-19.
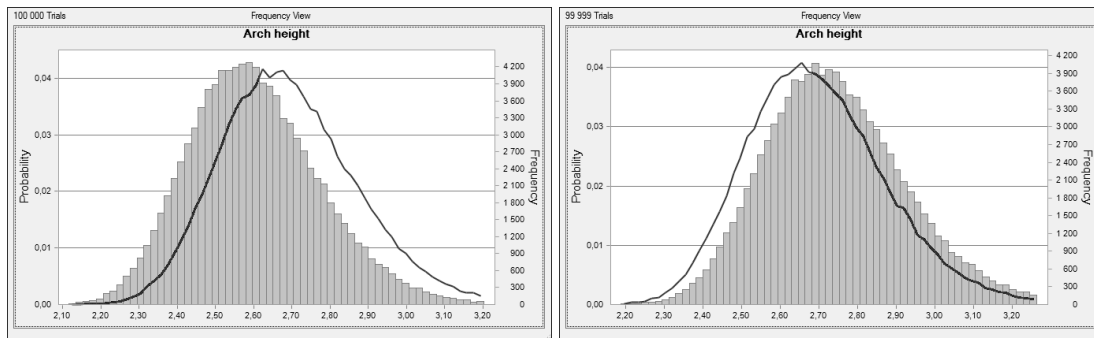
Figure 4-17 Arch height distributions; left) comparison between Calculation 1_1, line, and Calculation 2_5, column, right) comparison between Calculation 1_1, line, and Calculation 2_6, column
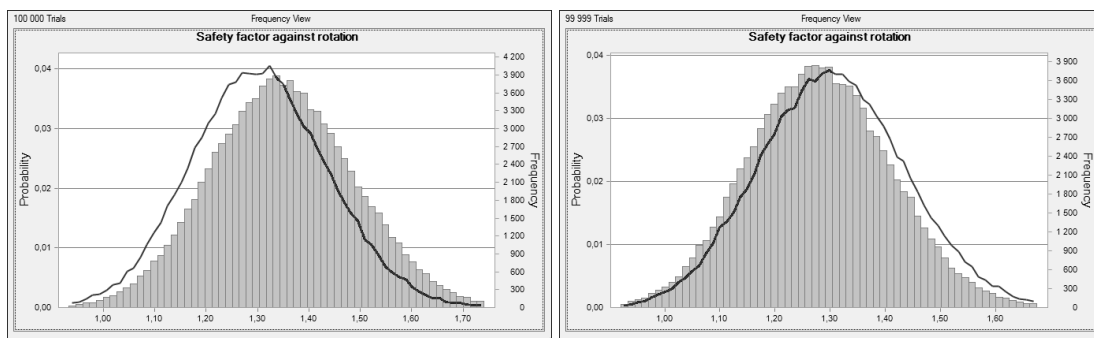
Figure 4-18 Safety factor against rotation distributions; left) comparison between Calculation 1_1, line, and Calculation 2_5, column, right) comparison between Calculation 1_1, line, and Calculation 2_6, column
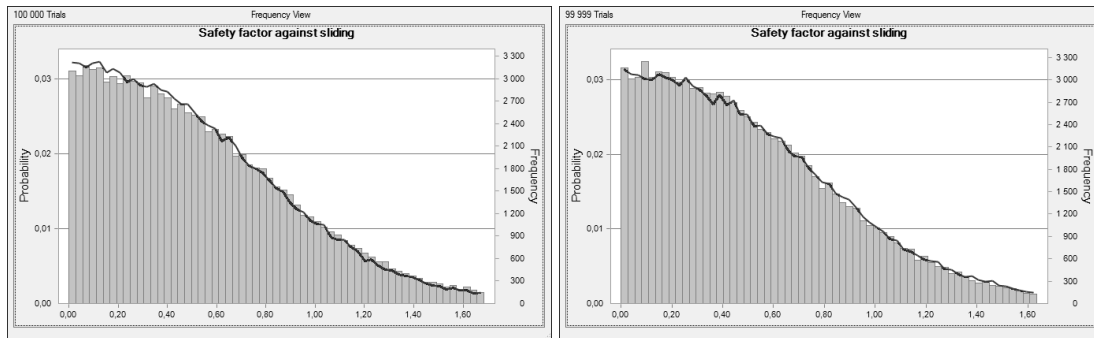
Figure 4-19 Safety factor against sliding distributions; left) comparison between Calculation 1_1, line, and Calculation 2_5, column, right) comparison between Calculation 1_1, line, and Calculation 2_6, column

4.5.2 Analysis Model 2

The uncertainty for the horizontal stress influence the uncertainty for the height of the arch more than the uncertainties for all the other parameters combined. In Calculation 2_1 and 2_7 the uncertainty of the horizontal stress is changed and both these calculations show larger changes in the uncertainty of the arch height than the results from Calculation 2_2 and 2_8, where the uncertainties for all other parameters are changed. When all parameters except the horizontal stress have their uncertainties doubled or halved the safety factor against rotation show larger changes in the uncertainty than if only the horizontal stress has changed. This due to that the changes in the uncertainty of the rock cover that occur when all parameters except the horizontal stress are changed are larger than the changes that occur in the uncertainty of the arch height when the uncertainty of the horizontal stress is changed. The uncertainty in the horizontal stress has a minor role in the uncertainty of the safety factor against sliding.

When the most probable value for the horizontal stress is changed the most probable value for the arch height is changed. This change also affects the uncertainty of the arch height with the same amount. The same thing happens with the safety factor against rotation. Calculation 2_3 to 2_6 shows that the size of the horizontal pressure is important to estimate size of the safety factor against sliding.

The results from Model 2 shows that it is more important to have a good estimation on how large the most probable value for the horizontal stress is than it is to have a low spread in the measured data.

5 Results

The results from Model 1 show that the parameter that gives the largest uncertainties in the estimation of the height of the arch is the horizontal stress. When the horizontal stress is the only varying parameter the uncertainty in the estimation of the arch height is approximately the same as it is when all parameters are varying. The uncertainty in the estimation of the rock cover has a minor role for the uncertainty in the estimation of the arch height but looking at the uncertainty in the safety factor against rotation it has a bigger impact than the uncertainty in horizontal stress. Only the friction angle and the fracture dip affect the uncertainty for the equivalent friction angle. By comparing the two calculations it shows that the friction angle has the biggest influence on the uncertainty.

In Model 2 where the uncertainties in the horizontal stress and its influence are further studied it is shown that changes in the uncertainty for the horizontal stress has a larger impact on the uncertainty in the arch height than a corresponding change for all other parameters have. Looking at the safety factor against rotation it is instead the changes in all parameters except the horizontal stress that shows the largest changes. If the horizontal stress is doubled the most probable arch height decreases with almost 30 % and if it is halved the most probable arch height increases with about 40 %. In both cases the same change can be seen in the 5-percentile and the difference between the 5-percentile and 95-percentile. The most probable value for the safety factor against rotation increases with about 40 % when the uncertainty in horizontal stress is halved. When the horizontal stress uncertainty is doubled the most probable value decreases with almost 30 % Just as the uncertainty for the arch height follows the changes in most probable arch height the uncertainties for the safety factor against rotation increases or decreases with the most probable safety factor against rotation.

Table 5.2 shows a compilation of all calculation results. Calculation 0_0 is the basic model. Model 1, Calculation 1_1 to 1_9, is the parameter study. Model 2, Calculation 2_1 to 2_8, is the study of the effects of changes in the horizontal stress and in the uncertainties for the horizontal stress. The different calculations made are described in Chapter 4 and in Table 5.1

Table 5.1 Calculations made in Model 0, Model 1 and Model 2

Calculations

Parameter	0_0		1_1	1_2	1_3	1_4	1_5	1_6	1_7	1_8	1_9		2_1	2_2	2_3	2_4	2_5	2_6	2_7	2_8
φ			▓	▓										-						+
φ			▓		▓									-						+
σ_h	Model 0		▓			▓						Model 2	-		+	-	+	-	+	
L			▓				▓							-						+
B			▓					▓						-						+
D_soil			▓						▓					-						+
ρ			▓							▓				-						+
γ			▓								▓			-						+

(Model 1 label appears in the spanning column before 1_1.)

Legend:

- □ Fixed value
- ▓ (gray) Varying value, according to Chapter 3.3
- [+] Varying value, doubled uncertainty
- [-] Varying value, halved uncertainty
- + Varying value, doubled value
- - Varying value, halved value
- [+] (dark) Varying value, doubled depth dependency
- [-] (dark) Varying value, halved depth dependency

Table 5.2 Compilation of calculation results

Parameter		Calculation																	
		0.0	1.1	1.2	1.3	1.4	1.5	1.6	1.7	1.8	1.9	2.1	2.2	2.3	2.4	2.5	2.6	2.7	2.8
f	m	2.67	2.67	2.67	2.67	2.64	2.66	2.67	2.67	2.67	2.67	2.66	2.65	1.88	3.75	2.56	2.70	2.58	2.67
5%		–	2.42	–	–	2.44	2.61	2.63	2.63	2.66	2.60	2.51	2.44	1.72	3.43	2.34	2.47	2.26	2.38
95%		–	3.01	–	–	2.98	2.76	2.70	2.70	2.67	2.73	2.86	2.99	2.13	4.26	2.91	3.07	3.46	3.09
α	degrees	37.89	37.69	37.89	37.89	37.65	37.89	37.89	37.89	37.88	37.88	37.85	37.89	28.63	47.55	36.71	38.19	36.99	37.72
5%		–	35.27	–	–	–	–	–	–	–	–	36.32	35.38	26.57	44.99	34.35	35.74	33.28	34.82
95%		–	41.08	–	–	–	–	–	–	–	–	39.56	41.00	31.65	50.98	40.09	41.62	45.11	41.36
Φ'	degrees	7.02	8.83	1.91	4.45	7.01	7.02	7.02	7.02	7.02	7.02	8.24	1.56	8.60	9.07	8.59	8.81	8.75	11.95
5%		–	1.65	1.01	1.35	–	–	–	–	–	–	1.64	0.71	1.63	1.61	1.64	1.66	1.63	0.71
95%		–	48.65	45.09	32.45	–	–	–	–	–	–	49.22	25.70	49.04	48.48	48.81	48.82	48.88	57.65
$p(f<B)$	-	1.00	0.99	1.00	1.00	1.00	1.00	1.00	1.00	1.00	1.00	1.00	1.00	0.20	1.00	0.99	0.99	0.94	0.91
FS_{rot}	-	1.31	1.30	1.31	1.31	1.32	1.31	1.32	1.31	1.31	1.31	1.31	1.31	1.84	0.92	1.34	1.27	1.30	1.28
5%		–	1.09	–	–	1.18	1.27	1.14	1.29	1.31	1.28	1.12	1.15	1.54	0.77	1.12	1.07	0.98	0.93
95%		–	1.52	–	1.44	1.44	1.34	1.48	1.33	1.32	1.34	1.50	1.46	2.16	1.08	1.58	1.49	1.61	1.67
$p(\alpha<\Phi')$	-	0.00	0.13	0.09	0.01	0.00	0.00	0.00	0.00	0.00	0.00	0.13	0.01	0.25	0.05	0.14	0.12	0.13	0.25
FS_{slide}	-	0.19	0.23	0.05	0.12	0.19	0.19	0.19	0.19	0.19	0.19	0.22	0.04	0.30	0.19	0.23	0.23	0.15	0.33
5%		–	0.04	0.03	0.04	0.17	–	0.18	0.18	0.18	0.18	0.04	0.02	0.06	0.03	0.04	0.04	0.04	0.05
95%		–	1.28	1.19	0.86	0.20	–	0.19	0.19	0.19	0.19	1.30	0.68	1.70	1.01	1.33	1.27	1.30	1.53

6 Analysis

Model 1 showed that the parameter used in the analysis of the arch stability that influenced the uncertainty in the arch height the most is the horizontal stress, see Table 6.1. It is also the parameter that has the biggest influence on the angle, of the arch, at the support. Both the influence on the arch height and the angle of the pressure line is much larger for the horizontal stress than any other input parameter. For the uncertainties in the factor of safety against rotation the horizontal stress also has a major role, but when the rock cover is as low as it is in these calculations the uncertainties in the measurements of this has an even bigger influence on the uncertainty. Variations in the rock cover has a minor role when it comes to the load on the tunnel roof, but it creates large variations in the rock mass where it is possible for the arch to form. Only two parameters affect the equivalent friction angle, friction angle and fracture dip. Of these, it is the friction angle that influences the uncertainty most. The uncertainty in safety factor against sliding is mainly decided by the friction angle and fracture dip and their uncertainties. Therefore it is important to continuously update the distribution for the friction angle and fracture dip during the construction process.

Table 6.1 Matrix showing a ranking of how much the uncertainties in the input parameters influence the uncertainty in the different output parameters; 1 = most influencial, 6 = least influencial, - = no influence

	Input parameter							
Output parameter	ϕ	φ	σ_h	L	D_{rock}	D_{soil}	ρ	γ
f	-	-	1	2	4	4	5	3
α	-	-	1	-	3	4	5	2
Φ'	1	2	-	-	-	-	-	-
FS_{rot}	-	-	2	3	1	5	6	4
FS_{slide}	1	2	3	-	4	4	4	4

Model 2 showed what happened with the arch height and the safety factors against rotation and sliding when modifications were made to the horizontal stress. It showed that the shape of the distribution for the arch height had less importance than the estimation of the most probable value. When the rock cover is low, the horizontal stress also is low and a change in most probable value of 0.5 MPa will give a big change in all three observed values. Both equations proposed by Stephansson (1993) suggest that different horizontal stresses should be used compared to the one proposed by SKB (2009). One would lead to an almost doubled horizontal stress, the other to a greatly lowered horizontal stress. This is interesting since the equation proposed by Stephansson is used as an estimate if no other values for the horizontal stress can be used. The horizontal stress is difficult to observe, but during construction new measurements of the stress regime can be done inside the tunnel and this gives a more detailed understanding of the local stress regime.

7 Discussion

The performed analyses on tunnels with low rock cover shows that using a probabilistic approach with account for uncertainties in the different parameters gives insight to the risk of collapse. In some cases this can be used to lower the rock cover or the amount of reinforcement, in others to increase them instead.

The results that have been found show that it is important to have a good estimation of the horizontal stress regime where the tunnel is going to be constructed. It also highlights that the simplification of the Scandinavian stress regime is not valid for parts of Sweden. By increasing the knowledge about the local stress regime it is possible to lower the safety margin without increasing the risk of failure. This result that tunnels can be constructed closer to the surface, and for train tunnels where the gradient of the track cannot be too steep, this means that the tunnels can be shorter. Shorter tunnels means a decreased cost for the project and the money saved can be used to finance the stress measurements. The knowledge on the location of the pressured arch can be used to change the design of the abutment and roof to reduce the amount of reinforcements needed since a changed design can reduce the risk of falling blocks. Rock bolts can be used to create a pressured arch in the roof that also lowers the risk of falling blocks but this takes time from the excavation process which increases the construction time and increases the construction costs.

To perform a probabilistic analysis of the arch stability little or no extra data needs to be collected, compared with a deterministic analysis. All that is needed is to use the data that is collected for the deterministic calculation and instead of using the calculated mean values all data is put in to a program that can perform Monte-Carlo simulations, e.g. Excel with Crystal Ball.

Further studies are suggested to be undertaken to increase the knowledge about how the friction angle and the fracture dip influence the uncertainty for the safety factor against sliding. It is also recommended to perform more stress measurements to get a better understanding of the local stress regime at low depth.

8 References

Atlas Copco (2012). *Ortdrivningsaggregat.* [Electronic] Ortdrivningsaggregat Boomer XE3 C and XE4 C Available: http://www.atlascopco.se/sesv/products /navigationbyproduct/ProductGroup.aspx?id=1401284 [2012-02-09]

Bagheri, M. (2009). *Model uncertainty of design tools to analyze block stability*. Lic.-thesis. Royal Institute of Technology, KTH. Stockholm: KTH

Banverket (2001). *Utställningen*. [Electronic] Dokument för Varberg dubbelspår (tunnel) inkl resecentrum: Samråd. Borlänge: Banverket. Available: http://www.trafikverket.se/PageFiles/2956/Utst_web.pdf [2011-10-13]

Banverket (2002). *Folder*. [Electronic] Dokument för Varberg dubbelspår (tunnel) inkl resecentrum: Utställelse. Borlänge: Banverket. Available: http://www.trafikverket.se/PageFiles/2956/Folder0204.pdf [2011-12-20]

Berg, S. (2005). *Bergspänningsmätningar på litet djup*. Master thesis. Luleå University of Technology, LTU. Luleå: LTU

Bergström, M. (1998). *Banverket Västra Regionen, PM, VKB Varberg-Hamra Förprojektering*. Göteborg: Petro Bloc AB

Eriksson, M. Nord, G. Stille, H. (2005). *Kompendium i Bergmekanik*. Stockholm: KTH

Hegardt, E. Meland, E. (2011). *Geofysiska undersökningar Gerumsberget*. Göteborg: Bergab

Heidbach, O. Tingay, M. Barth, A. Reinecker, J. Kurfeß, D. Müller, B. (2008). *World Stress Map database release 2008 doi:10.1594/GFZ.WSM.Rel2008.* [Electronic]. Potsdam: German Research Centre for Geosciences. Available: http://www.world-stress-map.org [2011-11-03]

Hoek, E, Brown, E. T. (1994). *Underground Excavations in Rock.* London: Institution of Mining and Metallurgy

Johansson, F. (2005). S*tability analyses of large structures founded on rock – An introductory study*. Lic.-thesis. Royal Institute of Technology, KTH. Stockholm: KTH

Larsson, R. (2008). *Jords egenskaper*. Linköping: SGI

Lindblom, U. (2010). *Bergbyggnad*. Malmö: Liber.

Lindblom, U. Albertsson, A. Sjöholm, A. (1999). *Krav på Injektering vid tunnelbyggande*. Göteborg: Chalmers University of Technology, CTH, Institutionen för geoteknik. (Rapport B 1999:5)

Nelson, M. (1998). *Bergmekanisk dimensionering med statistiska metoder – En förstudie*. Stockholm: Stiftelsen svensk bergteknisk forskning (SveBeFo Rapport, 39)

Nilsen, B. Palmström, A. (2000). *Engineering geology and rock engineering.* Oslo: Norwegian Soil and Rock Engineering Association.

Nordlund, E. Rådberg, G. Sjöberg, J (1998). *Bergmekanikens grunder*. Luleå: Luleå University of Technology, LTU

Oracle (2011). *Crystal Ball User's Guide, 11.1.2* [Electronic]. Oracle. Available: http://docs.oracle.com/cd/E17236_01/epm.1112/cb_user.pdf [2011-11-20]

Palisade (2011). *Monte Carlo Simulation* [Electronic]. Palisade. Available: http://www.palisade.com/risk/monte_carlo_simulation.asp [2011-12-20]

Swedish Nuclear Fuel and Waste Management Co, SKB (2009). *Site engineering report Laxemar - Guidelines for underground design - Step D2*. Stockholm: SKB (R-08-88).

Stephansson, O. (1993). R*ock stress in the Fennoscandian shield. Comprehensive Rock Engineering*, vol. 3, pp 445-459.

Stille, H. (1980). *Valvbildning i sprickigt hårt berg – Del 1: Teori*. Stockholm: Royal Institute of Technology, KTH

Stille, H. (1993) *Undermarksbyggande i svagt berg*. Stockholm: Stiftelsen Bergteknisk forskning

Töyrä, J. (2004). *Stability of shallow seated constructions in hard rock – A pilot study*. Luleå: Luleå University of Technology, LTU

Vägverket (1988). *Handbok i sprängteknik*. Stockholm: Vägverket

Appendix 1. Tunnel profile

Normal section of the tunnel underneath Varberg

Appendix 2. Map over the tunnel

Area of interest

Map over the suggested stretch for the Varberg tunnel, the black box shows the part of the tunnel where the rock cover is low

Appendix 3. Types of buildings above the tunnel

Picture showing the type of housing that exist above the tunnel at the area of interest

Appendix 4. Calculations

Calculations — Input parameters for the different calculations

Parameters (units): φ (degrees), Φ (degrees), σh (Mpa), L (m), Drock (m), Dsoil (m), ρ (kg/m3), γ (kN/m3)

Model	Calc	φ 5%	φ	φ 95%	Φ 5%	Φ	Φ 95%	σh	std	L 5%	L	L 95%	Drock 5%	Drock	Drock 95%	Dsoil 5%	Dsoil	Dsoil 95%	ρ 5%	ρ	ρ 95%	γ 5%	γ	γ 95%
Model 0	0_0	-	33.81	-	-	63.21	-	1+0.022*Drock	-	-	13.7	-	-	3.5	-	-	10.0	-	-	2650	-	-	18.5	-
Model 1	1_1	20.55	33.81	71.72	19.41	63.21	84.70	1+0.022*Drock	0.12*oh	13.4	13.7	14.2	3.0	3.5	4.0	9.5	10.0	10.5	2600	2650	2700	17.0	18.5	20.0
Model 1	1_2	20.55	33.81	71.72	-	63.21	-	1+0.022*Drock	-	-	13.7	-	-	3.5	-	-	10.0	-	-	2650	-	-	18.5	-
Model 1	1_3	-	33.81	-	19.41	63.21	84.70	1+0.022*Drock	-	-	13.7	-	-	3.5	-	-	10.0	-	-	2650	-	-	18.5	-
Model 1	1_4	-	33.81	-	-	63.21	-	1+0.022*Drock	0.12*oh	-	13.7	-	-	3.5	-	-	10.0	-	-	2650	-	-	18.5	-
Model 1	1_5	-	33.81	-	-	63.21	-	1+0.022*Drock	-	13.4	13.7	14.2	-	3.5	-	-	10.0	-	-	2650	-	-	18.5	-
Model 1	1_6	-	33.81	-	-	63.21	-	1+0.022*Drock	-	-	13.7	-	3.0	3.5	4.0	-	10.0	-	-	2650	-	-	18.5	-
Model 1	1_7	-	33.81	-	-	63.21	-	1+0.022*Drock	-	-	13.7	-	-	3.5	-	9.5	10.0	10.5	-	2650	-	-	18.5	-
Model 1	1_8	-	33.81	-	-	63.21	-	1+0.022*Drock	-	-	13.7	-	-	3.5	-	-	10.0	-	2600	2650	2700	-	18.5	-
Model 1	1_9	-	33.81	-	-	63.21	-	1+0.022*Drock	-	-	13.7	-	-	3.5	-	-	10.0	-	-	2650	-	17.0	18.5	20.0
Model 2	2_1	20.55	33.81	71.72	19.41	63.21	84.70	1+0.022*Drock	0.06*oh	13.4	13.7	14.2	3.0	3.5	4.0	9.5	10.0	10.5	2600	2650	2700	17.0	18.5	20.0
Model 2	2_2	27.18	33.81	52.77	41.31	63.21	73.95	1+0.022*Drock	0.12*oh	13.55	13.7	13.95	3.25	3.5	3.75	9.75	10.0	10.25	2625	2650	2675	17.75	18.5	19.25
Model 2	2_3	20.55	33.81	71.72	19.41	63.21	84.70	2+0.044*Drock	0.12*oh	13.4	13.7	14.2	3.0	3.5	4.0	9.5	10.0	10.5	2600	2650	2700	17.0	18.5	20.0
Model 2	2_4	20.55	33.81	71.72	19.41	63.21	84.70	0.5+0.011*Drock	0.12*oh	13.4	13.7	14.2	3.0	3.5	4.0	9.5	10.0	10.5	2600	2650	2700	17.0	18.5	20.0
Model 2	2_5	20.55	33.81	71.72	19.41	63.21	84.70	1+0.044*Drock	0.12*oh	13.4	13.7	14.2	3.0	3.5	4.0	9.5	10.0	10.5	2600	2650	2700	17.0	18.5	20.0
Model 2	2_6	20.55	33.81	71.72	19.41	63.21	84.70	1+0.011*Drock	0.12*oh	13.4	13.7	14.2	3.0	3.5	4.0	9.5	10.0	10.5	2600	2650	2700	17.0	18.5	20.0
Model 2	2_7	20.55	33.81	71.72	19.41	63.21	84.70	1+0.022*Drock	0.24*oh	13.4	13.7	14.2	3.0	3.5	4.0	9.5	10.0	10.5	2600	2650	2700	17.0	18.5	20.0
Model 2	2_8	7.29	33.81	90	17.00	63.21	90	1+0.022*Drock	0.12*oh	13.1	13.7	14.7	2.5	3.5	4.5	9.0	10.0	11.0	2550	2650	2750	15.5	18.5	21.5

Input parameters for the different calculations

Model 0/Basic solution

The normal way of calculating the arch stability is a deterministic calculation and does not take the uncertainty of the input data into consideration. Model 0 only contains one calculation and the parameters used have fixed values, see Table 3.1.

Calculation 0_0

This is the basic calculation where none of the input parameters are varying, the reason for this is to see what the arch stability would be if no uncertainties in the input values existed.

Input

$$\varphi = 63.21°$$
$$\phi = 33.81°$$
$$L = 13.7m$$
$$B = 3.5m$$
$$D_{soil} = 10m$$
$$q_{ext} = 50kN/m^2$$
$$\rho = 2650kg/m^3$$
$$\gamma = 18.5kN/m^3$$
$$g = 9.82m/s^2$$

Output

$$f = 2.67m$$
$$\alpha = 37.89°$$
$$\phi' = 7.02°$$
$$p(f < B) = 1.0$$
$$p(\alpha < \phi') = 0.0$$
$$FS_{rot} = 1.31$$
$$FS_{sliding} = 0.19$$

Results Calculation 0_0

The height of the arch is 2.67 m which is 0.83 m less than the rock cover, see Figure 1, this gives a factor of safety against rotating blocks of 1.31. At the supporting points the angle of the arch is 37.89 degrees and compared to the equivalent friction angle this is much more. The factor of safety against sliding is 0.19, this result in that failure due to slip in joints is expected
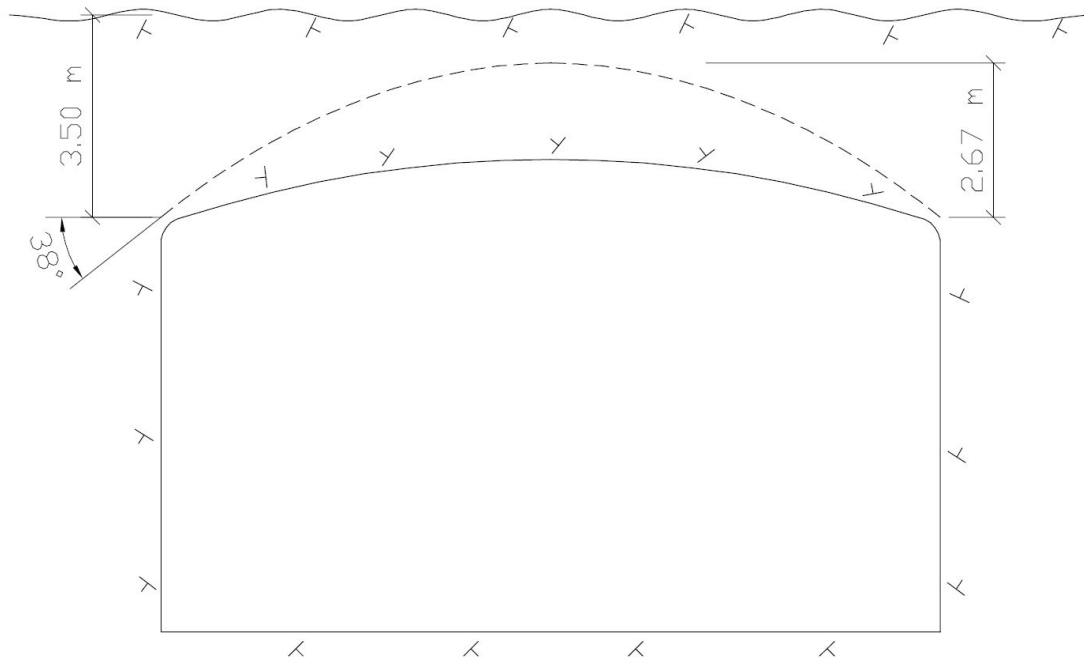
Figure 1 The pressured arch inside the rock mass.

Model 0 results

The rock cover is sufficient enough to be able to form a compressed arch within it. Problems will occur due to sliding blocks since the equivalent friction angle is much lower than the angle of the pressure line at the support points.

Analysis Model 0

The results from Calculation 0_0 show that the height of the arch is around 0.8 m lower than the rock cover. This is sufficient even if the rock cover, due to the uncertainties in the estimation of the position of the rock surface, would be 0.5 m lower. The results do also show that measurements need to be taken to prevent slip in joints, this is due to the fact that the equivalent friction angle is much lower than the angle of the arch at the supporting points.

Model 1/Parameter study

Model 1 is used to see which parameter with its uncertainty that has most influence on the uncertainties in the result. The uncertainties are the ones listed in chapter 3.3. The input parameters are described with their most probable value, 5 % and 95 % or the mean value and the standard deviation. For the output parameters f, α, FS_{rot} and FS_{slide} are given as the most probable value with its 5 % and 95 %, if they have any distribution, otherwise they are just given as mean values, and $p(f < B)$ and $p(\alpha < \phi')$ are given as mean values. The study is made by first including all uncertainty in the parameters, Calculation 1_1, and then study the influence of each parameter respectively, Calculation 1_2 to 1_9. By comparing these it will be shown which parameter that have the greatest influence on the overall uncertainty.

Calculation 1_1

In this calculation every parameter is varying according to chapter 3.3, see Figure 3-9 to Figure 3-8. This gives a value on how much all input uncertainties affect the uncertainty in the result.

Input

$\varphi = 63.21°$

$\varphi_{5\%} = 19.41°$

$\varphi_{95\%} = 84.70°$

$\phi = 33.81°$

$\phi_{5\%} = 20.55°$

$\phi_{95\%} = 71.72°$

$L = 13.7m$

$L_{5\%} 13.4m$

$L_{95\%} = 14.2m$

$B = 3.5m$

$B_{5\%} = 3.0m$

$B_{95\%} = 4.0m$

$g = 9.82m/s^2$

$D_{soil} = 10m$

$D_{soil,5\%} = 9.5m$

$D_{soil,95\%} = 10.5m$

$q_{ext} = 50kN/m^2$

$\rho = 2650kg/m^3$

$\rho_{5\%} = 2600kg/m^3$

$\rho_{95\%} = 2700kg/m^3$

$\gamma = 18.5kN/m^3$

$\gamma_{5\%} = 17.0kN/m^3$

$\gamma_{95\%} = 20.0kN/m^3$

$\sigma_h = 1 + 0.022B$

$\sigma_{h,std} = 0.12 \cdot \sigma_h$

Output

$f = 2.65m$

$f_{5\%} = 2.42m$

$f_{95\%} = 3.01m$

$\alpha = 37.69°$

$\alpha_{5\%} = 35.27°$

$\alpha_{95\%} = 41.08°$

$\phi' = 8.83°$

$\phi'_{5\%} = 1.65°$

$\phi'_{95\%} = 48.65°$

$p(f < B) = 0.99$

$p(\alpha < \phi') = 0.13$

$FS_{rot} = 1.30$

$FS_{rot,5\%} = 1.09$

$FS_{rot,95\%} = 1.52$

$FS_{slide} = 0.23$

$FS_{slide,5\%} = 0.04$

$FS_{slide,95\%} = 1.28$

Results Calculation 1_1

Calculation 1_1 shows that the most probable value for the arch height is 2.65 m. This is 0.02 m less than in Calculation 0_0. The 5-percentile is 2.42 m and the 95-percentile is 3.01 m, see Figure 2. For the angle of the pressure line the most probable value is 37.69 degrees, which is 0.20 degrees less than in Calculation 0_0. The 5-percentile is 35.27 degrees and the 95-percentile is 41.08 degrees, see Figure 3. Most probable equivalent friction angle is 8.83 degrees, which is 1.81 degrees more than in Calculation 0_0. The 5-percentile is 1.65 degrees and the 95-percentile is 48.65 degrees, Figure 4. The probability that the arch height is less than the bedding plane is 0.99, which is 0.01 less than in Calculation 0_0. Most probable value for the factor of safety against rotation is 1.30, which is 0.01 less than Calculation 0_0. The 5-percentile is 1.09 and the 95-percentile is 1.52, see Figure 5. The probability that the angle of the pressure line is lower than the equivalent friction angle is 0.13, which is 0.13 more than in Calculation 0_0. Most probable value for the factor of safety against sliding is 0.23, which is 0.04 more than Calculation 0_0. The 5-percentile is 0.04 and the 95-percentile is 1.28, see Figure 6.
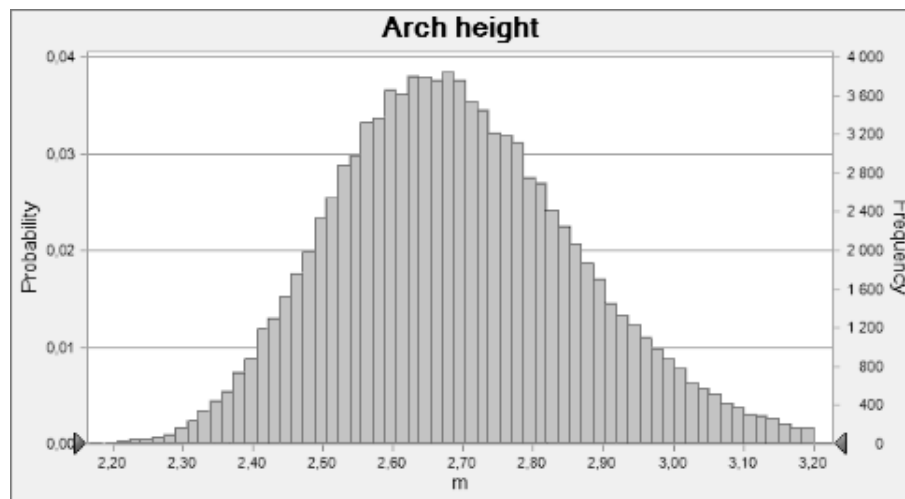
Figure 2 Arch height distribution in Calculation 1_1 [m]
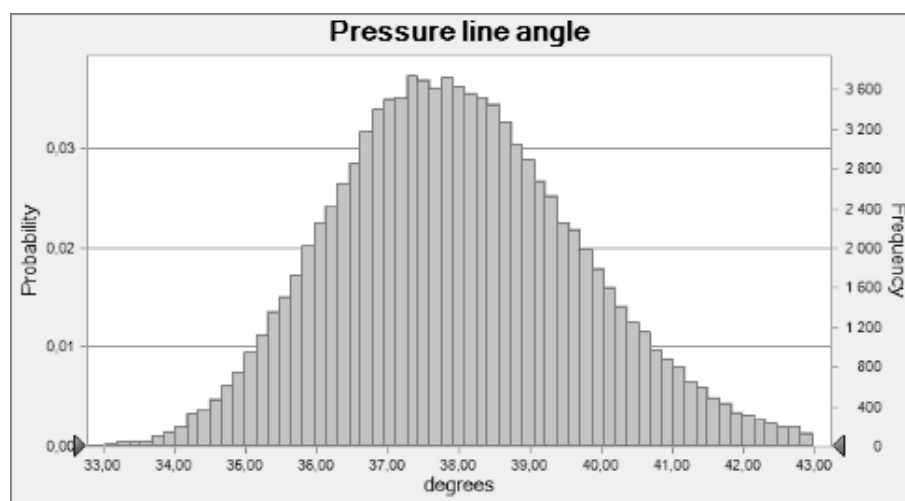
Figure 3 Pressure line angle distribution in Calculation 1_1 [degrees]
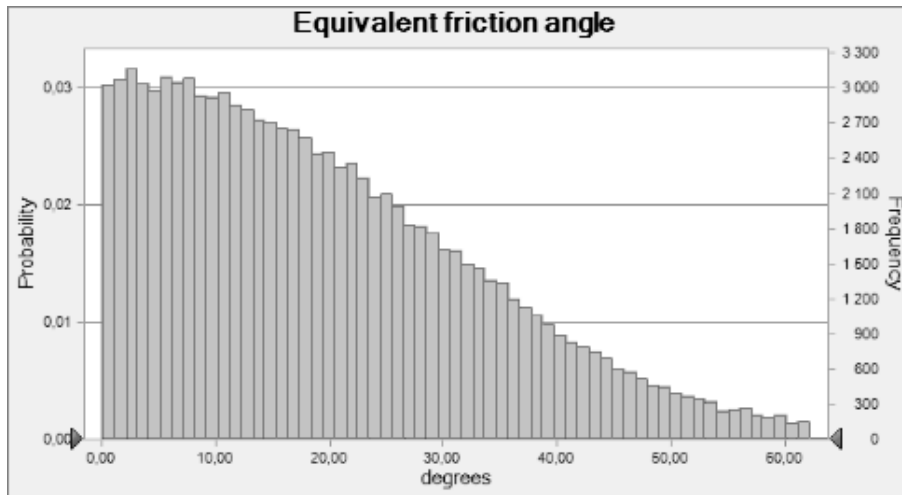
Figure 4 Equivalent friction angle distribution in Calculation 1_1 [degrees]
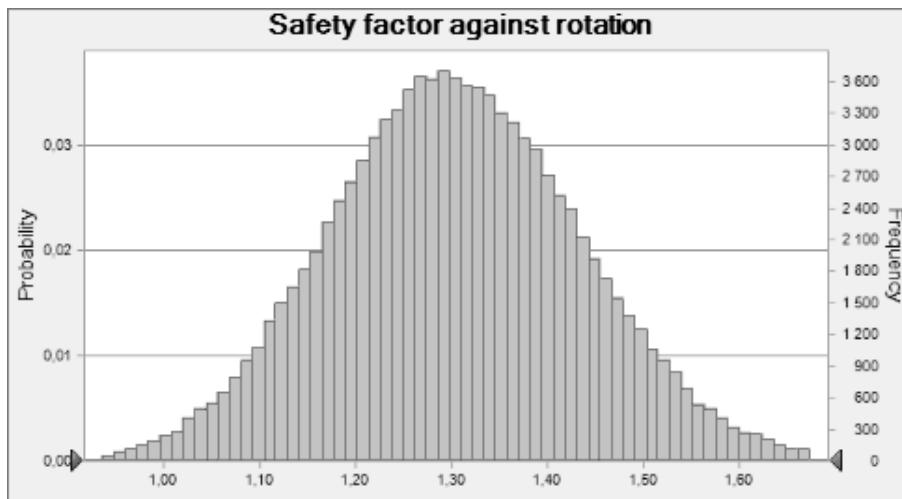
Figure 5 Safety factor against rotation distribution in Calculation 1_1 [-]
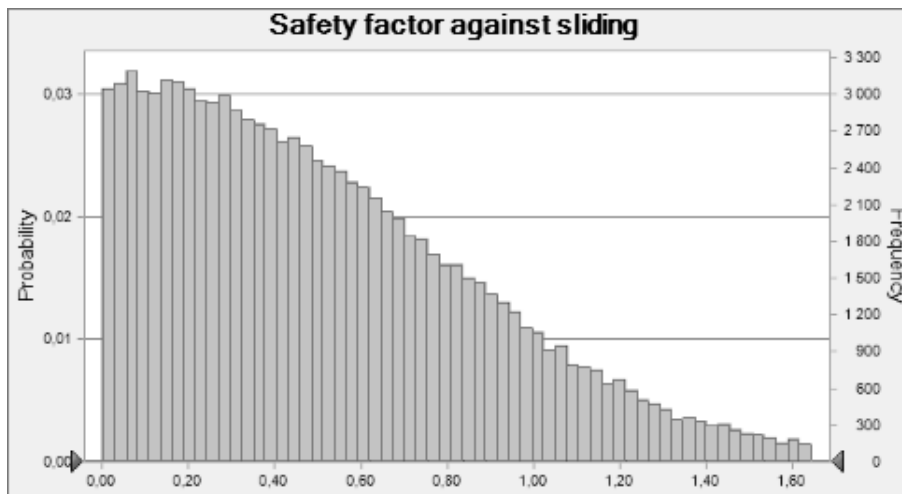
Figure 6 Safety factor against sliding distribution in Calculation 1_1 [-]

Calculation 1_2

In this calculation the friction angle is the only parameter that is varying, see Figure 3-9. The other parameters are the same as the mean value or the most probable value from Calculation 1_1.

Input

$\varphi = 63.21°$

$\phi = 33.81°$

$\phi_{5\%} = 20.55°$

$\phi_{95\%} = 71.72°$

$L = 13.7m$

$B = 3.5m$

$g = 9.82m/s^2$

$D_{soil} = 10m$

$q_{ext} = 50kN/m^2$

$\rho = 2650kg/m^3$

$\gamma = 18.5kN/m^3$

$\sigma_h = 1 + 0.022B$

Output

$f = 2.67m$

$\alpha = 37.89°$

$\phi' = 1.91°$

$\phi'_{5\%} = 1.01°$

$\phi'_{95\%} = 45.09°$

$p(f < B) = 1.0$

$p(\alpha < \phi') = 0.09$

$FS_{rot} = 1.31$

$FS_{slide} = 0.05$

$FS_{slide,5\%} = 0.03$

$FS_{slide,95\%} = 1.19$

Results Calculation 1_2

Calculation 1_2 shows that the most probable value for the arch height is 2.67 m. This is 0.02 m more than in Calculation 1_1, see Figure 7. For the angle of the pressure line the most probable value is 37.89 degrees, which is 0.20 degrees more than in Calculation 1_1, see Figure 8. Most probable equivalent friction angle is 1.91 degrees, which is 6.92 degrees less than in Calculation 1_1. The 5-percentile decreases with 0.64 degrees to 1.01 degrees and the 95-percentile decreases with 3.56 degrees to 45.09 degrees, see Figure 9. The probability that the arch height is less than the bedding plane is 1.0, which is 0.01 more than in Calculation 1_1. Most probable value for the factor of safety against rotation is 1.31, which is 0.01 more than in Calculation 1_1, see Figure 10. The probability that the angle of the pressure line is lower than the equivalent friction angle is 0.09, which is 0.04 less than in Calculation 1_1. Most probable value for the factor of safety against sliding is 0.05,

which is 0.17 less than in Calculation 1_1. The 5-percentile decreases with 0.01 to 0.03 and the 95-percentile decreases with 0.09 to 1.19, see Figure 11.
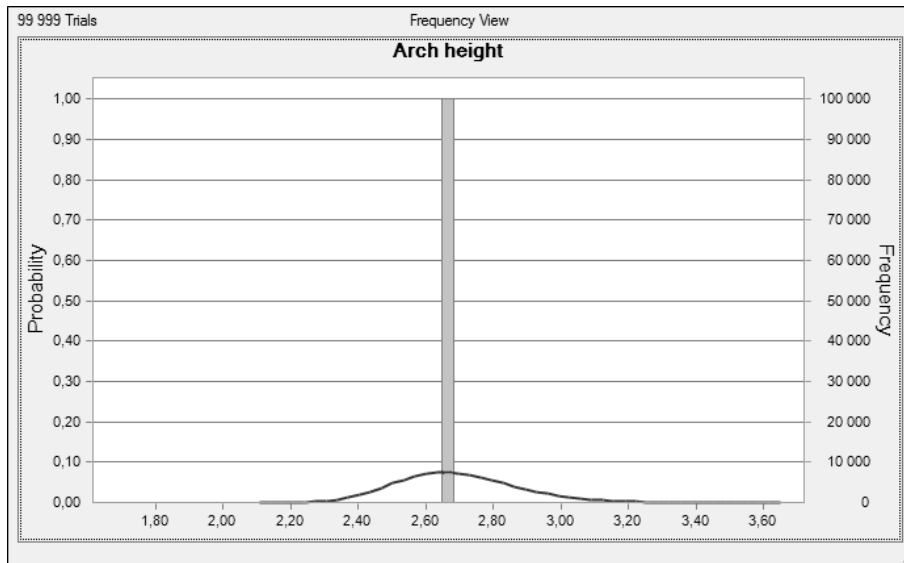
Figure 7 Comparison between the distribution of the arch height in Calculation 1_1, line, and Calculation 1_2, column
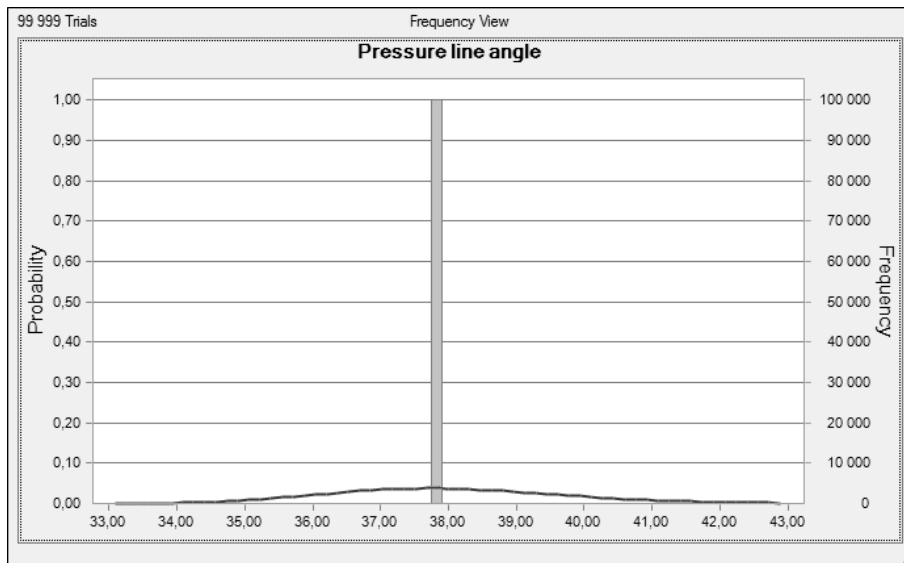
Figure 8 Comparison between the distribution of the pressure line angle in Calculation 1_1, line, and Calculation 1_2, column
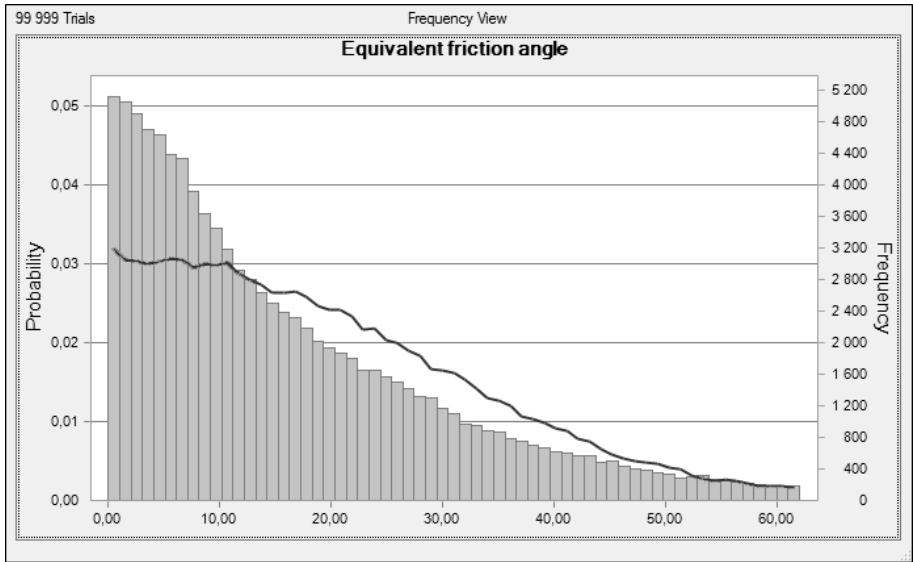
Figure 9 Comparison between the distribution of the equivalent friction angle in Calculation 1_1, line, and Calculation 1_2, column
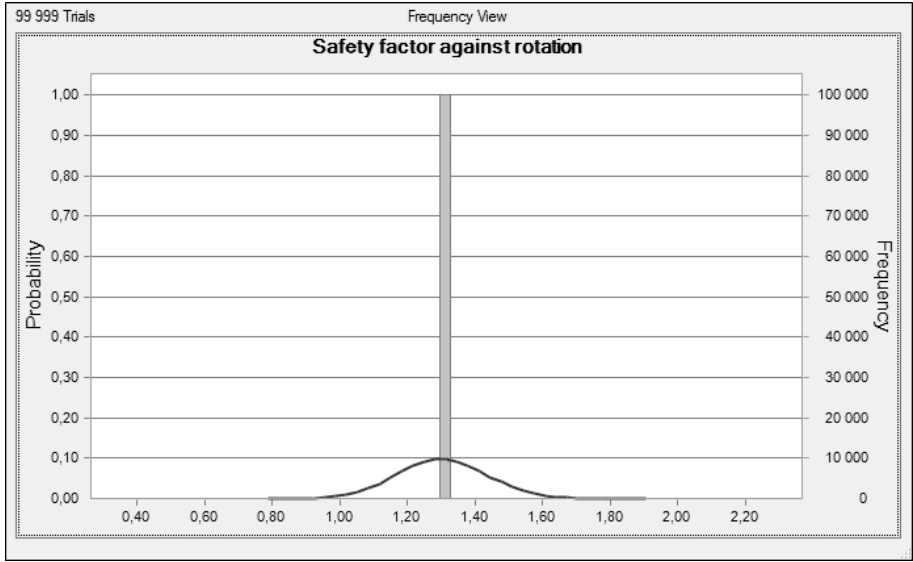
Figure 10 Comparison between the distribution of the safety factor against rotation in Calculation 1_1, line, and Calculation 1_2, column
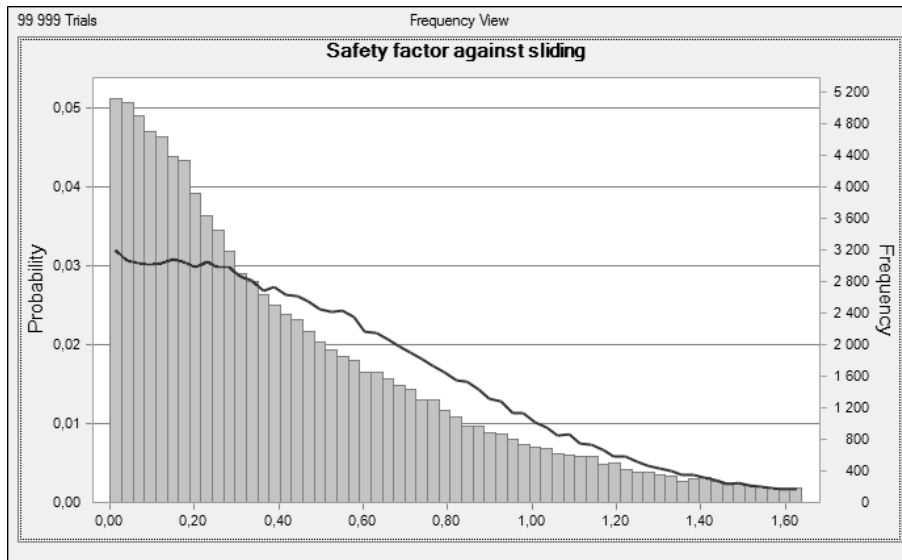
Figure 11 Comparison between the distribution of the safety factor against sliding in Calculation 1_1, line, and Calculation 1_2, column

Calculation 1_3

In this calculation the only parameter that is varying is the fracture dip, see Figure 3-10. The other parameters are the same as the mean value or the most probable value from Calculation 1_1.

Input

$\varphi = 63.21°$

$\varphi_{5\%} = 19.41°$

$\varphi_{95\%} = 84.70°$

$\phi = 33.81°$

$L = 13.7m$

$B = 3.5m$

$g = 9.82m/s^2$

$D_{soil} = 10m$

$q_{ext} = 50kN/m^2$

$\rho = 2650kg/m^3$

$\gamma = 18.5kN/m^3$

$\sigma_h = 1 + 0.022B$

Output

$$f = 2.67m$$

$$\alpha = 37.89°$$

$$\phi' = 4.45°$$

$$\phi'_{5\%} = 1.35°$$

$$\phi'_{95\%} = 32.45°$$

$$p(f < B) = 1.0$$

$$p(\alpha < \phi') = 0.01$$

$$FS_{rot} = 1.31$$

$$FS_{slide} = 0.12$$

$$FS_{slide,5\%} = 0.04$$

$$FS_{slide,95\%} \, 0.86$$

Results Calculation 1_3

Calculation 1_3 shows that the most probable value for the arch height is 2.67 m. This is 0.02 m more than in Calculation 1_1, see Figure 12. For the angle of the pressure line the most probable value is 37.89 degrees, which is 0.20 degrees more than in Calculation 1_1, see Figure 13. Most probable equivalent friction angle is 4.45 degrees, which is 4.38 degrees less than in Calculation 1_1. The 5-percentile decreases with 0.3 degrees to 1.35 degrees and the 95-percentile decreases with 16.2 degrees to 32.45 degrees, see Figure 14. The probability that the arch height is less than the bedding plane is 1.0, which is 0.01 more than in Calculation 1_1. Most probable value for the factor of safety against rotation is 1.31, which is 0.01 more than in Calculation 1_1, see Figure 15. The probability that the angle of the pressure line is lower than the equivalent friction angle is 0.01, which is 0.12 less than in Calculation 1_1. Most probable value for the factor of safety against sliding is 0.12, which is 0.11 less than in Calculation 1_1. The 5-percentile is unchanged at 0.04 and the 95-percentile decreases with 0.42 to 0.86, see Figure 16.
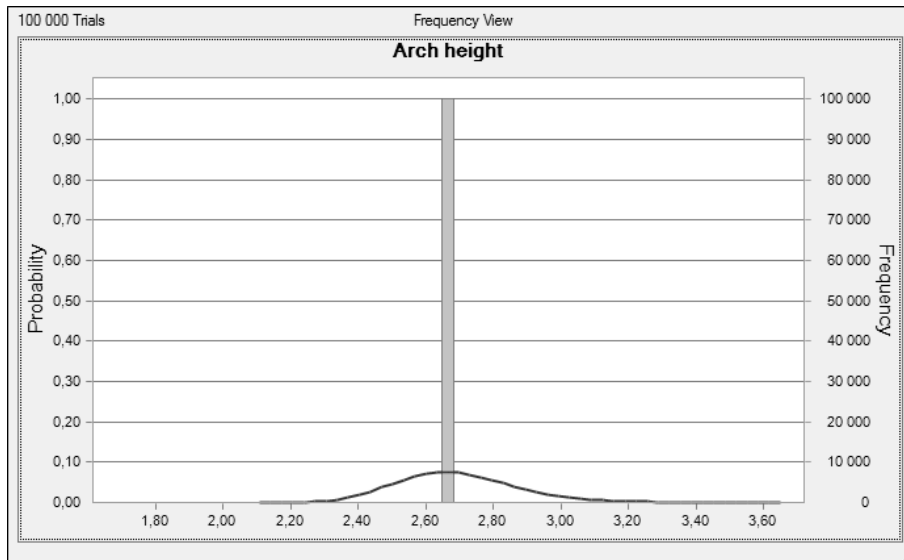
Figure 12 Comparison between the distribution of the arch height in Calculation 1_1, line, and Calculation 1_3, column
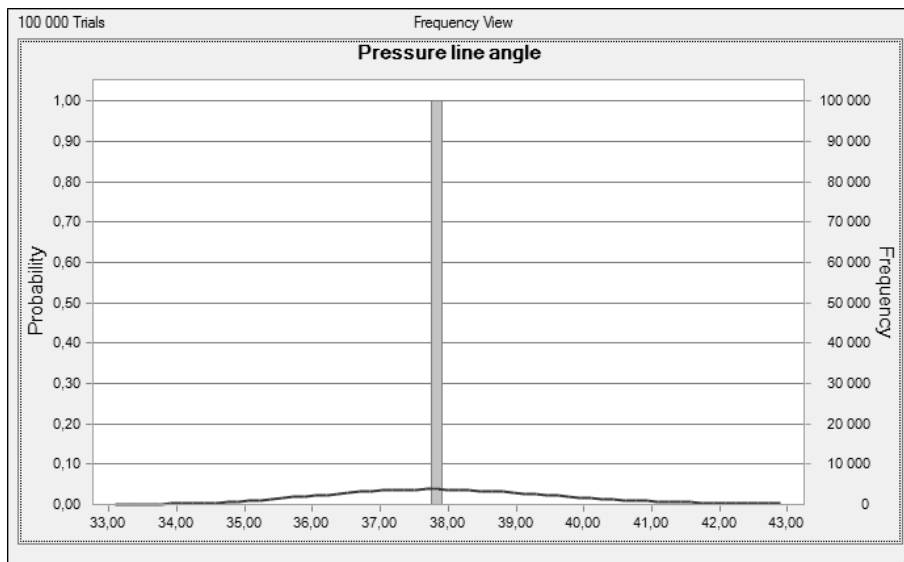
Figure 13 Comparison between the distribution of the pressure line angle in Calculation 1_1, line, and Calculation 1_3, column
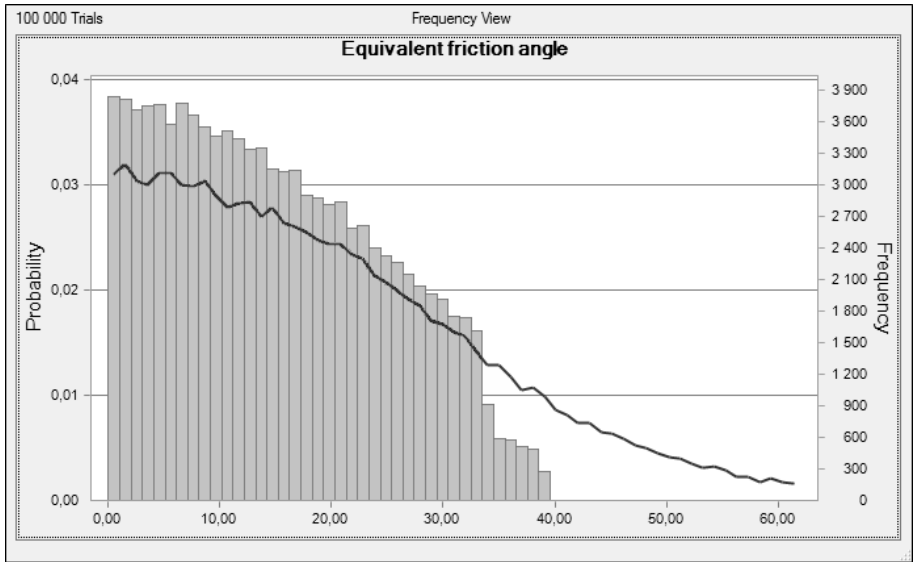
Figure 14 Comparison between the distribution of the equivalent friction angle in Calculation 1_1, line, and Calculation 1_3, column
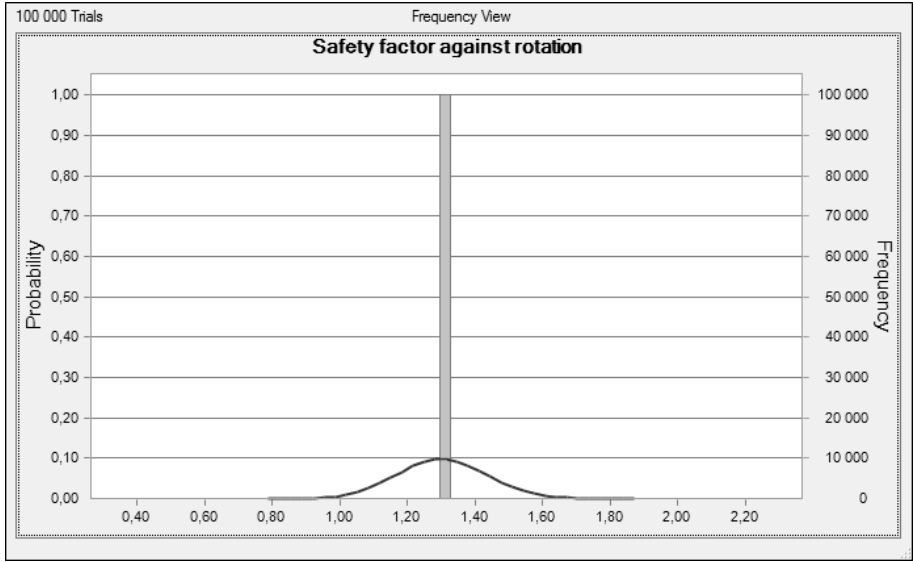
Figure 15 Comparison between the distribution of the safety factor against rotation in Calculation 1_1, line, and Calculation 1_3, column
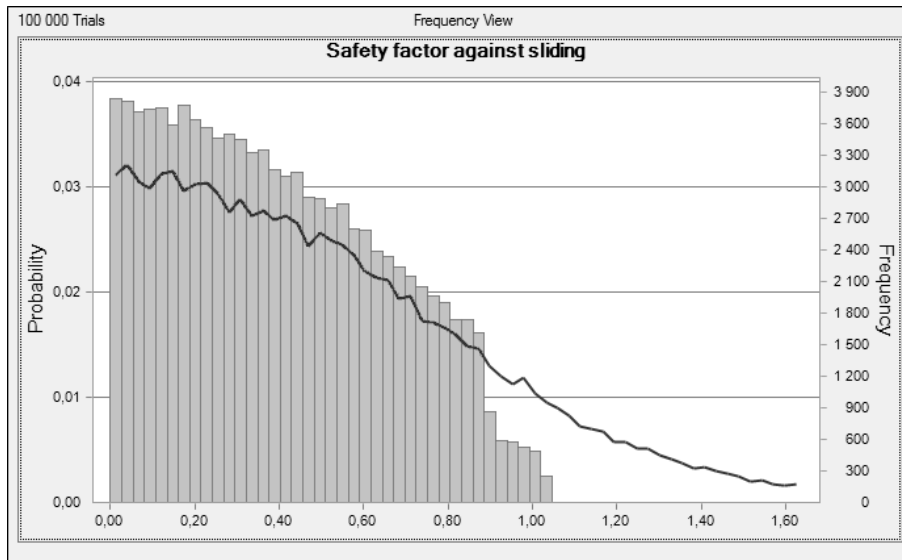
Figure 16 Comparison between the distribution of the safety factor against sliding in Calculation 1_1, line, and Calculation 1_3, column

Calculation 1_4

In this calculation the horizontal stress is the only parameter that is varying, see Figure 3-3. The other parameters are the same as the mean value or the most probable value from Calculation 1_1.

Input

$\varphi = 63.21°$

$\phi = 33.81°$

$L = 13.7m$

$B = 3.5m$

$g = 9.82m/s^2$

$D_{soil} = 10m$

$q_{ext} = 50kN/m^2$

$\rho = 2650kg/m^3$

$\gamma = 18.5kN/m^3$

$\sigma_h = 1 + 0.022B$

$\sigma_{h,std} = 0.12 \cdot \sigma_h$

Output

$$f = 2.64m$$
$$f_{5\%} = 2.44m$$
$$f_{95\%} = 2.98m$$
$$\alpha = 37.65°$$
$$\alpha_{5\%} = 35.42°$$
$$\alpha_{95\%} = 40.98°$$
$$\phi' = 7.01°$$
$$p(f < B) = 1.0$$
$$p(\alpha < \phi') = 0.0$$
$$FS_{rot} = 1.32$$
$$FS_{rot,5\%} = 1.18$$
$$FS_{rot,95\%} = 1.44$$
$$FS_{slide} = 0.19$$
$$FS_{slide,5\%} = 0.17$$
$$FS_{slide,95\%} = 0.20$$

Results Calculation 1_4

Calculation 1_4 shows that the most probable value for the arch height is 2.64 m. This is 0.01 m less than in Calculation 1_1. The 5-percentile increases with 0.02 m to 2.44 m and the 95-percentile decreases with 0.03 m to 2.98 m, see Figure 17. For the angle of the pressure line the most probable value is 37.65 degrees, which is 0.04 degrees less than in Calculation 1_1. The 5-percentile increases with 0.15 degrees to 35.42 degrees and the 95-percentile decreases with 0.10 degrees to 40.98 degrees, see Figure 18. Most probable equivalent friction angle is 7.01 degrees, which is 1.82 degrees less than in Calculation 1_1, see Figure 19. The probability that the arch height is less than the bedding plane is 1.0, which is 0.01 more than in Calculation 1_1. Most probable value for the factor of safety against rotation is 1.32, which is 0.02 more than in Calculation 1_1. The 5-percentile increases with 0.09 to 1.18 and the 95-percentile decreases with 0.08 to 1.44, see Figure 20. The probability that the angle of the pressure line is lower than the equivalent friction angle is 0.0, which is 0.13 less than in Calculation 1_1. Most probable value for the factor of safety against sliding is 0.19, which is 0.04 less than in Calculation 1_1. The 5-percentile increases with 0.13 to 0.17 and the 95-percentile decreases with 1.08 to 0.20, see Figure 21.
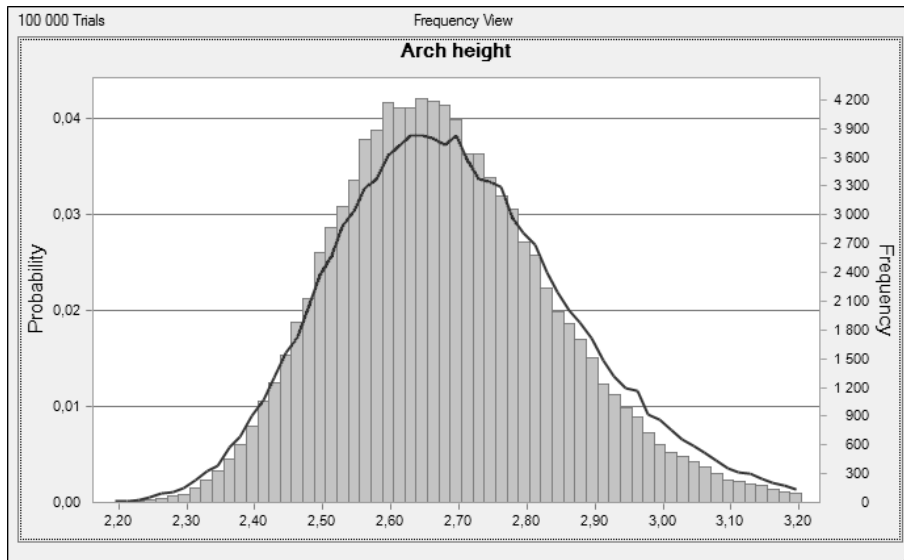
Figure 17 Comparison between the distribution of the arch height in Calculation 1_1, line, and Calculation 1_4, column
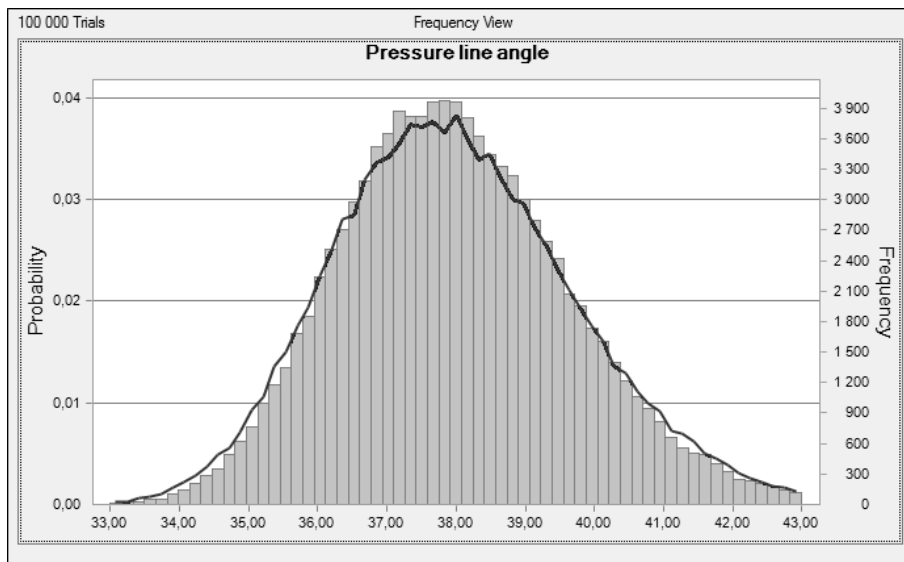
Figure 18 Comparison between the distribution of the pressure line angle in Calculation 1_1, line, and Calculation 1_4, column
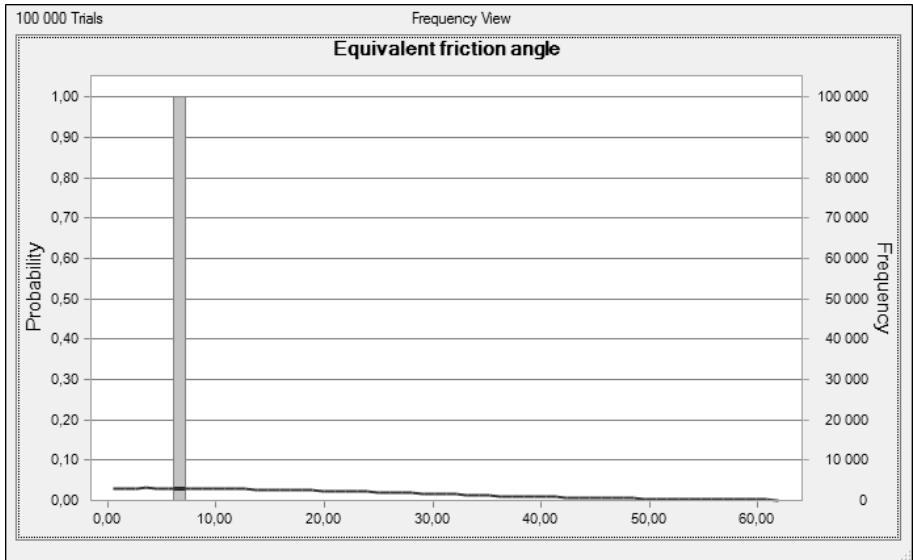
Figure 19 Comparison between the distribution of the equivalent friction angle in Calculation 1_1, line, and Calculation 1_4, column
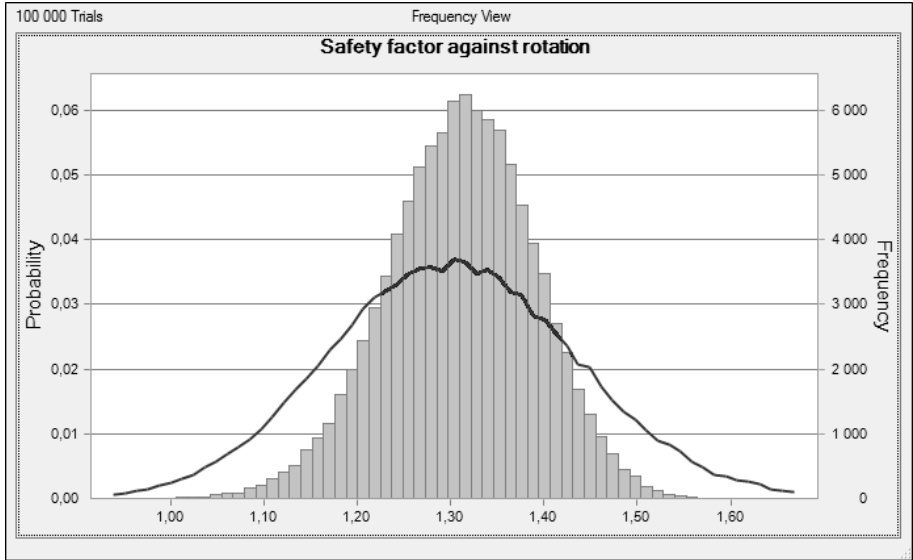
Figure 20 Comparison between the distribution of the safety factor against rotation in Calculation 1_1, line, and Calculation 1_4, column
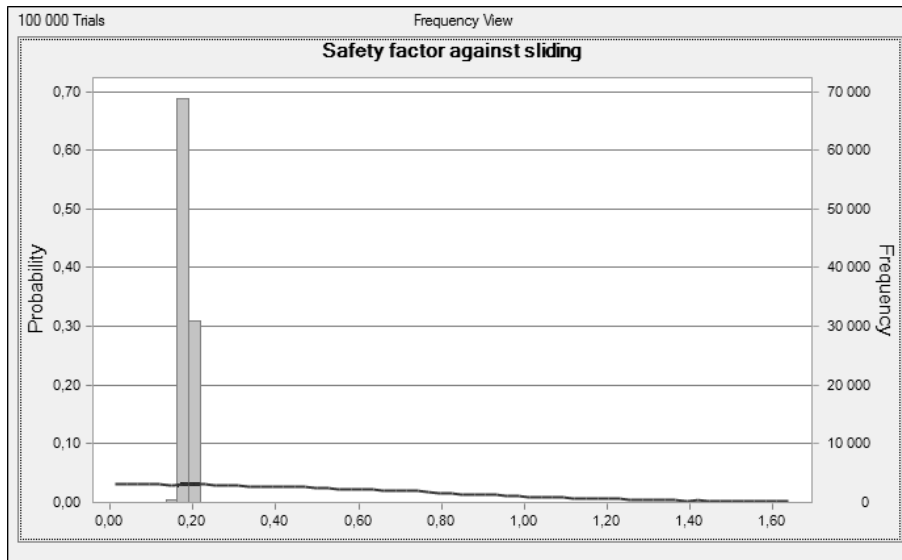
Figure 21 Comparison between the distribution of the safety factor against sliding in Calculation 1_1, line, and Calculation 1_4, column

Calculation 1_5

In this calculation is the tunnel width the only parameter that is varying, see Figure 3-8. The other parameters are the same as the mean value or the most probable value from Calculation 1_1.

Input

$\varphi = 63.21°$

$\phi = 33.81°$

$L = 13.7m$

$L_{5\%} 13.4m$

$L_{95\%} = 14.2m$

$B = 3.5m$

$g = 9.82m/s^2$

$D_{soil} = 10m$

$q_{ext} = 50kN/m^2$

$\rho = 2650kg/m^3$

$\gamma = 18.5kN/m^3$

$\sigma_h = 1 + 0.022B$

Output

$$f = 2.66m$$
$$f_{5\%} = 2.61m$$
$$f_{95\%} = 2.76m$$
$$\alpha = 37.89°$$
$$\phi' = 7.02°$$
$$p(f < B) = 1.0$$
$$p(\alpha < \phi') = 0.0$$
$$FS_{rot} = 1.31$$
$$FS_{rot,5\%} = 1.27$$
$$FS_{rot,95\%} = 1.34$$
$$FS_{slide} = 0.19$$

Results Calculation 1_5

Calculation 1_5 shows that the most probable value for the arch height is 2.66 m. This is 0.01 m more than in Calculation 1_1. The 5-percentile increases with 0.19 m to 2.61 m and the 95-percentile decreases with 0.25 m to 2.76 m, see Figure 22. For the angle of the pressure line the most probable value is 37.89 degrees, which is 0.20 degrees more than in Calculation 1_1, see Figure 23. Most probable equivalent friction angle is 7.02 degrees, which is 1.81 degrees less than in Calculation 1_1, see Figure 24. The probability that the arch height is less than the bedding plane is 1.0, which is 0.01 more than in Calculation 1_1. Most probable value for the factor of safety against rotation is 1.31, which is 0.01 more than in Calculation 1_1. The 5-percentile increases with 0.18 to 1.27 and the 95-percentile decreases with 0.18 to 1.34, see Figure 25. The probability that the angle of the pressure line is lower than the equivalent friction angle is 0.0, which is 0.13 less than in Calculation 1_1. Most probable value for the factor of safety against sliding is 0.19, which is 0.04 less than in Calculation 1_1, see Figure 26.
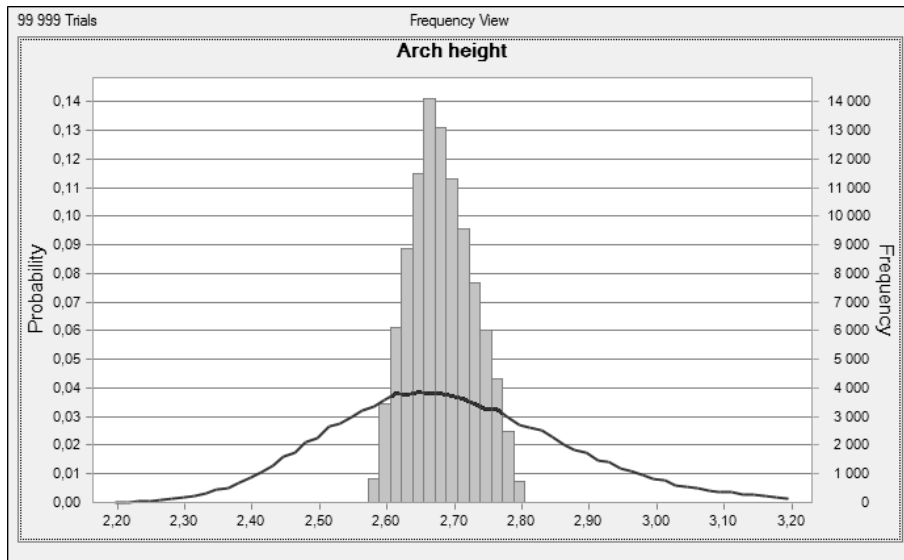
Figure 22 Comparison between the distribution of the arch height in Calculation 1_1, line, and Calculation 1_5, column
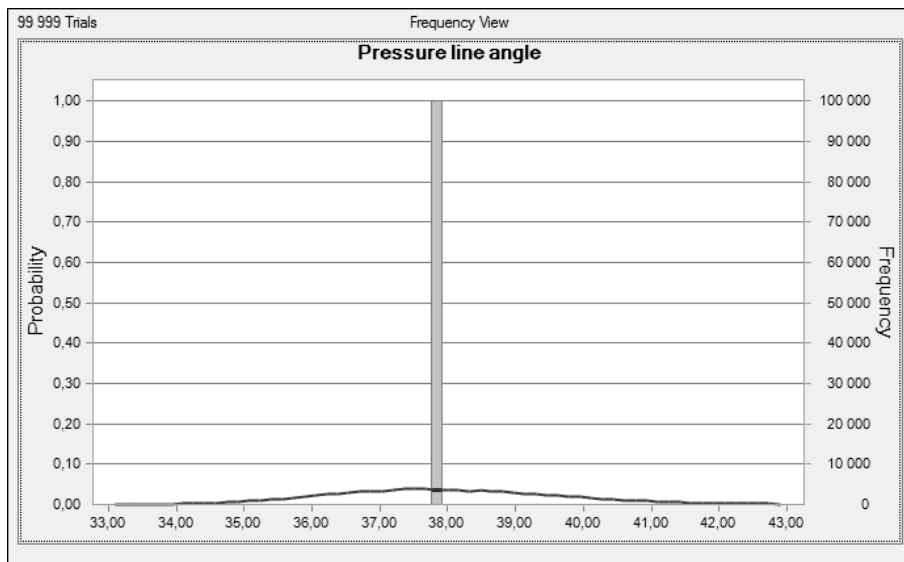
Figure 23 Comparison between the distribution of the pressure line angle in Calculation 1_1, line, and Calculation 1_5, column
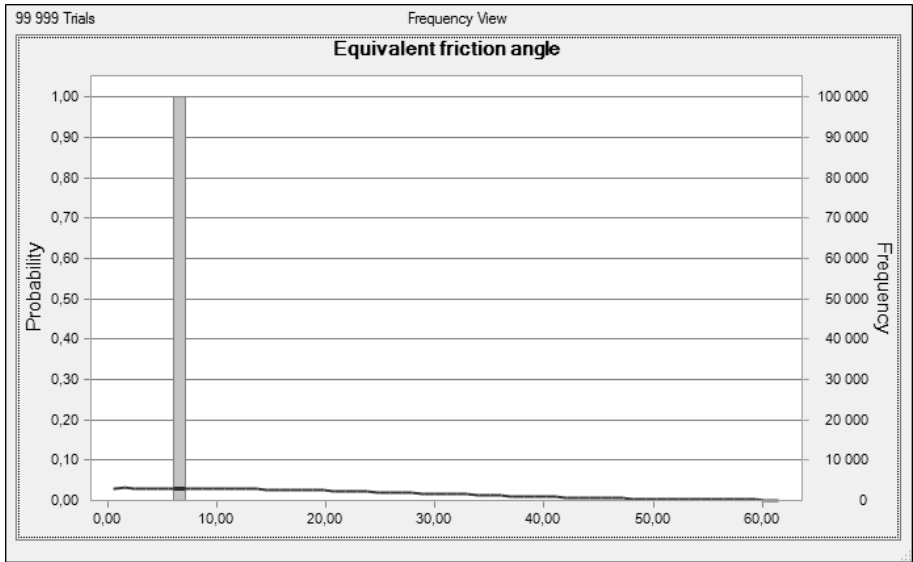
Figure 24 Comparison between the distribution of the equivalent friction angle in Calculation 1_1, line, and Calculation 1_5, column
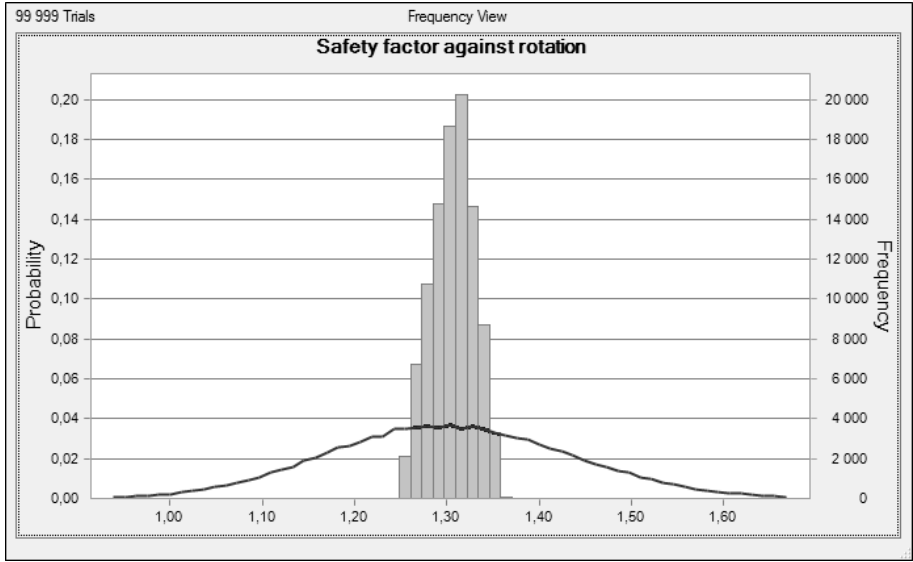
Figure 25 Comparison between the distribution of the safety factor against rotation in Calculation 1_1, line, and Calculation 1_5, column
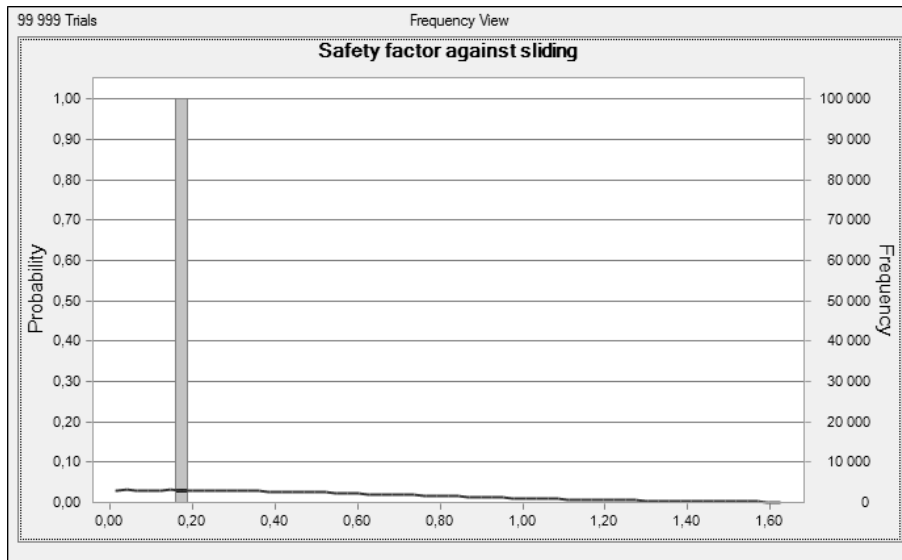
Figure 26 Comparison between the distribution of the safety factor against sliding in Calculation 1_1, line, and Calculation 1_5, column

Calculation 1_6

In this calculation the rock cover is the only parameter that is varying, see Figure 3-6. The other parameters are the same as the mean value or the most probable value from Calculation 1_1.

Input

$\varphi = 63.21°$

$\phi = 33.81°$

$L = 13.7m$

$B = 3.5m$

$B_{5\%} = 3.0m$

$B_{95\%} = 4.0m$

$g = 9.82m/s^2$

$D_{soil} = 10m$

$q_{ext} = 50kN/m^2$

$\rho = 2650kg/m^3$

$\gamma = 18.5kN/m^3$

$\sigma_h = 1 + 0.022B$

Output

$$f = 2.67m$$
$$f_{5\%} = 2.63m$$
$$f_{95\%} = 2.70m$$
$$\alpha = 37.89°$$
$$\alpha_{5\%} = 37.47°$$
$$\alpha_{95\%} = 38.29°$$
$$\phi' = 7.02°$$
$$p(f < B) = 1.0$$
$$p(\alpha < \phi') = 0.0$$
$$FS_{rot} = 1.32$$
$$FS_{rot,5\%} = 1.14$$
$$FS_{rot,95\%} = 1.48$$
$$FS_{slide} = 0.19$$
$$FS_{slide,5\%} = 0.18$$
$$FS_{slide,95\%} = 0.19$$

Results Calculation 1_6

Calculation 1_6 shows that the most probable value for the arch height is 2.67 m. This is 0.02 m more than in Calculation 1_1. The 5-percentile increases with 0.21 m to 2.63 m and the 95-percentile decreases with 0.31 m to 2.70 m, see Figure 27. For the angle of the pressure line the most probable value is 37.89 degrees, which is 0.20 degrees more than in Calculation 1_1. The 5-percentile increases with 2.2 degrees to 37.47 degrees and the 95-percentile decreases with 2.79 degrees to 38.29 degrees, see Figure 28. Most probable equivalent friction angle is 7.02 degrees, which is 1.81 degrees less than in Calculation 1_1, see Figure 29. The probability that the arch height is less than the bedding plane is 1.0, which is 0.01 more than in Calculation 1_1. Most probable value for the factor of safety against rotation is 1.31, which is 0.01 more than in Calculation 1_1. The 5-percentile increases with 0.20 to 1.29 and the 95-percentile decreases with 0.19 to 1.33, see Figure 30. The probability that the angle of the pressure line is lower than the equivalent friction angle is 0.0, which is 0.13 less than in Calculation 1_1. Most probable value for the factor of safety against sliding is 0.19, which is 0.04 less than in Calculation 1_1. The 5-percentile increases with 0.14 to 0.18 and the 95-percentile decreases with 1.09 to 0.19, see Figure 31.
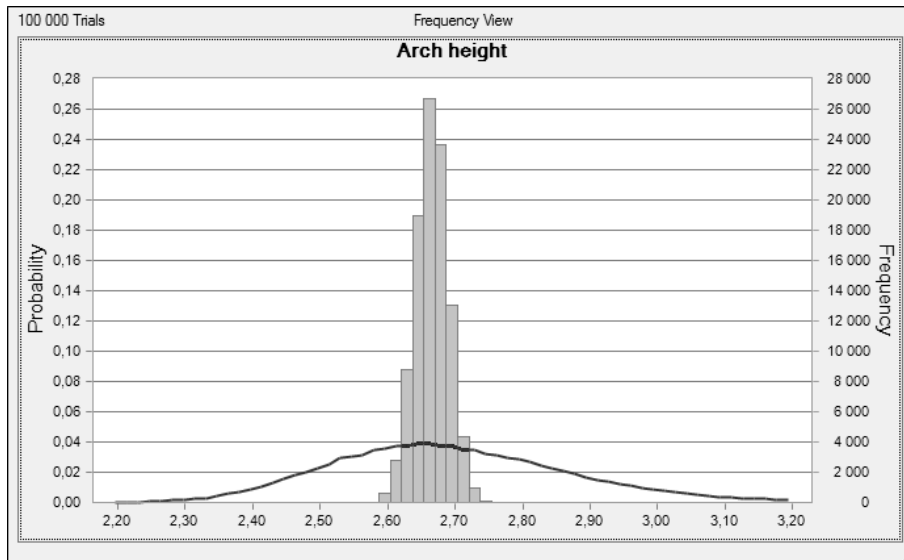
Figure 27 Comparison between the distribution of the arch height in Calculation 1_1, line, and Calculation 1_6, column
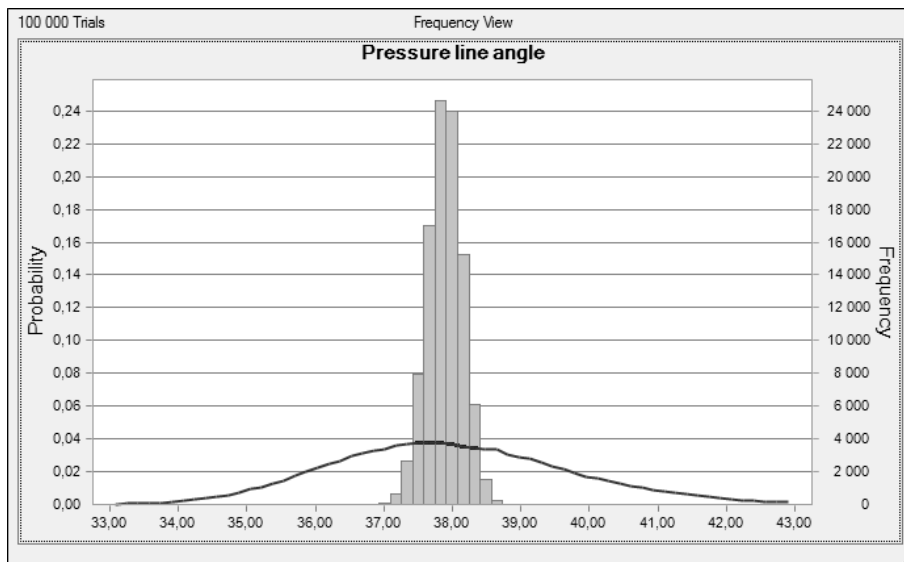
Figure 28 Comparison between the distribution of the pressure line angle in Calculation 1_1, line, and Calculation 1_6, column
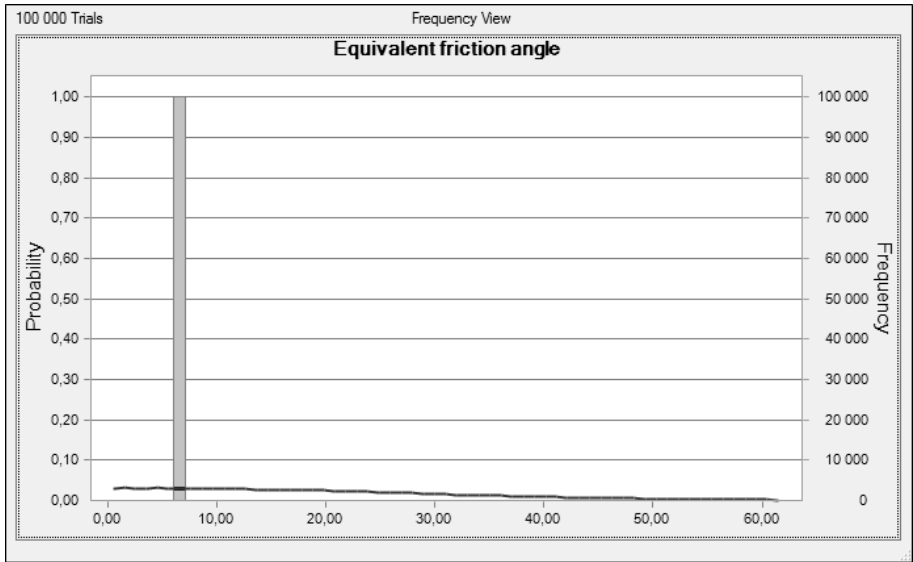
Figure 29 Comparison between the distribution of the equivalent friction angle in Calculation 1_1, line, and Calculation 1_6, column
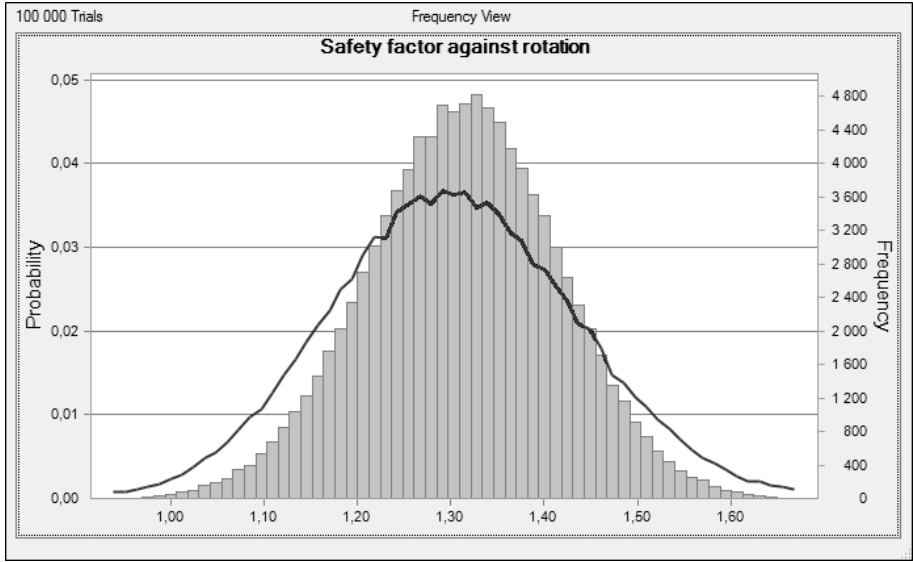
Figure 30 Comparison between the distribution of the safety factor against rotation in Calculation 1_1, line, and Calculation 1_6, column
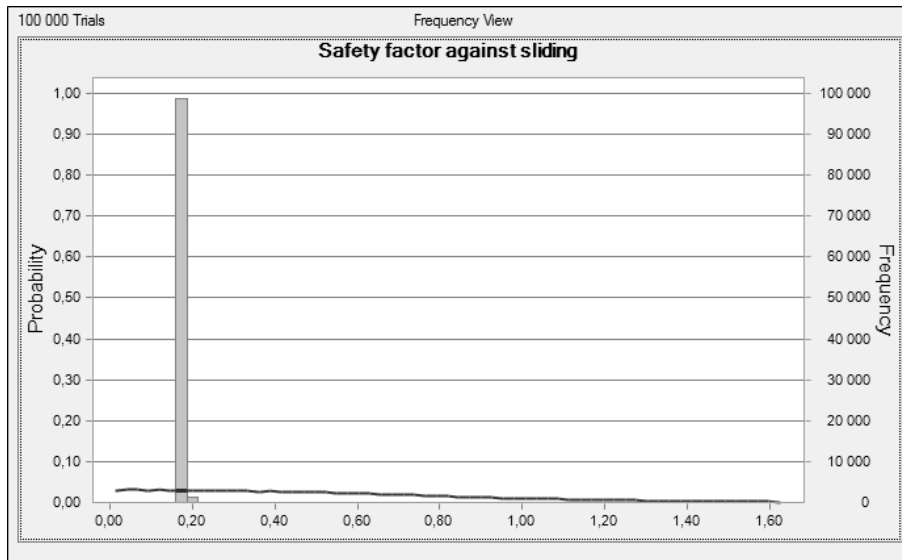
Figure 31 Comparison between the distribution of the safety factor against sliding in Calculation 1_1, line, and Calculation 1_6, column

Calculation 1_7

In this calculation the only parameter that is varying is the soil depth, see Figure 3-7. The other parameters are the same as the mean value or the most probable value from Calculation 1_1.

Input

$$D_{soil} = 10m$$

$$D_{soil,5\%} = 9.5m$$

$$\varphi = 63.21°$$

$$\phi = 33.81°$$

$$D_{soil,95\%} = 10.5m$$

$$L = 13.7m$$

$$q_{ext} = 50kN/m^2$$

$$B = 3.5m$$

$$\rho = 2650kg/m^3$$

$$g = 9.82m/s^2$$

$$\gamma = 18.5kN/m^{3^3}$$

$$\sigma_h = 1 + 0.022B$$

Output

$$f = 2.67m$$
$$f_{5\%} = 2.63m$$
$$f_{95\%} = 2.70m$$
$$\alpha = 37.89°$$
$$\alpha_{5\%} = 37.49°$$
$$\alpha_{95\%} = 38.28°$$
$$\phi' = 7.02°$$
$$p(f < B) = 1.0$$
$$p(\alpha < \phi') = 0.0$$
$$FS = 1.31$$
$$FS_{5\%} = 1.29$$
$$FS_{95\%} = 1.33$$
$$FS_{slide} = 0.19$$
$$FS_{slide,5\%} = 0.18$$
$$FS_{slide,95\%} = 0.19$$

Results Calculation 1_7

Calculation 1_7 shows that the most probable value for the arch height is 2.67 m. This is 0.02 m more than in Calculation 1_1. The 5-percentile increases with 0.21 m to 2.63 m and the 95-percentile decreases with 0.31 m to 2.70 m, see Figure 32. For the angle of the pressure line the most probable value is 37.89 degrees, which is 0.20 degrees more than in Calculation 1_1. The 5-percentile increases with 2.22 degrees to 37.49 degrees and the 95-percentile decreases with 2.80 degrees to 38.28 degrees, see Figure 33. Most probable equivalent friction angle is 7.02 degrees, which is 1.81 degrees less than in Calculation 1_1, see Figure 34. The probability that the arch height is less than the bedding plane is 1.0, which is 0.01 more than in Calculation 1_1. Most probable value for the factor of safety against rotation is 1.31, which is 0.01 more than in Calculation 1_1. The 5-percentile increases with 0.20 to 1.29 and the 95-percentile decreases with 0.19 to 1.33, see Figure 35. The probability that the angle of the pressure line is lower than the equivalent friction angle is 0.0, which is 0.13 less than in Calculation 1_1. Most probable value for the factor of safety against sliding is 0.19, which is 0.04 less than in Calculation 1_1. The 5-percentile increases with 0.14 to 0.18 and the 95-percentile decreases with 1.09 to 0.19, see Figure 36.
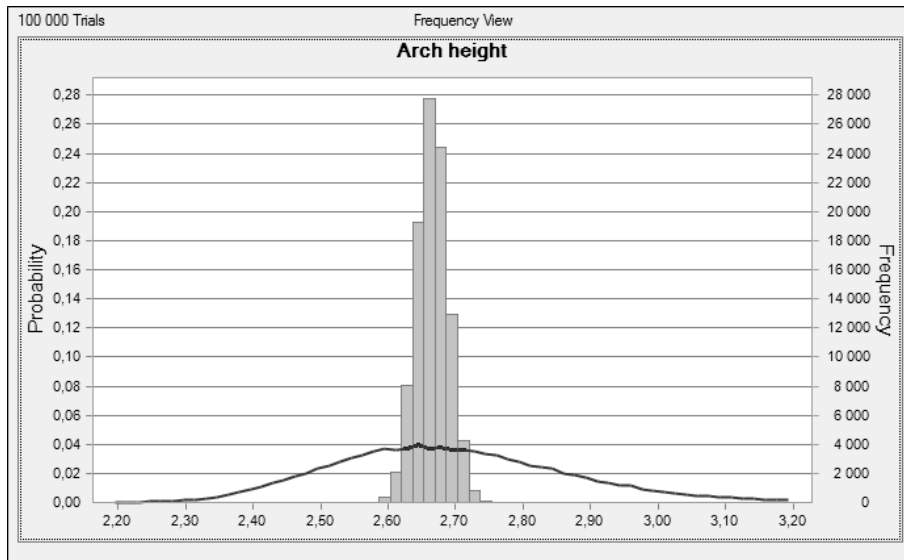
Figure 32 Comparison between the distribution of the arch height in Calculation 1_1, line, and Calculation 1_7, column
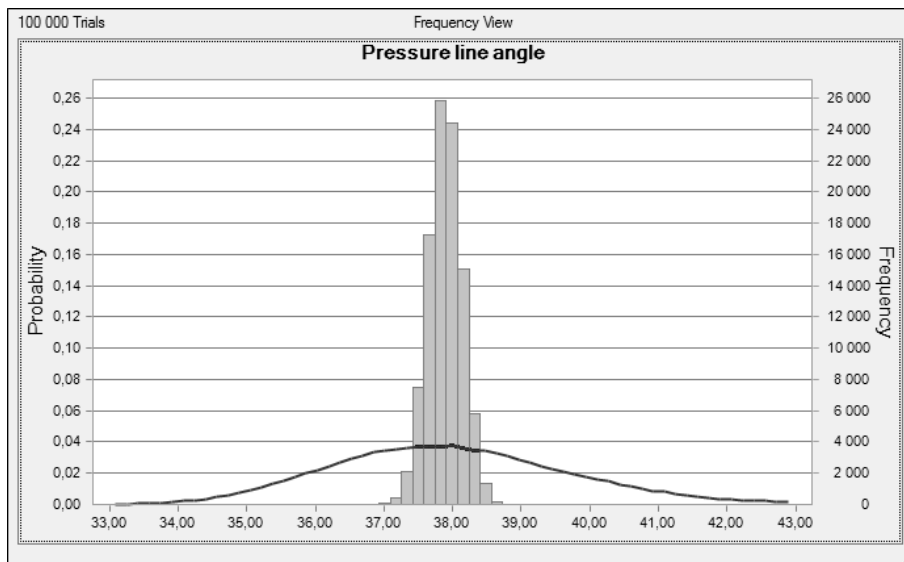
Figure 33 Comparison between the distribution of the pressure line angle in Calculation 1_1, line, and Calculation 1_7, column
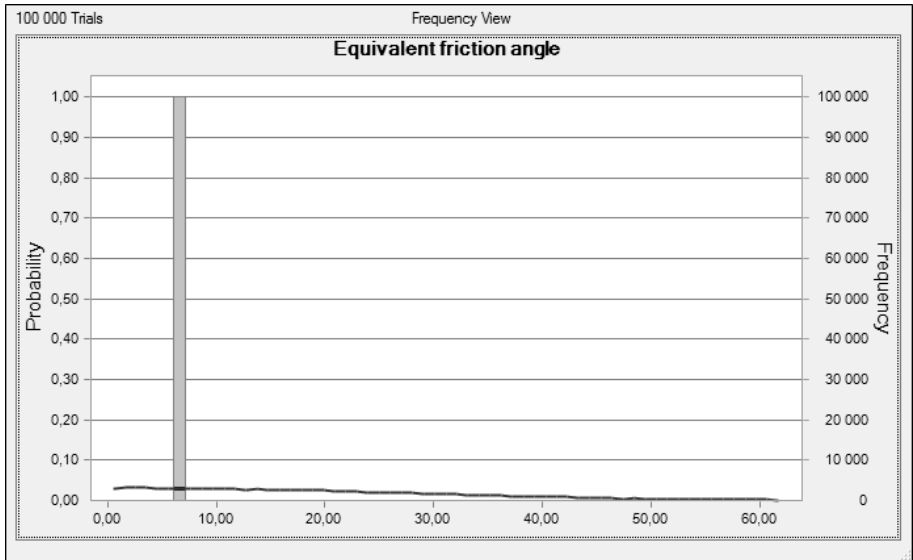
Figure 34 Comparison between the distribution of the equivalent friction angle in Calculation 1_1, line, and Calculation 1_7, column
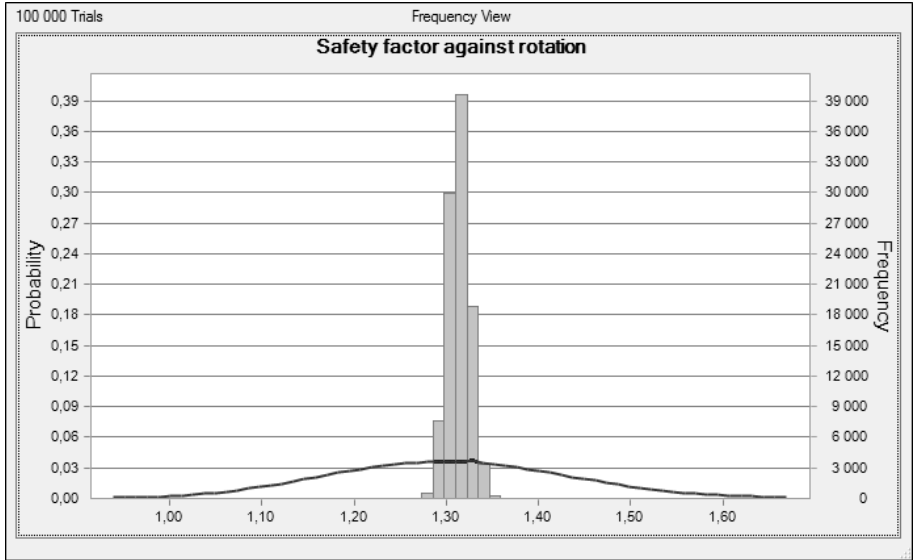
Figure 35 Comparison between the distribution of the safety factor against rotation in Calculation 1_1, line, and Calculation 1_7, column
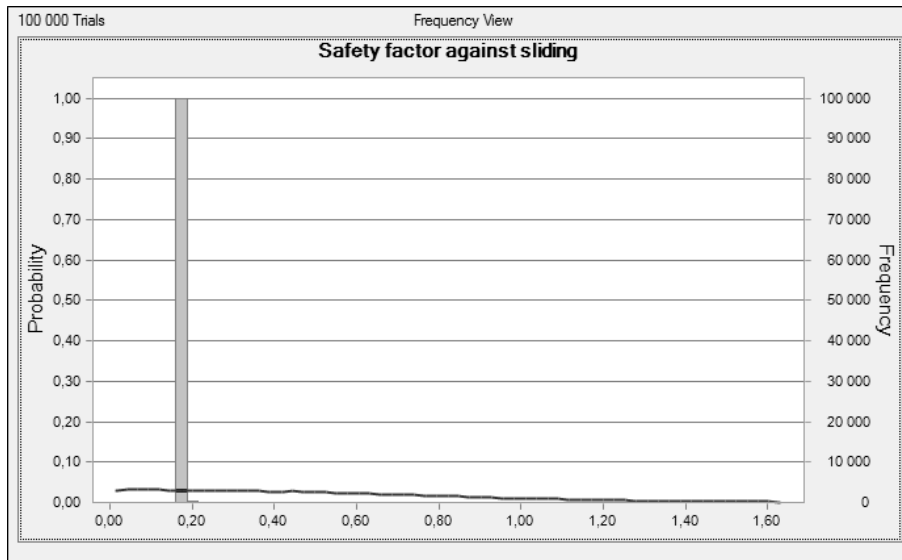
Figure 36 Comparison between the distribution of the safety factor against sliding in Calculation 1_1, line, and Calculation 1_7, column

Calculation 1_8

In this calculation the only parameter that is varying is the density of the rock, see Figure 3-4. The other parameters are the same as the mean value or the most probable value from Calculation 1_1.

Input

$$D_{soil} = 10m$$

$$\varphi = 63.21°$$

$$q_{ext} = 50kN/m^2$$

$$\phi = 33.81°$$

$$\rho = 2650kg/m^3$$

$$L = 13.7m$$

$$\rho_{5\%} = 2600kg/m^3$$

$$B = 3.5m$$

$$\rho_{95\%} = 2700kg/m^3$$

$$g = 9.82m/s^2$$

$$\gamma = 18.5kN/m^{3^3}$$

$$\sigma_h = 1 + 0.022B$$

Output

$f = 2.67m$

$f_{5\%} = 2.66m$

$f_{95\%} = 2.67m$

$\alpha = 37.89°$

$\alpha_{5\%} = 37.82°$

$\alpha_{95\%} = 37.96°$

$\phi' = 7.02°$

$p(f < B) = 1.0$

$p(\alpha < \phi') = 0.0$

$FS_{rot} = 1.31$

$FS_{rot,5\%} = 1.31$

$FS_{rot,95\%} = 1.32$

$FS_{slide} = 0.19$

$FS_{5\%,slide} = 0.18$

$FS_{95\%,slide} = 0.19$

Results Calculation 1_8

Calculation 1_8 shows that the most probable value for the arch height is 2.67 m. This is 0.02 m more than in Calculation 1_1. The 5-percentile increases with 0.24 m to 2.66 m and the 95-percentile decreases with 0.34 m to 2.67 m, see Figure 37. For the angle of the pressure line the most probable value is 37.89 degrees, which is 0.20 degrees more than in Calculation 1_1. The 5-percentile increases with 0.13 degrees to 37.82 degrees and the 95-percentile decreases with 3.12 degrees to 37.96 degrees, see Figure 38. Most probable equivalent friction angle is 7.02 degrees, which is 1.81 degrees less than in Calculation 1_1, see Figure 39. The probability that the arch height is less than the bedding plane is 1.0, which is 0.01 more than in Calculation 1_1. Most probable value for the factor of safety against rotation is 1.31, which is 0.01 more than in Calculation 1_1. The 5-percentile increases with 0.22 to 1.31 and the 95-percentile decreases with 0.20 to 1.32, see Figure 40. The probability that the angle of the pressure line is lower than the equivalent friction angle is 0.0, which is 0.13 less than in Calculation 1_1. Most probable value for the factor of safety against sliding is 0.19, which is 0.04 less than in Calculation 1_1. The 5-percentile increases with 0.14 to 0.18 and the 95-percentile decreases with 1.09 to 0.19, see Figure 41.
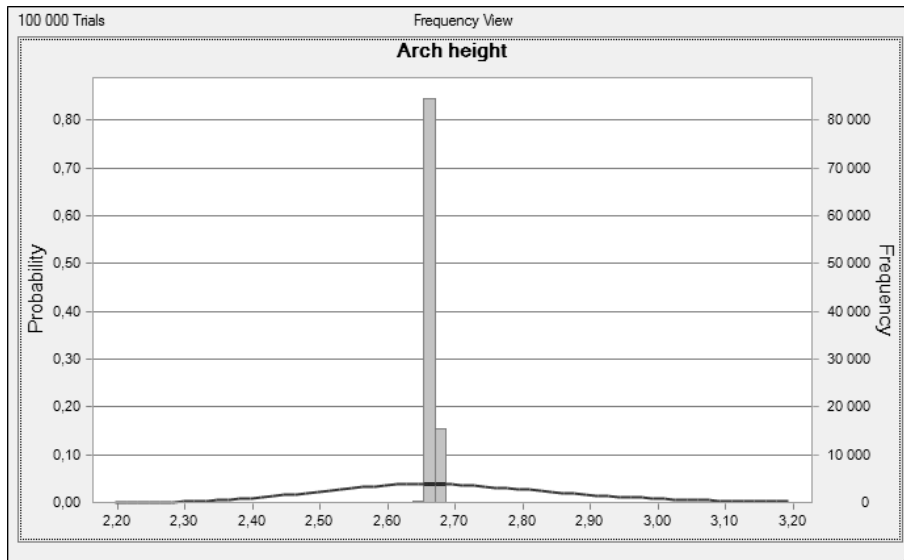
Arch height

Figure 37 **Comparison between the distribution of the arch height in Calculation 1_1, line, and Calculation 1_8, column**

Pressure line angle
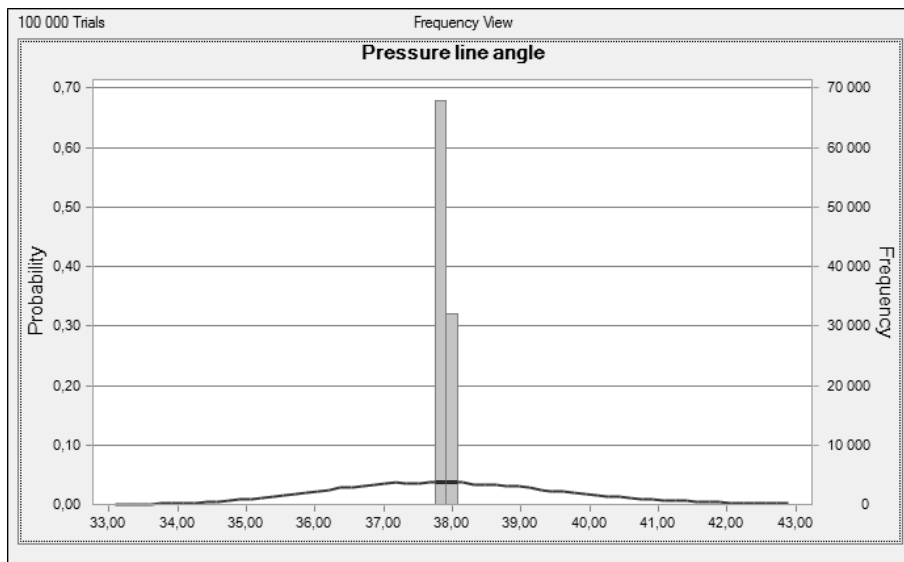
Figure 38 **Comparison between the distribution of the pressure line angle in Calculation 1_1, line, and Calculation 1_8, column**
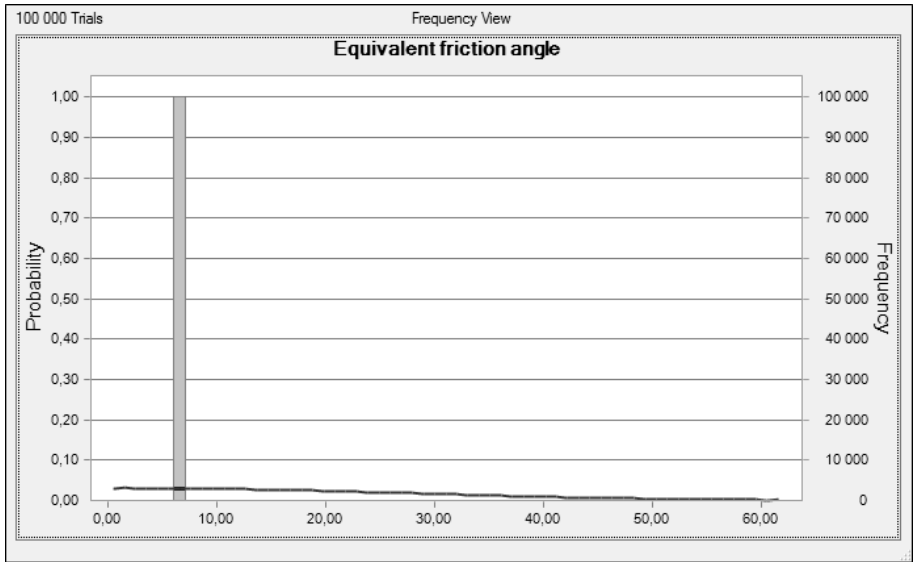
Figure 39 Comparison between the distribution of the equivalent friction angle in Calculation 1_1, line, and Calculation 1_8, column
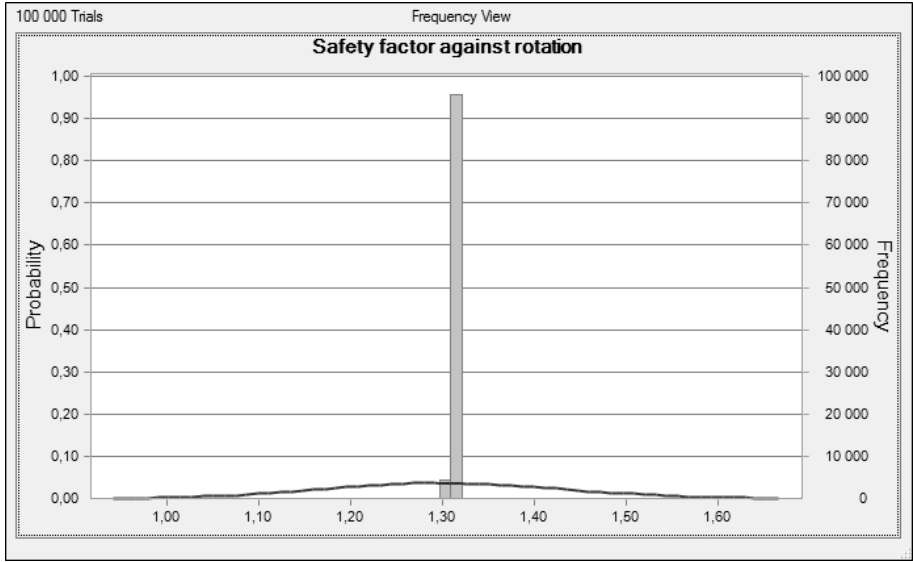
Figure 40 Comparison between the distribution of the safety factor against rotation in Calculation 1_1, line, and Calculation 1_8, column
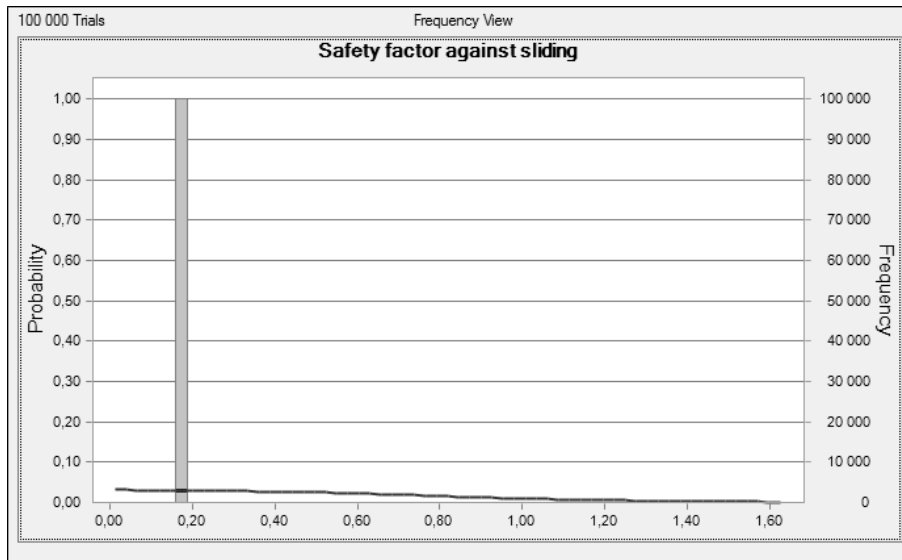
Figure 41 Comparison between the distribution of the safety factor against sliding in Calculation 1_1, line, and Calculation 1_8, column

Calculation 1_9

In this calculation the only parameter that is varying is the heaviness of the soil, see Figure 3-5. The other parameters are the same as the mean value or the most probable value from Calculation 1_1.

Input

$$D_{soil} = 10m$$

$$\varphi = 63.21°$$
$$\phi = 33.81°$$
$$L = 13.7m$$
$$B = 3.5m$$
$$g = 9.82m/s^2$$

$$q_{ext} = 50kN/m^2$$
$$\rho = 2650kg/m^3$$
$$\gamma = 18.5kN/m^3$$
$$\gamma_{5\%} = 17.0kN/m^3$$
$$\gamma_{95\%} = 20.0kN/m^3$$
$$\sigma_h = 1 + 0.022B$$

Output

$$f = 2.67m$$
$$f_{5\%} = 2.60m$$
$$f_{95\%} = 2.73m$$
$$\alpha = 37.88°$$
$$\alpha_{5\%} = 37.24°$$
$$\alpha_{95\%} = 38.51°$$
$$\phi' = 7.02°$$
$$p(f < B) = 1.0$$
$$p(\alpha < \phi') = 0.0$$
$$FS = 1.31$$
$$FS_{rot,5\%} = 1.28$$
$$FS_{rot,95\%} = 1.34$$
$$FS_{slide} = 0.19$$
$$FS_{slide,5\%} = 0.18$$
$$FS_{slide,95\%} = 0.19$$

Results Calculation 1_9

Calculation 1_9 shows that the most probable value for the arch height is 2.67 m. This is 0.02 m more than in Calculation 1_1. The 5-percentile increases with 0.18 m to 2.60 m and the 95-percentile decreases with 0.28 m to 2.73 m, see Figure 42. For the angle of the pressure line the most probable value is 37.88 degrees, which is 0.19 degrees more than in Calculation 1_1. The 5-percentile increases with 1.97 degrees to 37.24 degrees and the 95-percentile decreases with 0.28 degrees to 2.73 degrees, see Figure 43. Most probable equivalent friction angle is 7.02 degrees, which is 1.81 degrees more than in Calculation 1_1, see Figure 44. The probability that the arch height is less than the bedding plane is 1.0, which is 0.1 more than in Calculation 1_1. Most probable value for the factor of safety against rotation is 1.31, which is 0.01 more than in Calculation 1_1. The 5-percentile increases with 0.19 to 1.28 and the 95-percentile decreases with 0.18 to 1.34, see Figure 45. The probability that the angle of the pressure line is lower than the equivalent friction angle is 0.0, which is 0.13 less than in Calculation 1_1. Most probable value for the factor of safety against sliding is 0.19, which is 0.04 more than in Calculation 1_1. The 5-percentile increases with 0.14 to 0.18 and the 95-percentile decreases with 1.09 to 0.19, see Figure 46.
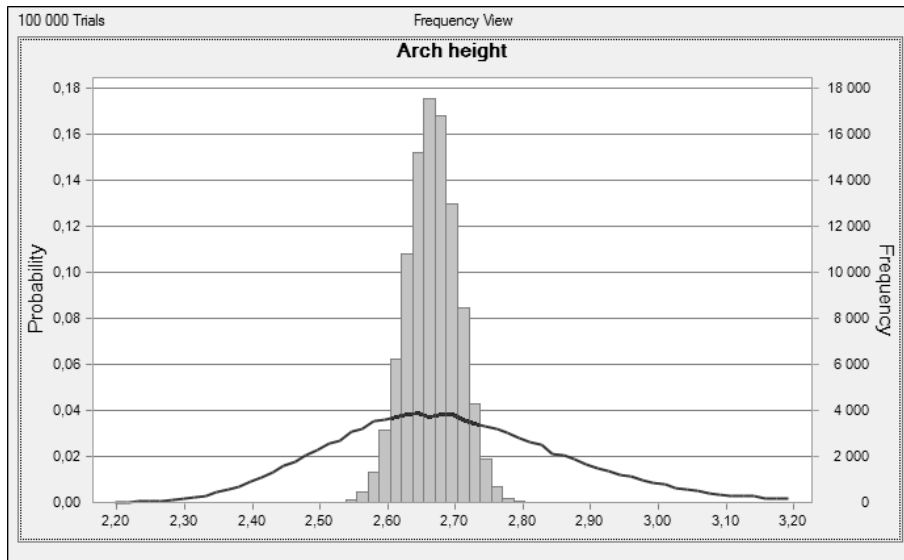
Figure 42 Comparison between the distribution of the arch height in Calculation 1_1, line, and Calculation 1_9, column
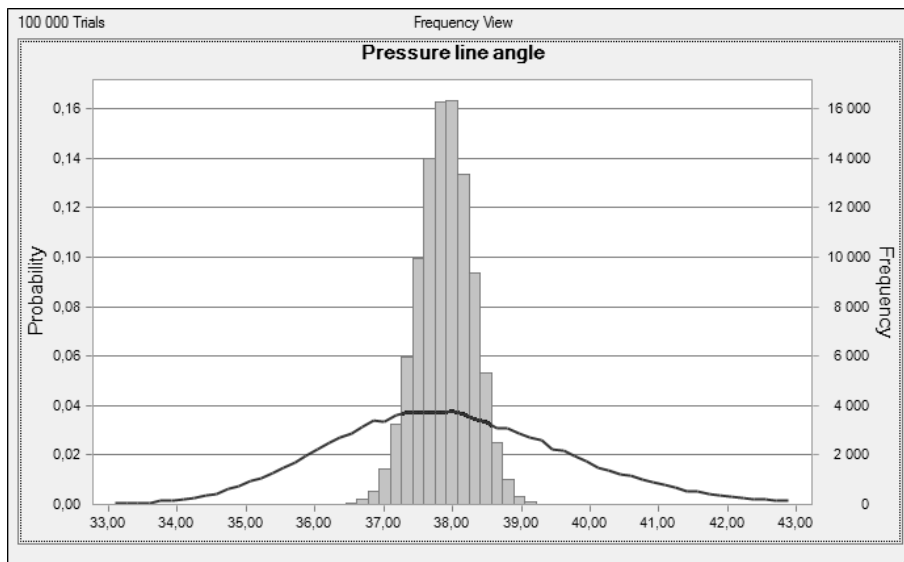
Figure 43 Comparison between the distribution of the pressure line angle in Calculation 1_1, line, and Calculation 1_9, column
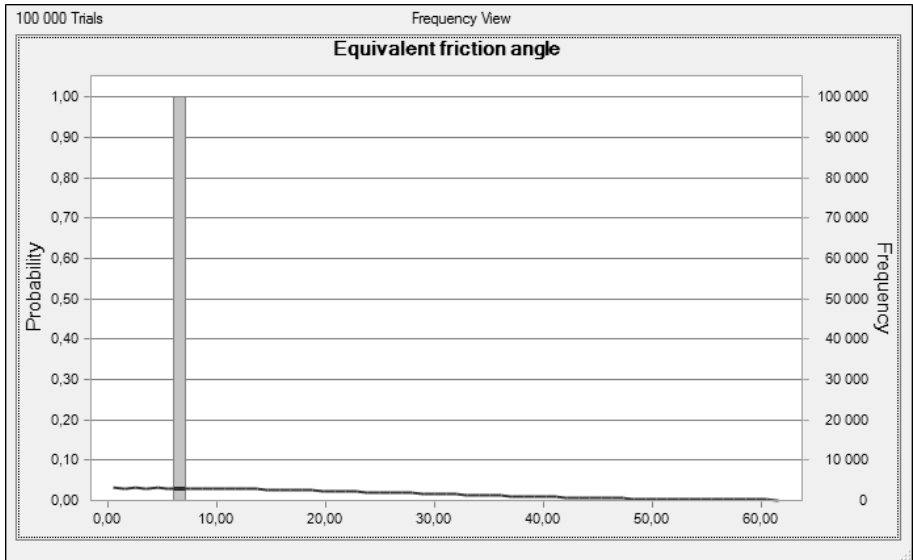
Figure 44 Comparison between the distribution of the equivalent friction angle in Calculation 1_1, line, and Calculation 1_9, column
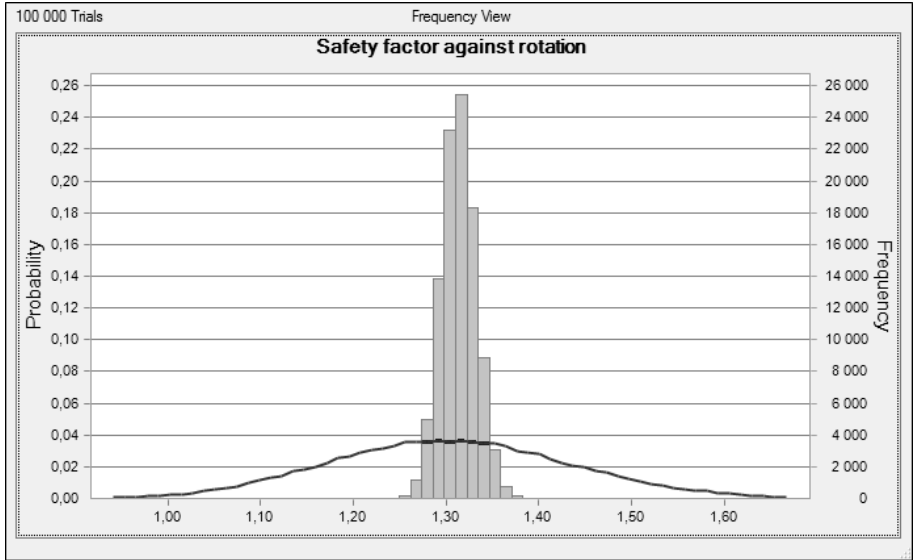
Figure 45 Comparison between the distribution of the safety factor against rotation in Calculation 1_1, line, and Calculation 1_9, column
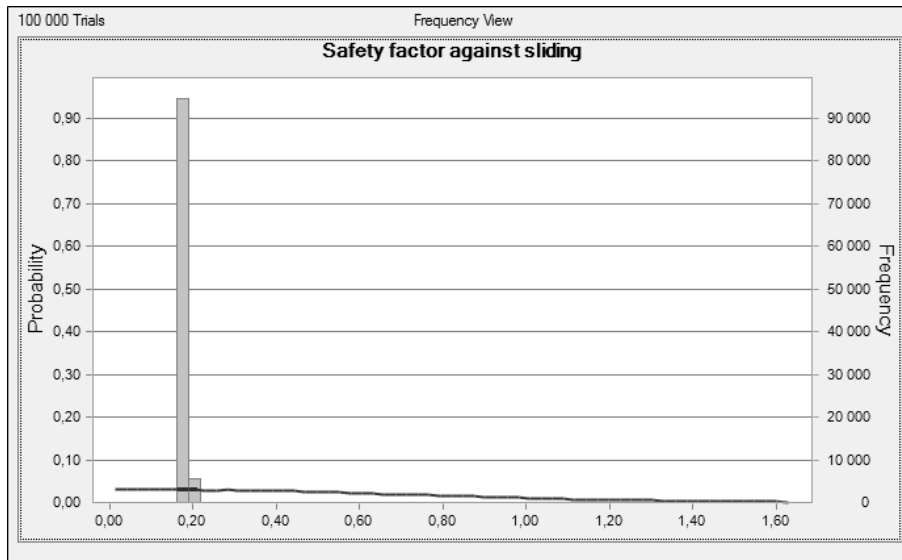
Figure 46 Comparison between the distribution of the safety factor against sliding in Calculation 1_1, line, and Calculation 1_9, column

Results Model 1

Table 1 Calculation results from Model 1

Parameter		Calculation								
		1_1	1_2	1_3	1_4	1_5	1_6	1_7	1_8	1_9
5%		2.42	-	-	2.44	2.61	2.63	2.63	2.66	2.60
f	m	2.65	2.67	2.67	2.64	2.66	2.67	2.67	2.67	2.67
95%		3.01	-	-	2.98	2.76	2.70	2.70	2.67	2.73
5%		35.27	-	-	35.42	-	37.47	37.49	37.82	37.24
α	degrees	37.69	37.89	37.89	37.65	37.89	37.89	37.89	37.89	37.88
95%		41.08	-	-	40.98	-	38.29	38.28	37.96	38.51
5%		1.65	1.01	1.35	-	-	-	-	-	-
Φ'	degrees	8.83	1.91	4.45	7.01	7.02	7.02	7.02	7.02	7.02
95%		48.65	45.09	32.45	-	-	-	-	-	-
$p(f<B)$	-	0.99	1.00	1.00	1.00	1.00	1.00	1.00	1.00	1.00
5%		1.09	-	-	1.18	1.27	1.14	1.29	1.31	1.28
FS_{rot}	-	1.30	1.31	1.31	1.32	1.31	1.32	1.31	1.31	1.31
95%		1.52	-	-	1.44	1.34	1.48	1.33	1.32	1.34
$p(α<Φ')$	-	0.13	0.09	0.01	0.00	0.00	0.00	0.00	0.00	0.00
5%		0.04	0.03	0.04	0.17	-	0.18	0.18	0.18	0.18
FS_{slide}	-	0.23	0.05	0.12	0.19	0.19	0.19	0.19	0.19	0.19
95%		1.28	1.19	0.86	0.20	-	0.19	0.19	0.19	0.19

The results from the calculations in Model 1, see Table 1, show that the input parameter that gives the largest uncertainties in the estimation of the height of the arch is the horizontal stress. In Calculation 1_1 the difference between $f_{5\%}$ and $f_{95\%}$ is 0.59 m and in Calculation 1_4 where the horizontal stress is the only varying parameter the difference between $f_{5\%}$ and $f_{95\%}$ is 0.54 m. This is almost the same

range between the outer parts of the uncertainty graph and if it is compared to the other input parameters, as can be seen in Figure 7, Figure 12, Figure 17, Figure 22, Figure 27, Figure 32, Figure 37 and Figure 42, the uncertainties in the arch height has the highest uncertainty when the horizontal stress is varied.

All calculations show high probability that the arch height will be lower than the rock cover/bedding plane and this means that the risk for collapse due to rotating block is low. Looking at the safety factor for rotation the result from Calculation 1_6 is interesting. The difference between $f_{5\%}$ and $f_{95\%}$ is low, only 0.07 m but since the rock cover is varying the safety factor against rotation shows almost the same difference between the 5- and 95-percentile as Calculation 1_1, 0.34 in Calculation 1_6 and 0.43 in Calculation 1_1, see Figure 30. This is a little more than in Calculation 1_4, which had the largest variation in arch height, where the span between $FS_{rot,5\%}$ and $FS_{rot,95\%}$ is 0.26, see Figure 20.

The angle for the pressure line is depending on the arch height and the width of the tunnel. In Calculation 1_5 the results show that the variation in arch height created by the variation in tunnel width does not change the angle of the pressure line. So the parameter that has the largest influence in the angle of pressure line is the horizontal stress.

Only two parameters affect the equivalent friction angle, it is the friction angle and the dip of the fractures. The results from Calculation 1_2, variation in friction angle, and 1_3, variation in fracture dip, show that the variation in the friction angle has the largest influence on the uncertainties for the equivalent friction angle, see Figure 16.

For all calculations except 1_1, 1_2 and 1_3 the risk of collapse due to sliding blocks is 100 %. In Calculation 1_1 the risk is 83 %, in Calculation 1_2 it is 81 % and in Calculation 1_3 it is 99 %. The safety factor against sliding shows very low uncertainties for the calculations where the equivalent friction angle does not vary. The larger the uncertainty is in the equivalent friction angle, the larger the uncertainty is for the safety factor against sliding, see Figure 11.

Analysis Model 1

Model 1 show that the horizontal stress has the largest influence on the height of the compressed arch, see Table 2. This means that it has the largest influence on the angle at the supports for the arch. This influence is much larger than it is from the other parameters in the model. When it comes to the factor of safety against rotation, Model 1 shows that the rock cover has a major role, the changes in rock cover makes a small change in the total load on the tunnel roof but it creates a large variation in the rock mass where the arch can be formed.

Both the friction angle and the fracture dip cause large variations in the resulting equivalent friction angle. It seems that the variation in friction angle makes the model safer than the variation in fracture dip. This, since it makes the probability of the angle of the pressure line being less than the equivalent friction angle increase from 1 %, which it is when only the fracture dip is varying, to 9 %.

As a result of these findings more calculations are done in Model 2 to see what happens if more focus is put on the influence of the horizontal stress.

Table 2 Matrix showing a ranking of how much the uncertainties in the input parameters influence the uncertainty in the different output parameters; 1 = most influencial, 6 = least influencial, - = no influence

	Input parameter							
	ϕ	φ	σ_h	L	D_{rock}	D_{soil}	ρ	γ
f	-	-	1	2	4	4	5	3
α	-	-	1	-	3	4	5	2
Φ'	1	2	-	-	-	-	-	-
FS_{rot}	-	-	2	3	1	5	6	4
FS_{slide}	1	2	3	-	4	4	4	4

(Output parameter labels shown vertically at left of the rows)

Model 2/Horizontal stress study

In this model, the effect of the uncertainties in the horizontal stress will be further studied. It will also be seen what happens to the overall stability if the horizontal stress regime is doubled or halved. The calculations in Model 2 is done according to Table 3

Table 3 Calculations in Model 2

Parameter	ϕ	φ	σ_h	L	B	D_{soil}	ρ	γ
Model 2	In-depth study of the horizontal stress							
2_1			-					
2_2	-	-		-	-	-	-	-
2_3			+					
2_4			-					
2_5			+					
2_6			-					
2_7			+					
2_8	+	+		+	+	+	+	+

(grey)	Varying value, same as Model 1
+	Varying value, doubled uncertainty
-	Varying value, halved uncertainty
+	Varying value, doubled value
-	Varying value, halved value
+	Varying value, doubled depth dependency
-	Varying value halved depth dependency

Calculation 2_1

In this calculation every parameter except the horizontal stress will be the same as in Calculation 1_1. For the horizontal stress the standard deviation will be lowered from 12 % to 6 %, see Figure 47.

Figure 47 Distribution of the horizontal stress in Calculation 2_1

Input

$\varphi = 63.21°$

$\varphi_{5\%} = 19.41°$

$\varphi_{95\%} = 84.70°$

$\phi = 33.81°$

$\phi_{5\%} = 20.55°$

$\phi_{95\%} = 71.72°$

$L = 13.7m$

$L_{5\%} 13.4m$

$L_{95\%} = 14.2m$

$B = 3.5m$

$B_{5\%} = 3.0m$

$B_{95\%} = 4.0m$

$g = 9.82m/s^2$

$D_{soil} = 10m$

$D_{soil,5\%} = 9.5m$

$D_{soil,95\%} = 10.5m$

$q_{ext} = 50kN/m^2$

$\rho = 2650kg/m^3$

$\rho_{5\%} = 2600kg/m^3$

$\rho_{95\%} = 2700kg/m^3$

$\gamma = 18.5kN/m^3$

$\gamma_{5\%} = 17.0kN/m^3$

$\gamma_{95\%} = 20.0kN/m^3$

$\sigma_h = 1 + 0.022B$

$\sigma_{h,std} = 0.06 \cdot \sigma_h$

Output

$$f = 2.66m$$

$$f_{5\%} = 2.51m$$

$$f_{95\%} = 2.86m$$

$$\alpha = 37.85°$$

$$\alpha_{5\%} = 36.32°$$

$$\alpha_{95\%} = 39.56°$$

$$\phi' = 8.24°$$

$$\phi'_{5\%} = 1.64°$$

$$\phi'_{95\%} = 49.22°$$

$$p(f < B) = 1.0$$

$$p(\alpha < \phi') = 0.13$$

$$FS_{rot} = 1.31$$

$$FS_{rot,5\%} = 1.12$$

$$FS_{rot,95\%} = 1.50$$

$$FS_{slide} = 0.22$$

$$FS_{slide,5\%} = 0.04$$

$$FS_{slide,95\%} = 1.30$$

Results Calculation 2_1

Calculation 2_1 shows that the most probable value for the arch height is 2.66 m. This is 0.01 m more than in Calculation 1_1. The 5-percentile increases with 0.09 m to 2.51 m and the 95-percentile decreases with 0.15 m to 2.86 m, see Figure 48. For the angle of the pressure line the most probable value is 37.85 degrees, which is 0.16 degrees more than in Calculation 1_1. The 5-percentile increases with 1.05 degrees to 36.32 degrees and the 95-percentile decreases with 1.52 degrees to 39.56 degrees, see Figure 49. Most probable equivalent friction angle is 8.24 degrees, which is 0.59 degrees less than in Calculation 1_1. The 5-percentile decreases with 0.01 degrees to 1.64 degrees and the 95-percentile increases with 0.57 degrees to 49.22 degrees, see Figure 50. The probability that the arch height is less than the bedding plane is 1.0, which is 0.01 more than in Calculation 1_1. Most probable value for the factor of safety against rotation is 1.31, which is 0.01 more than in Calculation 1_1. The 5-percentile increases with 0.03 to 1.12 and the 95-percentile decreases with 0.02 to 1.50, see Figure 51. The probability that the angle of the pressure line is lower than the equivalent friction angle is 0.13, which is the same as in Calculation 1_1. Most probable value for the factor of safety against sliding is 0.22, which is 0.01 more than in Calculation 1_1. The 5-percentile does not increase and is 0.04 and the 95-percentile increases with 0.02 to 1.30, see Figure 52.
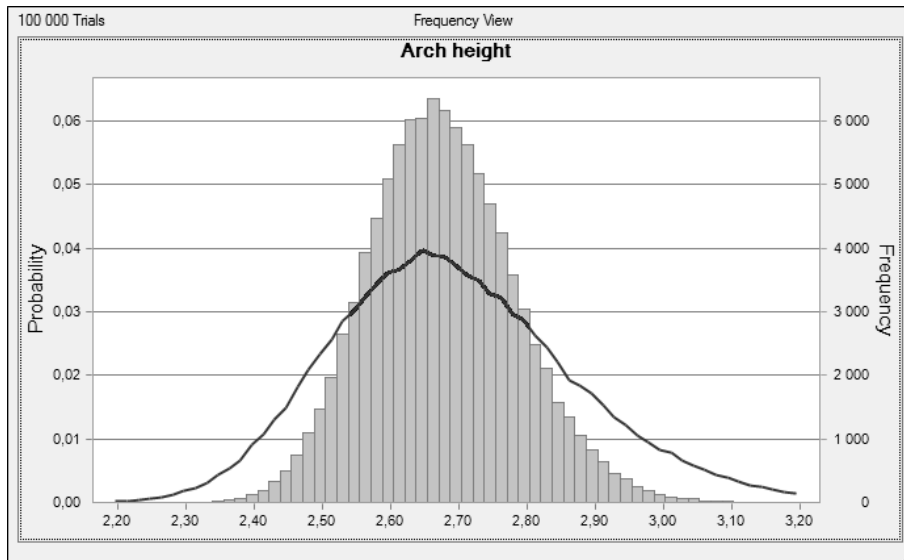
Figure 48 Comparison between the distribution of the arch height in Calculation 1_1, line, and Calculation 2_1, column
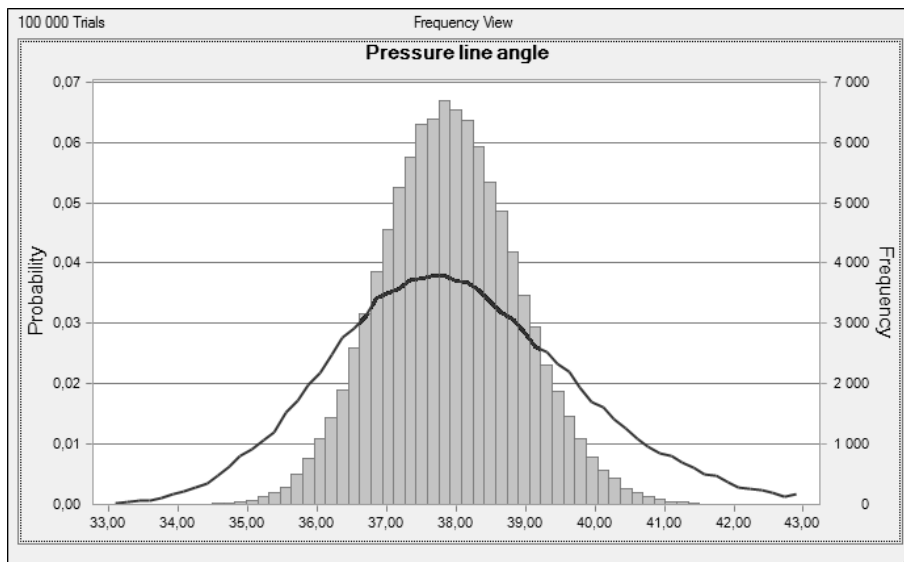
Figure 49 Comparison between the distribution of the pressure line angle in Calculation 1_1, line, and Calculation 2_1, column
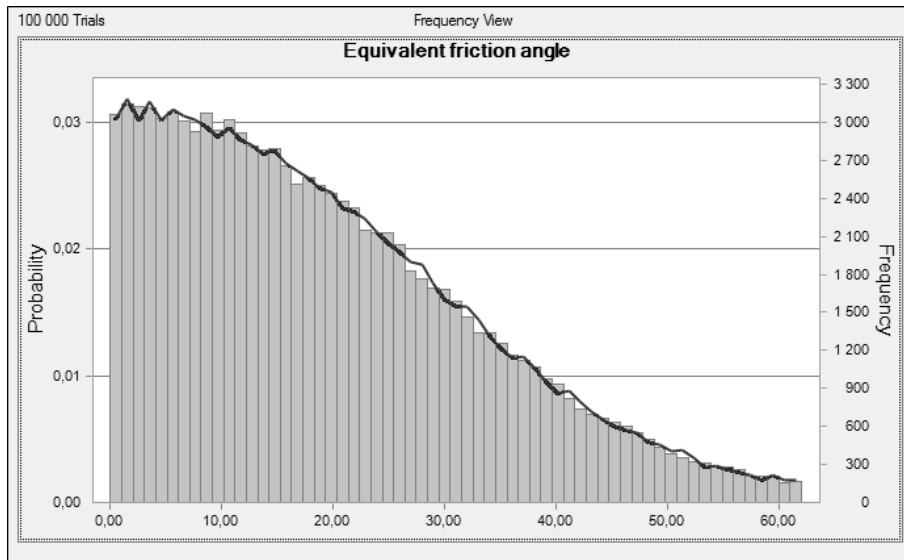
Figure 50 Comparison between the distribution of the equivalent friction angle in Calculation 1_1, line, and Calculation 2_1, column
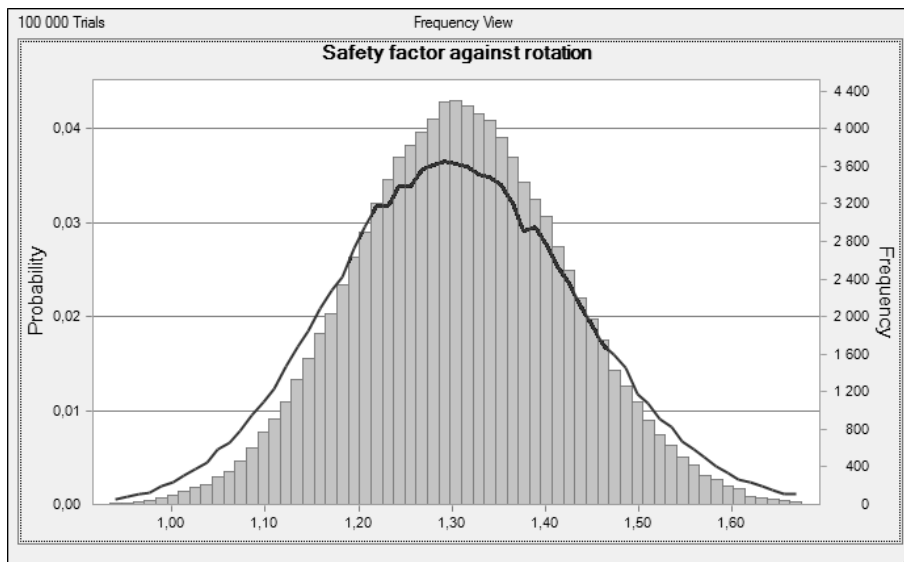
Figure 51 Comparison between the distribution of the safety factor against rotation in Calculation 1_1, line, and Calculation 2_1, column
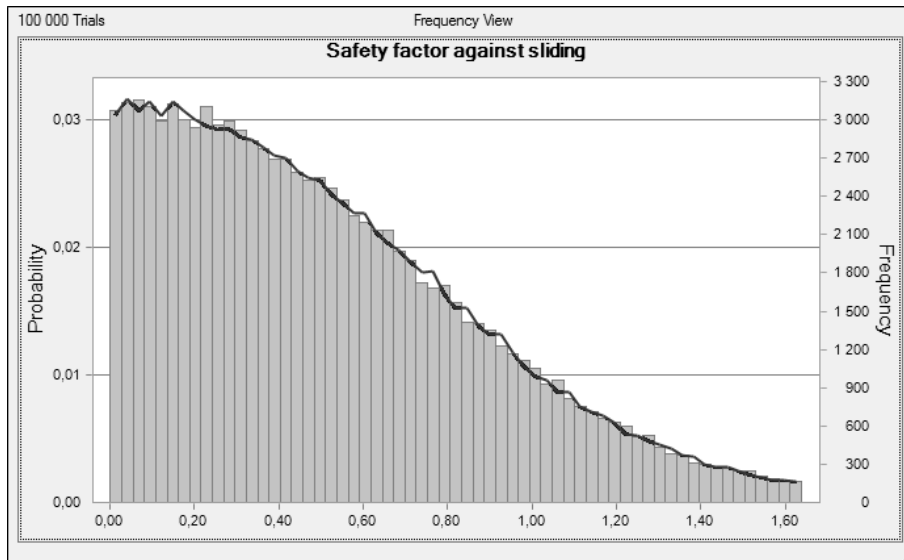
Figure 52 Comparison between the distribution of the safety factor against sliding in Calculation 1_1, line, and Calculation 2_1, column

Calculation 2_2

This calculation is the opposite from Calculation 2_1, now all parameters except the horizontal stress are halved compared to Calculation 1_1. This means the 5 % and 95 % will change so that the difference between them and the most probable value is halved, see Figure 53 to Figure 59.
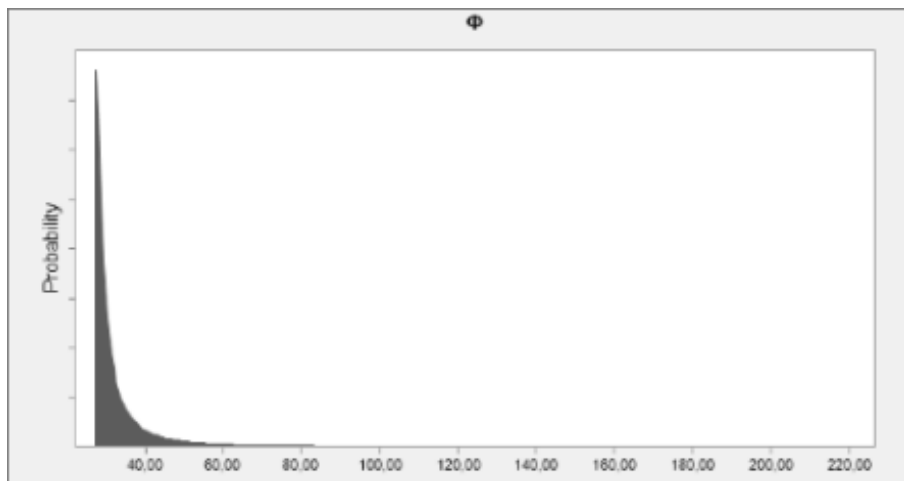
Figure 53 Distribution for the friction angle of fractures in Calculation 2_2
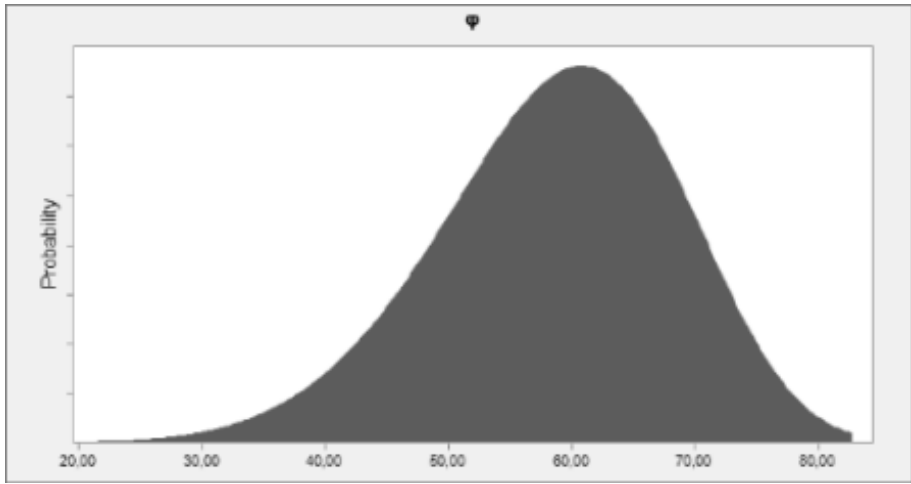
Figure 54 Distribution for the fracture dip in Calculation 2_2
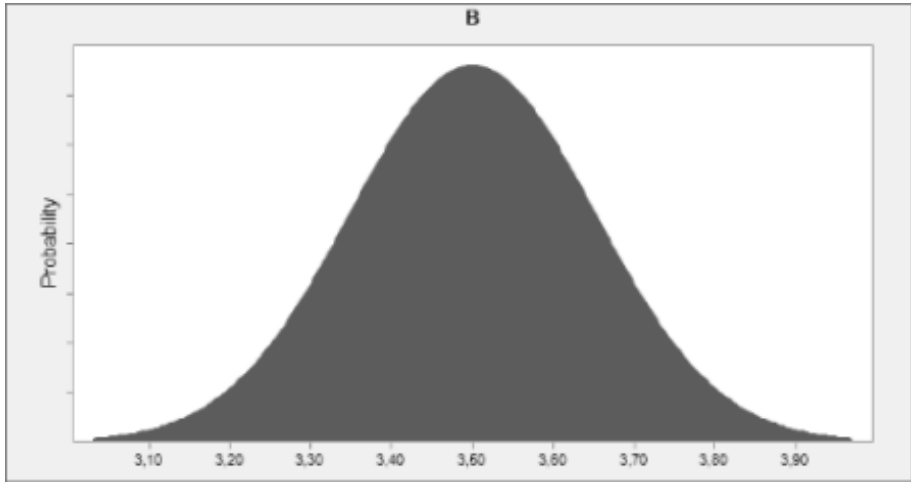
Figure 55 Distribution for the rock cover and height of the bedding plane in Calculation 2_2
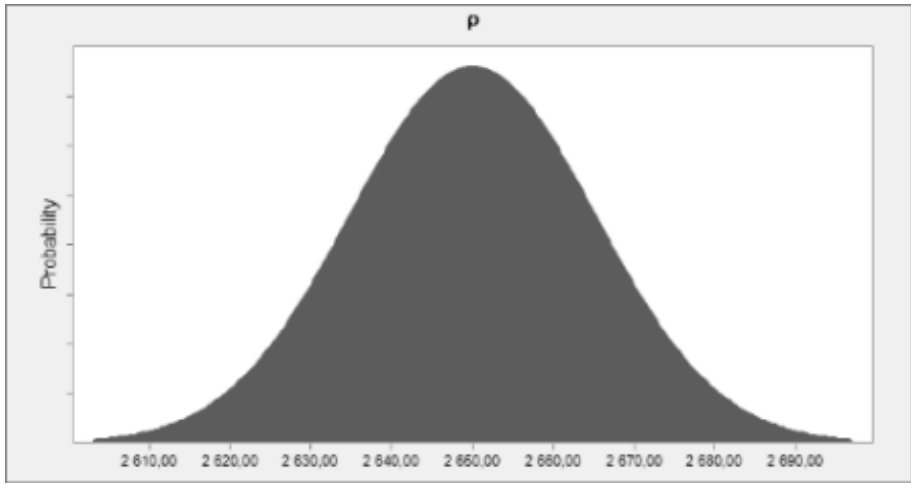
Figure 56 Distribution of the rock density in Calculation 2_2
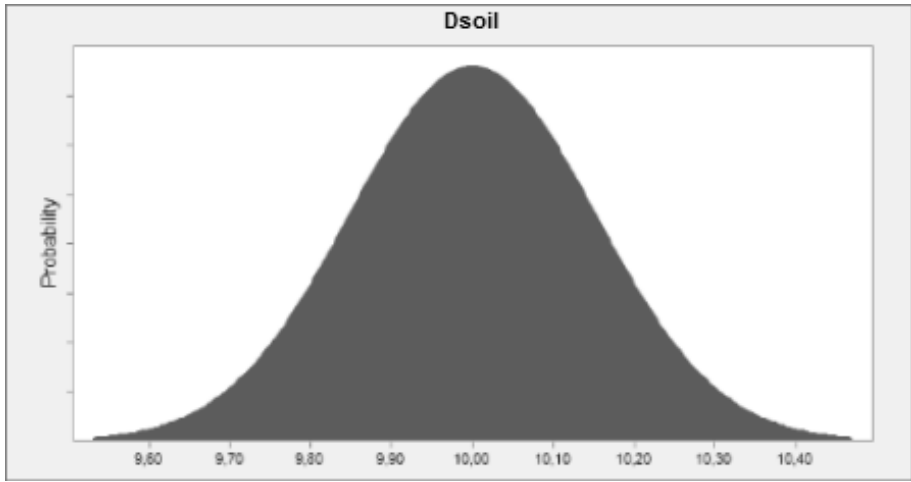
Figure 57 Distribution of the soil depth in Calculation 2_2
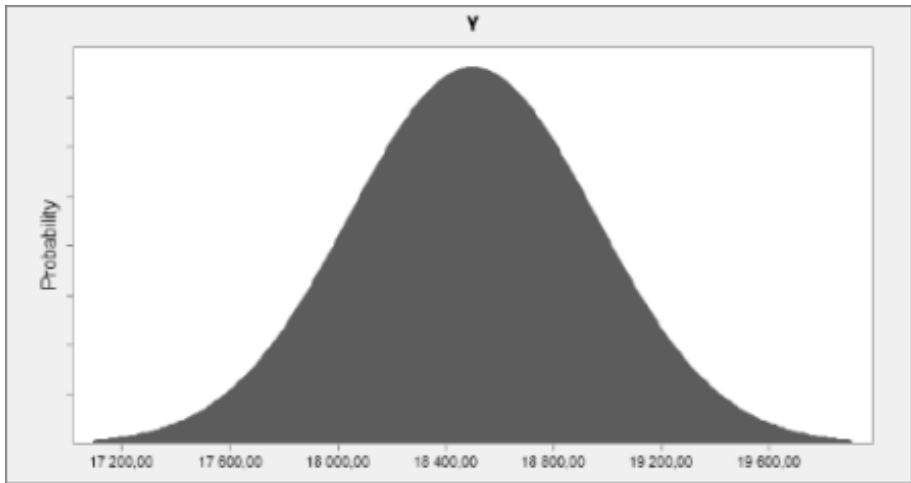
Figure 58 Distribution of the heaviness of the soil in Calculation 2_2
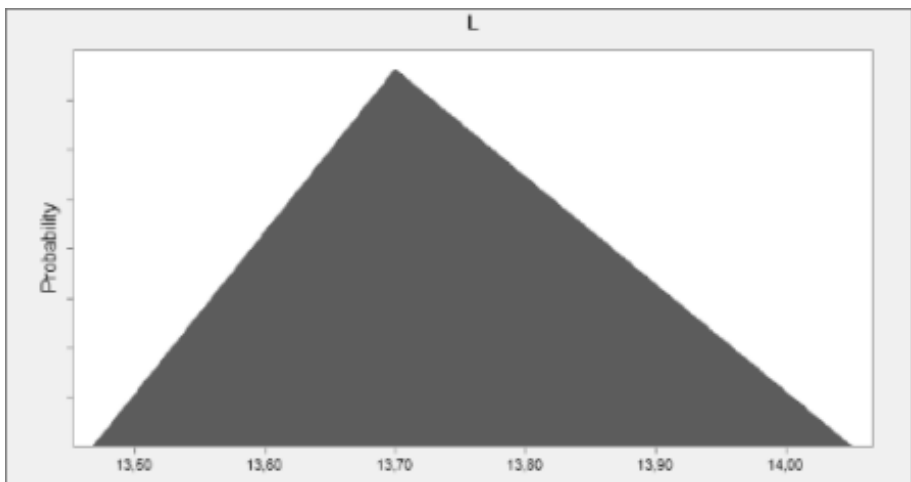
Figure 59 Distribution of the tunnel width in Calculation 2_2

Input

$\varphi = 63.21°$

$\varphi_{5\%} = 41.31°$

$\varphi_{95\%} = 73.95°$

$\phi = 33.81°$

$\phi_{5\%} = 27.18°$

$\phi_{95\%} = 52.77°$

$L = 13.7m$

$L_{5\%}13.55m$

$L_{95\%} = 13.95m$

$B = 3.5m$

$B_{5\%} = 3.25m$

$B_{95\%} = 3.75m$

$g = 9.82m/s^2$

$D_{soil} = 10m$

$D_{soil,5\%} = 9.75m$

$D_{soil,95\%} = 10.25m$

$q_{ext} = 50kN/m^2$

$\rho = 2650kg/m^3$

$\rho_{5\%} = 2625kg/m^3$

$\rho_{95\%} = 2675kg/m^3$

$\gamma = 18.5kN/m^3$

$\gamma_{5\%} = 17.75kN/m^3$

$\gamma_{95\%} = 19.25kN/m^3$

$\sigma_h = 1 + 0.022B$

$\sigma_{h,std} = 0.12 \cdot \sigma_h$

Output

$f = 2.65m$

$f_{5\%} = 2.44m$

$f_{95\%} = 2.99m$

$\alpha = 37.89°$

$\alpha_{5\%} = 35.38°$

$\alpha_{95\%} = 41.00°$

$\phi' = 1.56°$

$\phi'_{5\%} = 0.71°$

$\phi'_{95\%} = 25.70°$

$p(f < B) = 1.0$

$p(\alpha < \phi') = 0.01$

$FS_{rot} = 1.31$

$FS_{rot,5\%} = 1.15$

$FS_{rot,95\%} = 1.46$

$FS_{slide} = 0.04$

$FS_{slide,5\%} = 0.02$

$FS_{slide,95\%} = 0.68$

Results Calculation 2_2

Calculation 2_2 shows that the most probable value for the arch height is 2.65 m. This is the same as in Calculation 1_1. The 5-percentile increases with 0.02 m to 2.44 m and the 95-percentile decreases with 0.02 m to 2.99 m, see Figure 60. For the angle of

the pressure line the most probable value is 37.89 degrees, which is 0.20 degrees more than in Calculation 1_1. The 5-percentile increases with 0.11 degrees to 35.38 degrees and the 95-percentile decreases with 0.08 degrees to 41.00 degrees, see Figure 61. Most probable equivalent friction angle is 1.56 degrees, which is 7.27 degrees less than in Calculation 1_1. The 5-percentile decreases with 0.94 degrees to 0.71 degrees and the 95-percentile decreases with 22.95 degrees to 25.70 degrees, see Figure 62. The probability that the arch height is less than the bedding plane is 1.0, which is 0.01 more than in Calculation 1_1. Most probable value for the factor of safety against rotation is 1.31, which is 0.01 more than in Calculation 1_1. The 5-percentile increases with 0.06 to 1.15 and the 95-percentile decreases with 0.06 to 1.46, see Figure 63. The probability that the angle of the pressure line is lower than the equivalent friction angle is 0.01, which is 0.12 less than in Calculation 1_1. Most probable value for the factor of safety against sliding is 1.46, which is 0.19 less than in Calculation 1_1. The 5-percentile decreases with 0.02 to 0.02 and the 95-percentile decreases with 0.60 to 0.68, see Figure 64.
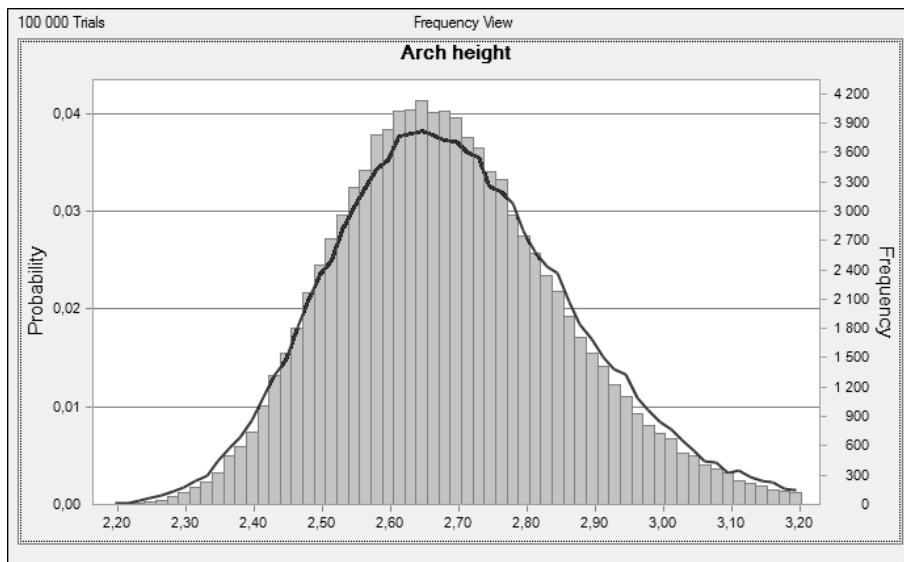
Figure 60 Comparison between the distribution of the arch height in Calculation 1_1, line, and Calculation 2_2, column
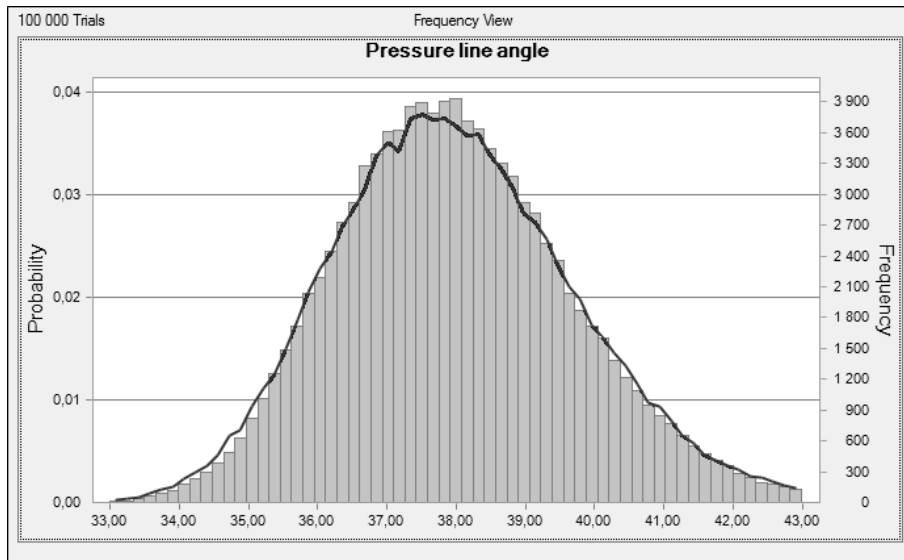
Figure 61 Comparison between the distribution of the pressure line angle in Calculation 1_1, line, and Calculation 2_2, column
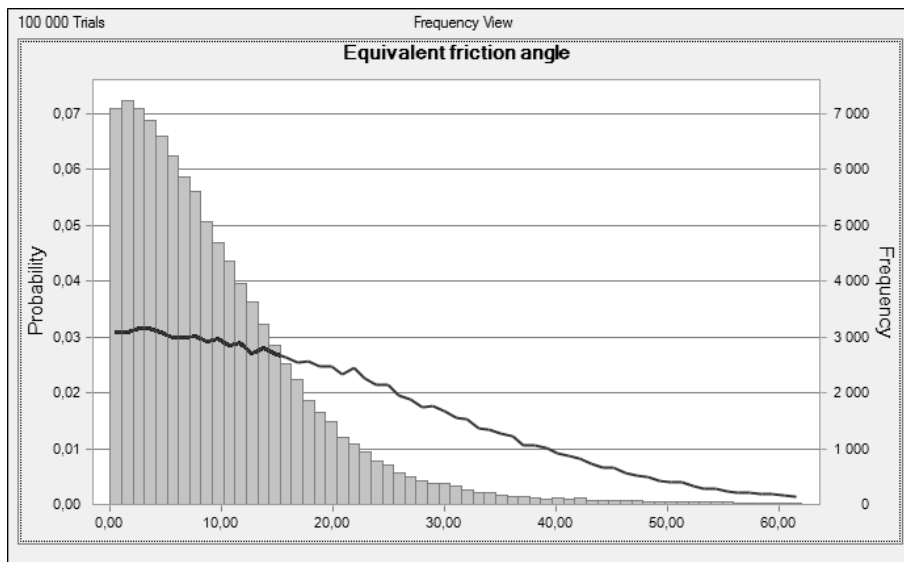
Figure 62 Comparison between the distribution of the equivalent friction angle in Calculation 1_1, line, and Calculation 2_2, column
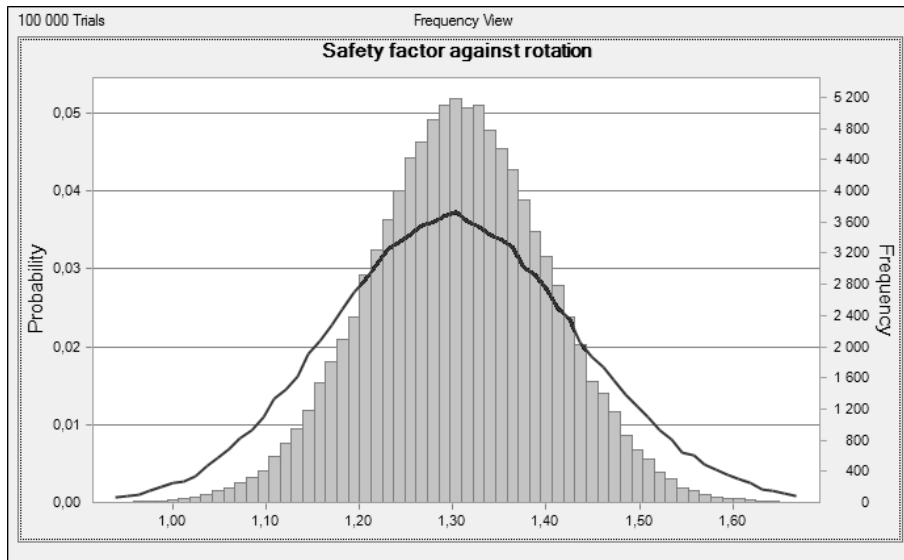
Figure 63 Comparison between the distribution of the safety factor against rotation in Calculation 1_1, line, and Calculation 2_2, column
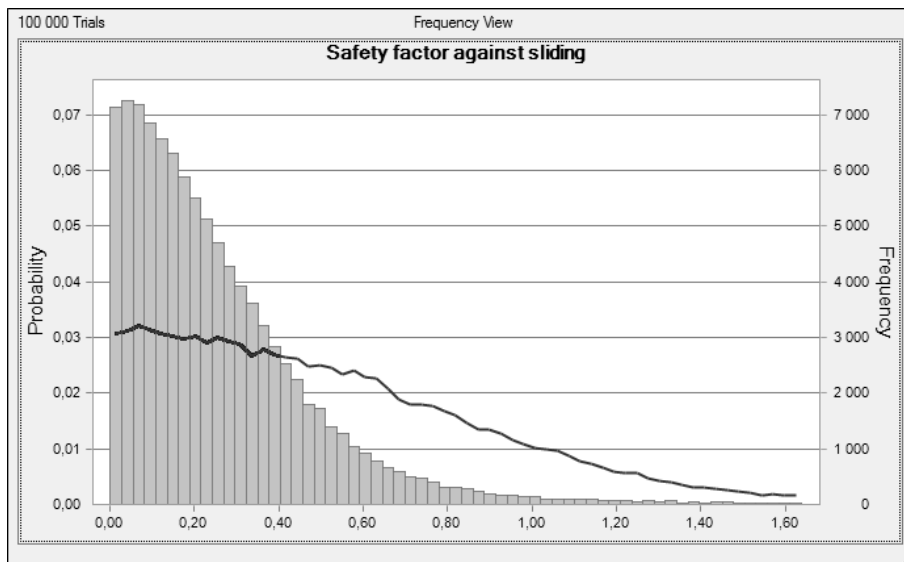
Figure 64 Comparison between the distribution of the safety factor against sliding in Calculation 1_1, line, and Calculation 2_2, column

Calculation 2_3

In this calculation the equation for the horizontal stress is doubled compared to Calculation 1_1, see Equation 1 and Figure 65, but with the same variation as in Calculation 1_1. The other parameters are the same as in Calculation 1_1.

$$\sigma_h = 2 + 0.044B \qquad\qquad\qquad\text{Equation 1}$$

Figure 65 Distribution for the horizontal stress in Calculation 2_3

Input

$\varphi = 63.21°$

$\varphi_{5\%} = 19.41°$

$\varphi_{95\%} = 84.70°$

$\phi = 33.81°$

$\phi_{5\%} = 20.55°$

$\phi_{95\%} = 71.72°$

$L = 13.7m$

$L_{5\%}13.4m$

$L_{95\%} = 14.2m$

$B = 3.5m$

$B_{5\%} = 3.0m$

$B_{95\%} = 4.0m$

$g = 9.82m/s^2$

$D_{soil} = 10m$

$D_{soil,5\%} = 9.5m$

$D_{soil,95\%} = 10.5m$

$q_{ext} = 50kN/m^2$

$\rho = 2650kg/m^3$

$\rho_{5\%} = 2600kg/m^3$

$\rho_{95\%} = 2700kg/m^3$

$\gamma = 18.5kN/m^3$

$\gamma_{5\%} = 17.0kN/m^3$

$\gamma_{95\%} = 20.0kN/m^3$

$\sigma_h = 2 + 0.044B$

$\sigma_{h,std} = 0.12 \cdot \sigma_h$

Output

$$f = 1.88m$$
$$f_{5\%} = 1.72m$$
$$f_{95\%} = 2.13m$$
$$\alpha = 28.63°$$
$$\alpha_{5\%} = 26.57°$$
$$\alpha_{95\%} = 31.65°$$
$$\phi' = 8.60°$$
$$\phi'_{5\%} = 1.63°$$
$$\phi'_{95\%} = 49.04°$$
$$p(f < B) = 1.0$$
$$p(\alpha < \phi') = 0.25$$
$$FS_{rot} = 1.84$$
$$FS_{rot,5\%} = 1.54$$
$$FS_{rot,95\%} = 2.16$$
$$FS_{slide} = 0.30$$
$$FS_{slide,5\%} = 0.06$$
$$FS_{slide,95\%} = 1.70$$

Results Calculation 2_3

Calculation 2_3 shows that the most probable value for the arch height is 1.88 m. This is 0.77 m less than in Calculation 1_1. The 5-percentile decreases with 0.70 m to 1.72 m and the 95-percentile decreases with 0.88 m to 2.13 m, see Figure 66. For the angle of the pressure line the most probable value is 28.63 degrees, which is 9.06 degrees less than in Calculation 1_1. The 5-percentile decreases with 8.70 degrees to 26.57 degrees and the 95-percentile decreases with 9.43 degrees to 31.65 degrees, see Figure 67. Most probable equivalent friction angle is 8.60 degrees, which is 0.23 degrees less than in Calculation 1_1. The 5-percentile decreases with 0.02 degrees to 1.63 degrees and the 95-percentile decreases with 0.39 degrees to 49.04 degrees, see Figure 68. The probability that the arch height is less than the bedding plane is 1.0, which is 0.01 more than in Calculation 1_1. Most probable value for the factor of safety against rotation is 1.84, which is 0.54 more than in Calculation 1_1. The 5-percentile increases with 0.02 to 1.52 and the 95-percentile increases with 0.64 to 2.16, see Figure 69. The probability that the angle of the pressure line is lower than the equivalent friction angle is 0.25, which is 0.12 more than in Calculation 1_1. Most probable value for the factor of safety against sliding is 0.30, which is 0.07 more than in Calculation 1_1. The 5-percentile increases with 0.02 to 0.06 and the 95-percentile increases with 0.42 to 1.70, see Figure 70.
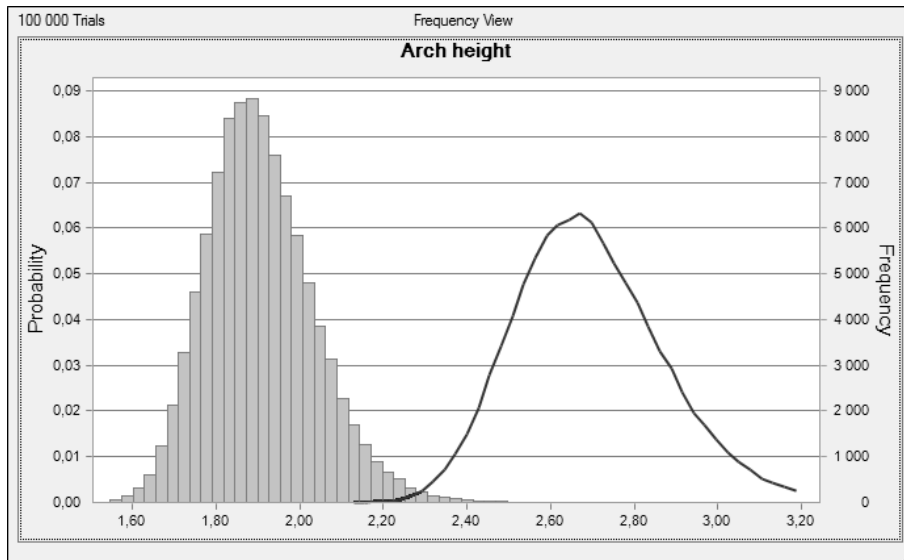
Figure 66 Comparison between the distribution of the arch height in Calculation 1_1, line, and Calculation 2_3, column
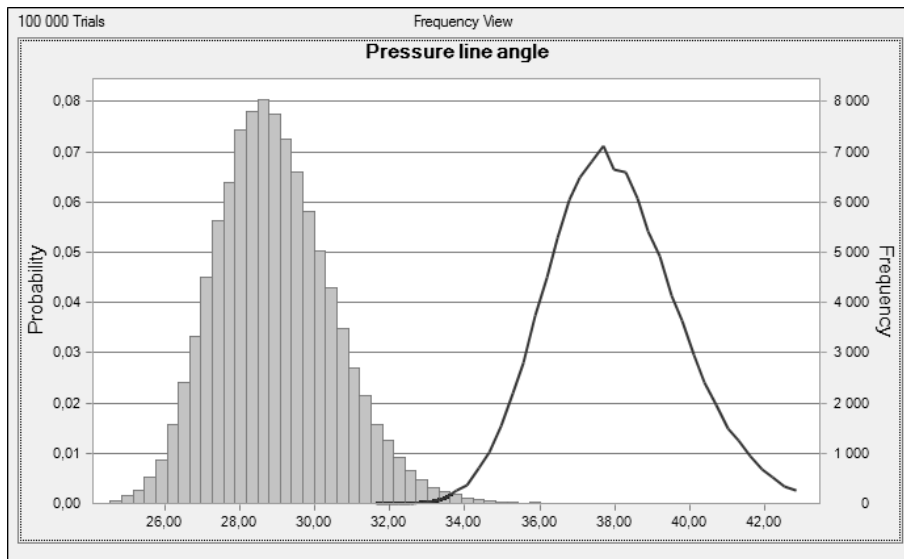
Figure 67 Comparison between the distribution of the pressure line angle in Calculation 1_1, line, and Calculation 2_3, column
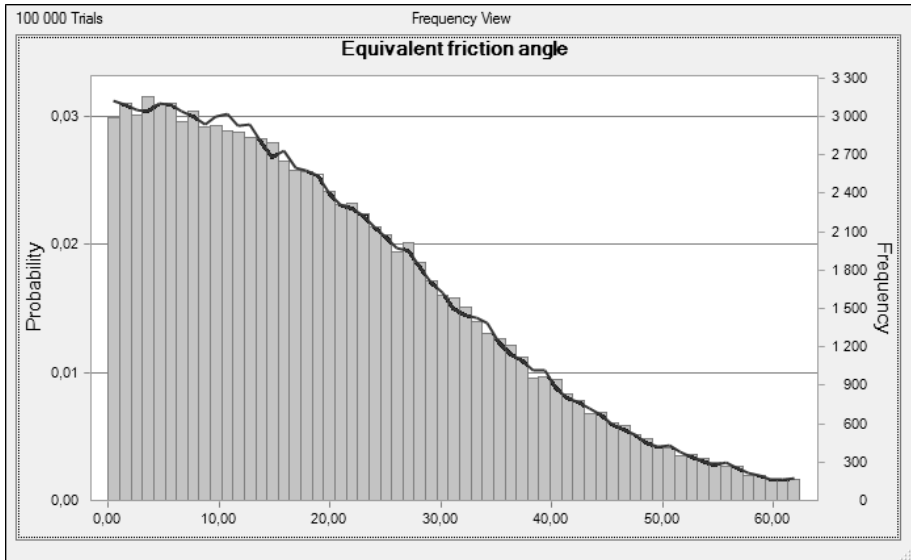
Figure 68 Comparison between the distribution of the equivalent friction angle in Calculation 1_1, line, and Calculation 2_3, column
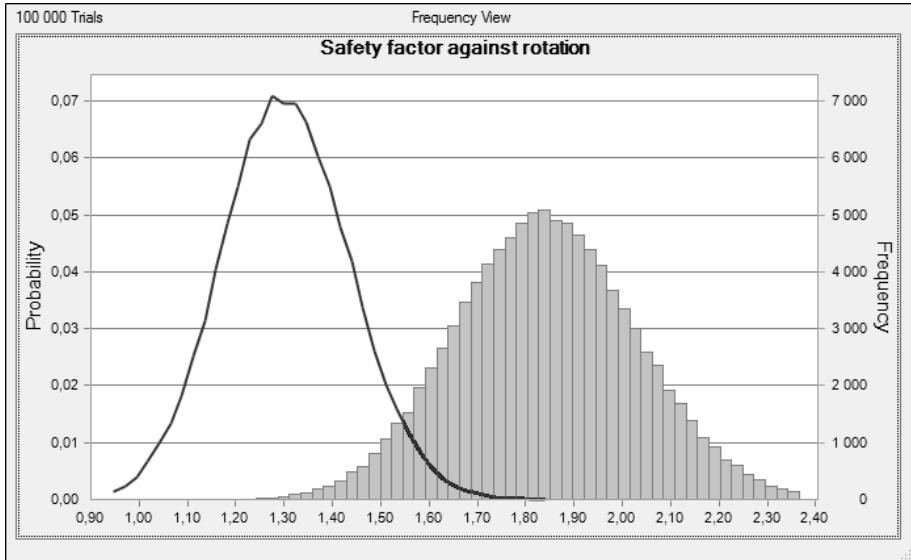
Figure 69 Comparison between the distribution of the safety factor against rotation in Calculation 1_1, line, and Calculation 2_3, column
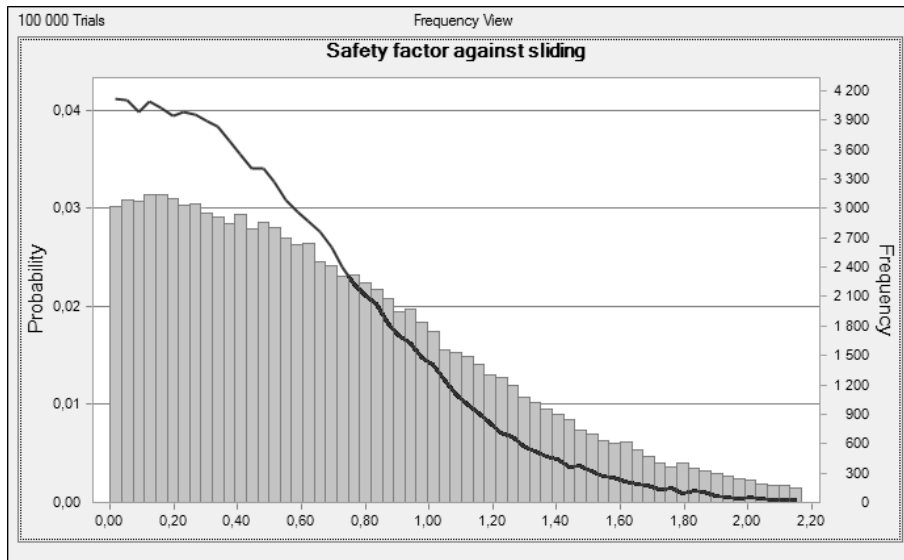
Figure 70 Comparison between the distribution of the safety factor against sliding in Calculation 1_1, line, and Calculation 2_3, column

Calculation 2_4

In this calculation the horizontal stress is half of that in Calculation 1_1, see Equation 2 and Figure 71, but the standard deviation is the same as well as all the other parameters.

$$\sigma_h = 0.5 + 0.011B \qquad\qquad \textbf{Equation 2}$$
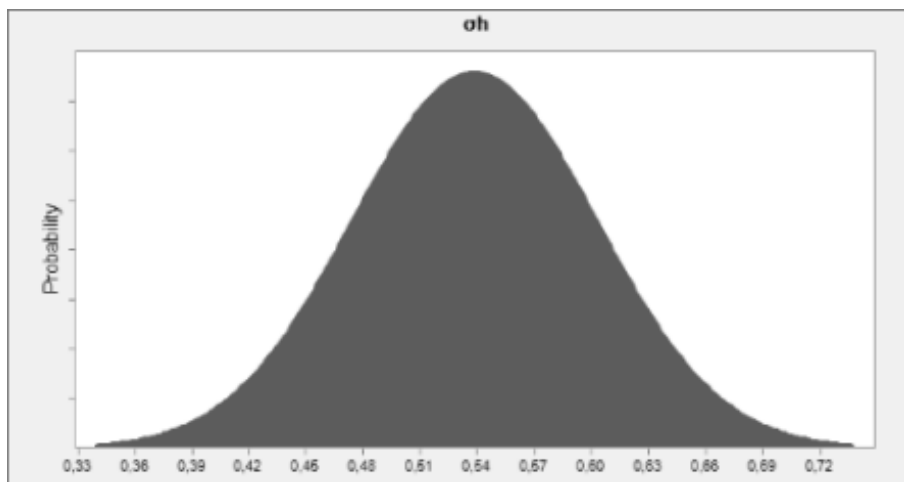
Figure 71 Distribution for the horizontal stress in Calculation 2_4

Input

$\varphi = 63.21°$ $D_{soil} = 10m$

$\varphi_{5\%} = 19.41°$ $D_{soil,5\%} = 9.5m$

$\varphi_{95\%} = 84.70°$ $D_{soil,95\%} = 10.5m$

$\phi = 33.81°$ $q_{ext} = 50kN/m^2$

$\phi_{5\%} = 20.55°$ $\rho = 2650kg/m^3$

$\phi_{95\%} = 71.72°$ $\rho_{5\%} = 2600kg/m^3$

$L = 13.7m$ $\rho_{95\%} = 2700kg/m^3$

$L_{5\%} 13.4m$ $\gamma = 18.5kN/m^3$

$L_{95\%} = 14.2m$ $\gamma_{5\%} = 17.0kN/m^3$

$B = 3.5m$ $\gamma_{95\%} = 20.0kN/m^3$

$B_{5\%} = 3.0m$ $\sigma_h = 0.5 + 0.011B$

$B_{95\%} = 4.0m$ $\sigma_{h,std} = 0.12 \cdot \sigma_h$

$g = 9.82m/s^2$

Output

$f = 3.75m$

$f_{5\%} = 3.43m$

$f_{95\%} = 4.26m$

$\alpha = 47.55°$

$\alpha_{5\%} = 44.99°$

$\alpha_{95\%} = 50.98°$

$\phi' = 9.07°$

$\phi'_{5\%} = 1.61°$

$\phi'_{95\%} = 48.48°$

$p(f < B) = 0.20$

$p(\alpha < \phi') = 0.05$

$FS_{rot} = 0.92$

$FS_{rot,5\%} = 0.77$

$FS_{rot,95\%} = 1.08$

$FS_{slide} = 0.19$

$FS_{slide,5\%} = 0.03$

$FS_{slide,95\%} = 1.01$

Results Calculation 2_4

Calculation 2_4 shows that the most probable value for the arch height is 3.75 m. This is 1.10 m more than in Calculation 1_1. The 5-percentile increases with 1.01 m to 3.43 m and the 95-percentile increases with 1.25 m to 4.26 m, see Figure 72. For the

angle of the pressure line the most probable value is 47.55 degrees, which is 9.86 degrees more than in Calculation 1_1. The 5-percentile increases with 9.72 degrees to 44.99 degrees and the 95-percentile increases with 9.90 degrees to 50.98 degrees, see Figure 73. Most probable equivalent friction angle is 9.07 degrees, which is 0.24 degrees more than in Calculation 1_1. The 5-percentile increases with 0.04 degrees to 1.61 degrees and the 95-percentile decreases with 0.17 degrees to 48.48 degrees, see Figure 74. The probability that the arch height is less than the bedding plane is 0.20, which is 0.79 less than in Calculation 1_1. Most probable value for the factor of safety against rotation is 0.92, which is 0.38 less than in Calculation 1_1. The 5-percentile decreases with 0.32 to 0.77 and the 95-percentile decreases with 0.44 to 1.08, see Figure 75. The probability that the angle of the pressure line is lower than the equivalent friction angle is 0.05, which is 0.08 less than in Calculation 1_1. Most probable value for the factor of safety against sliding is 0.19, which is 0.04 less than in Calculation 1_1. The 5-percentile decreases with 0.01 to 0.03 and the 95-percentile decreases with 0.27 to 1.01, see Figure 76.
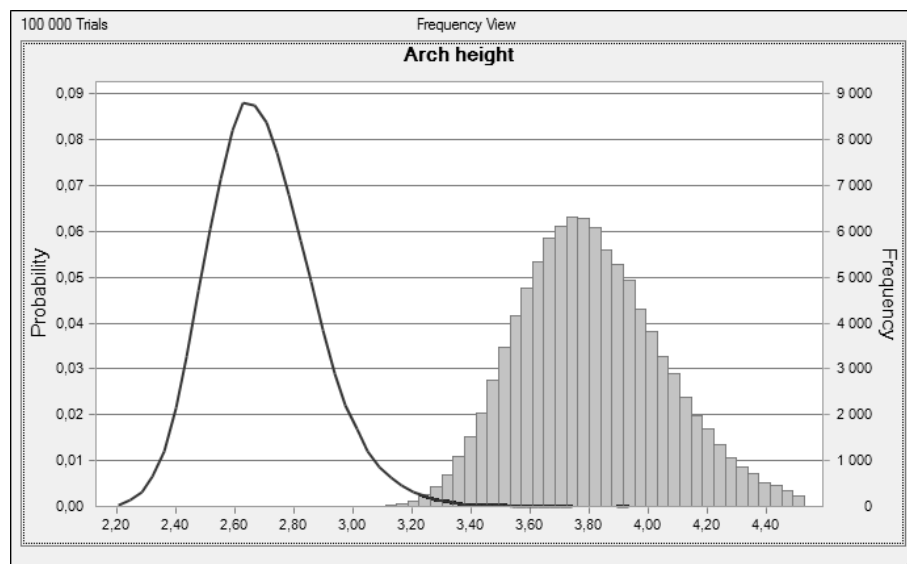
Figure 72 Comparison between the distribution of the arch height in Calculation 1_1, line, and Calculation 2_4, column
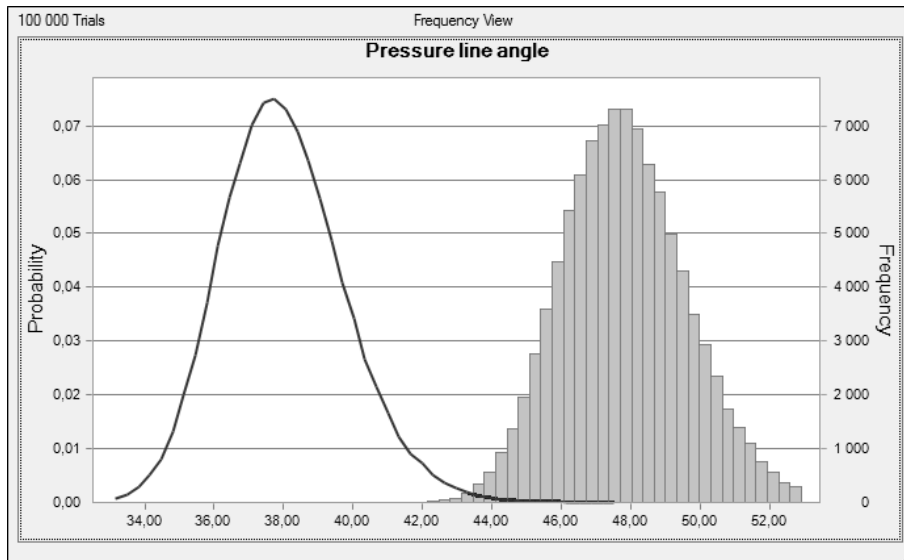
Figure 73 Comparison between the distribution of the pressure line angle in Calculation 1_1, line, and Calculation 2_4, column
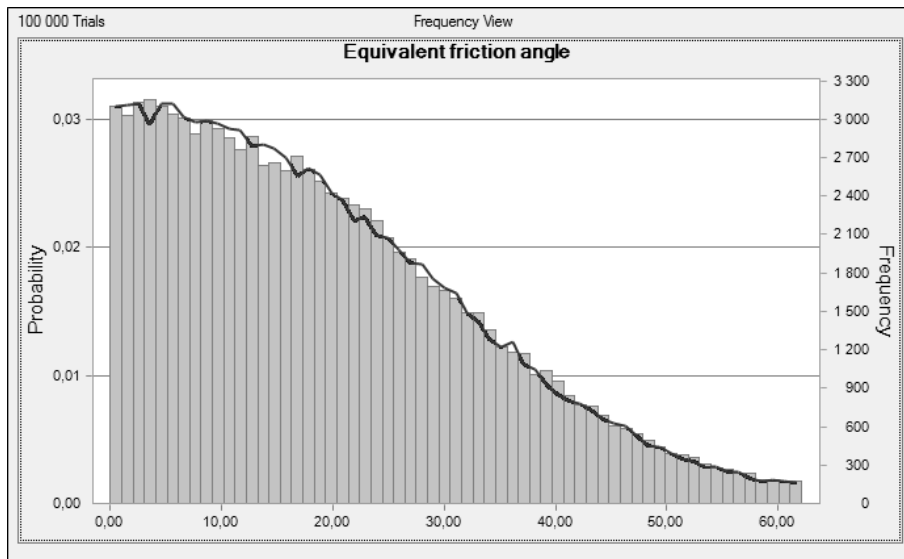
Figure 74 Comparison between the distribution of the equivalent friction angle in Calculation 1_1, line, and Calculation 2_4, column
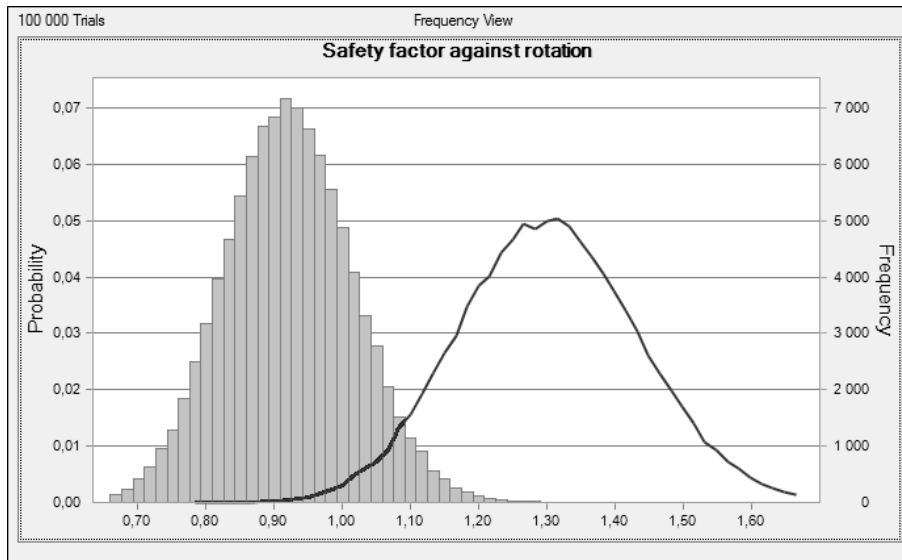
Figure 75 Comparison between the distribution of the safety factor against rotation in Calculation 1_1, line, and Calculation 2_4, column
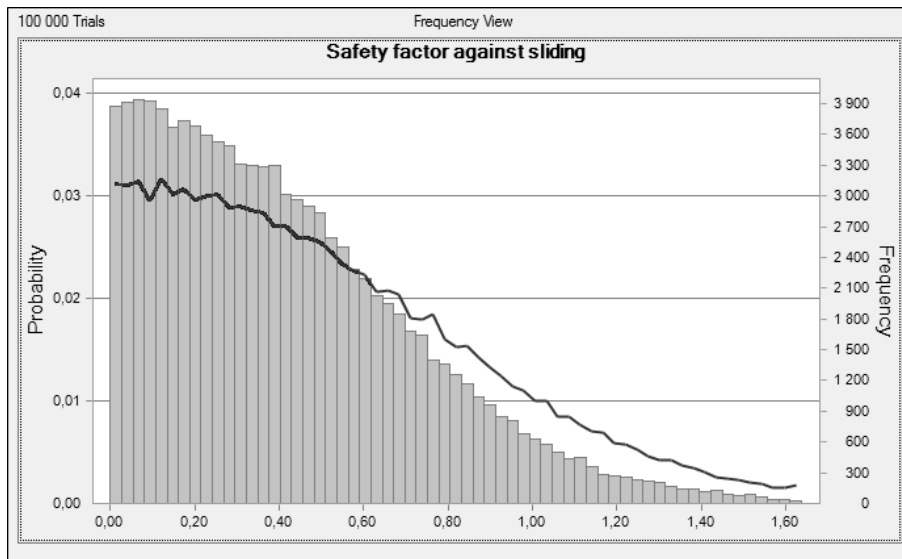
Figure 76 Comparison between the distribution of the safety factor against sliding in Calculation 1_1, line, and Calculation 2_4, column

Calculation 2_5

In this calculation the depth dependency of the horizontal stress equation is doubled compared to Calculation 1_1, see Equation 3 and Figure 77, all other input are the same.

$$\sigma_h = 1 + 0.044B \qquad\qquad \textbf{Equation 3}$$

Figure 77 Distribution for the horizontal stress in Calculation 2_5

Input

$\varphi = 63.21°$

$\varphi_{5\%} = 19.41°$

$\varphi_{95\%} = 84.70°$

$\phi = 33.81°$

$\phi_{5\%} = 20.55°$

$\phi_{95\%} = 71.72°$

$L = 13.7m$

$L_{5\%} 13.4m$

$L_{95\%} = 14.2m$

$B = 3.5m$

$B_{5\%} = 3.0m$

$B_{95\%} = 4.0m$

$g = 9.82m/s^2$

$D_{soil} = 10m$

$D_{soil,5\%} = 9.5m$

$D_{soil,95\%} = 10.5m$

$q_{ext} = 50kN/m^2$

$\rho = 2650kg/m^3$

$\rho_{5\%} = 2600kg/m^3$

$\rho_{95\%} = 2700kg/m^3$

$\gamma = 18.5kN/m^3$

$\gamma_{5\%} = 17.0kN/m^3$

$\gamma_{95\%} = 20.0kN/m^3$

$\sigma_h = 1 + 0.044B$

$\sigma_{h,std} = 0.12 \cdot \sigma_h$

Output

$$f = 2.56m$$
$$f_{5\%} = 2.34m$$
$$f_{95\%} = 2.91m$$
$$\alpha = 36.71°$$
$$\alpha_{5\%} = 34.35°$$
$$\alpha_{95\%} = 40.09°$$
$$\phi' = 8.59°$$
$$\phi'_{5\%} = 1.64°$$
$$\phi'_{95\%} = 48.81°$$
$$p(f < B) = 1.0$$
$$p(\alpha < \phi') = 0.14$$
$$FS_{rot} = 1.34$$
$$FS_{rot,5\%} = 1.12$$
$$FS_{rot,95\%} = 1.58$$
$$FS_{slide} = 0.23$$
$$FS_{slide,5\%} = 0.04$$
$$FS_{slide,95\%} = 1.33$$

Results Calculation 2_5

Calculation 2_5 shows that the most probable value for the arch height is 2.56 m. This is 0.09 m less than in Calculation 1_1. The 5-percentile decreases with 0.08 m to 2.34 m and the 95-percentile decreases with 0.10 m to 2.91 m, see Figure 78. For the angle of the pressure line the most probable value is 36.71 degrees, which is 0.02 degrees less than in Calculation 1_1. The 5-percentile decreases with 0.92 degrees to 34.35 degrees and the 95-percentile decreases with 0.99 degrees to 40.09 degrees, see Figure 79. Most probable equivalent friction angle is 8.59 degrees, which is 0.24 degrees less than in Calculation 1_1. The 5-percentile decreases with 0.01 degrees to 1.64 degrees and the 95-percentile increases with 0.16 degrees to 48.81 degrees, see Figure 80. The probability that the arch height is less than the bedding plane is 1.0, which is 0.01 more than in Calculation 1_1. Most probable value for the factor of safety against rotation is 1.34, which is 0.04 more than in Calculation 1_1. The 5-percentile increases with 0.03 to 1.12 and the 95-percentile increases with 0.06 to 1.58, see Figure 81. The probability that the angle of the pressure line is lower than the equivalent friction angle is 0.14, which is 0.01 more than in Calculation 1_1. Most probable value for the factor of safety against sliding is 0.23, which is the same as in Calculation 1_1. The 5-percentile remains at 0.04 and the 95-percentile increases with 0.05 to 1.33, see Figure 82.
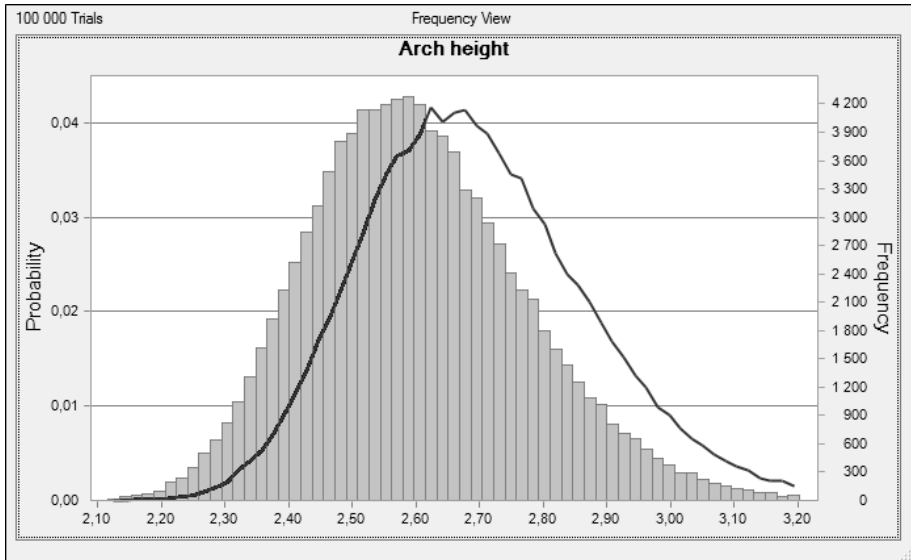
Figure 78 Comparison between the distribution of the arch height in Calculation 1_1, line, and Calculation 2_5, column
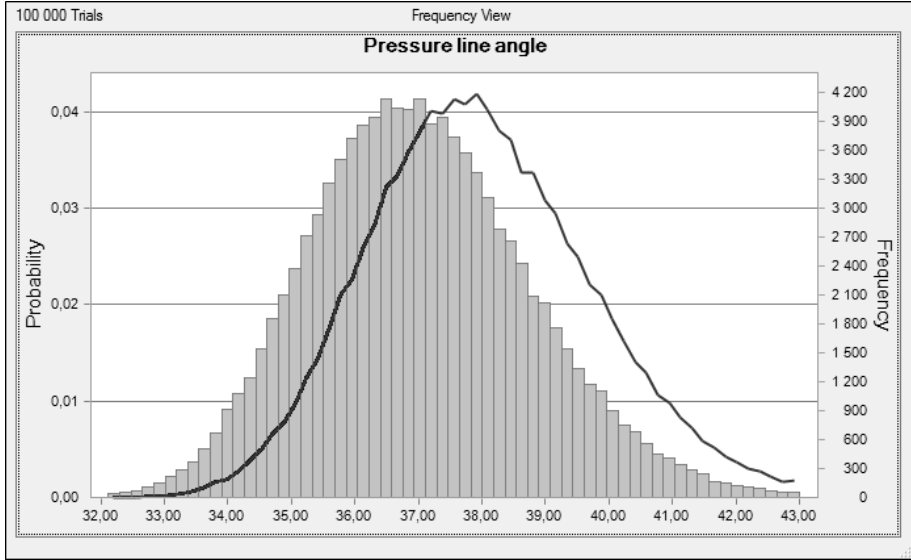
Figure 79 Comparison between the distribution of the pressure line angle in Calculation 1_1, line, and Calculation 2_5, column
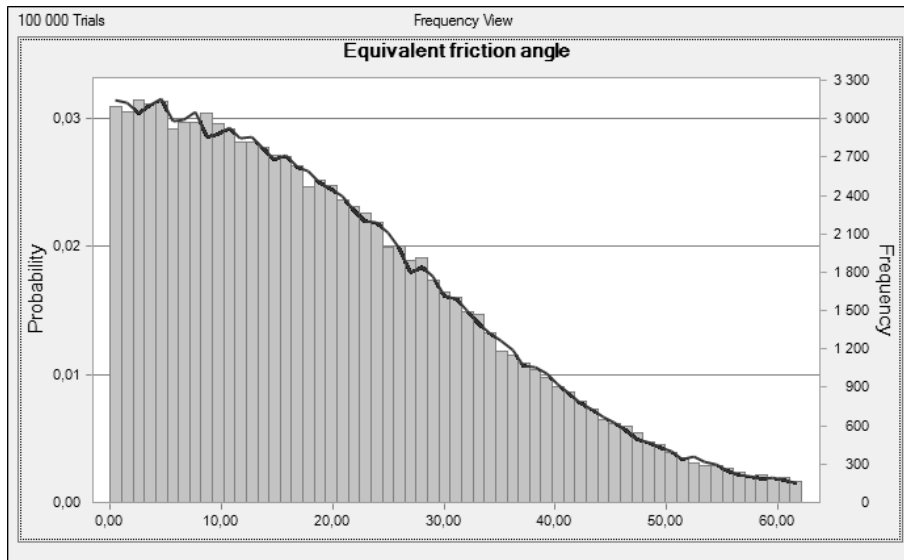
Figure 80 Comparison between the distribution of the equivalent friction angle in Calculation 1_1, line, and Calculation 2_5, column
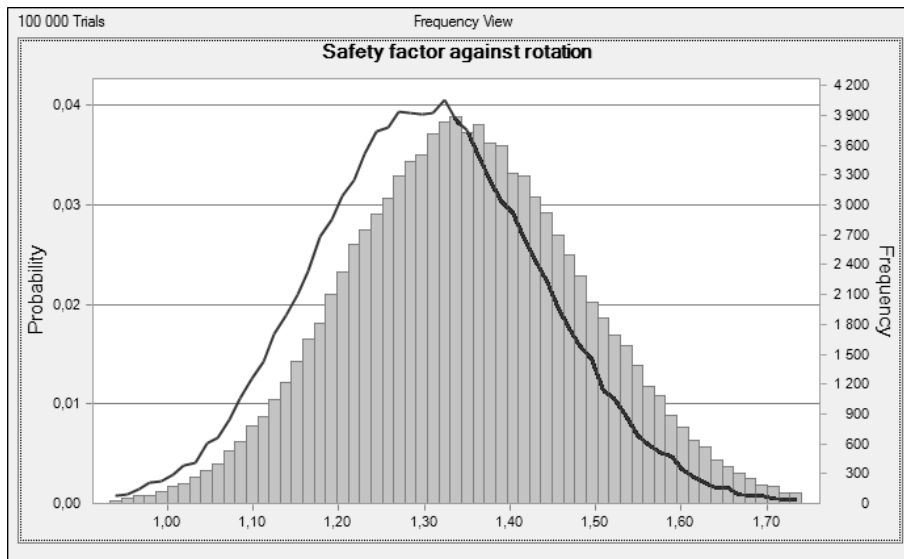
Figure 81 Comparison between the distribution of the safety factor against rotation in Calculation 1_1, line, and Calculation 2_5, column
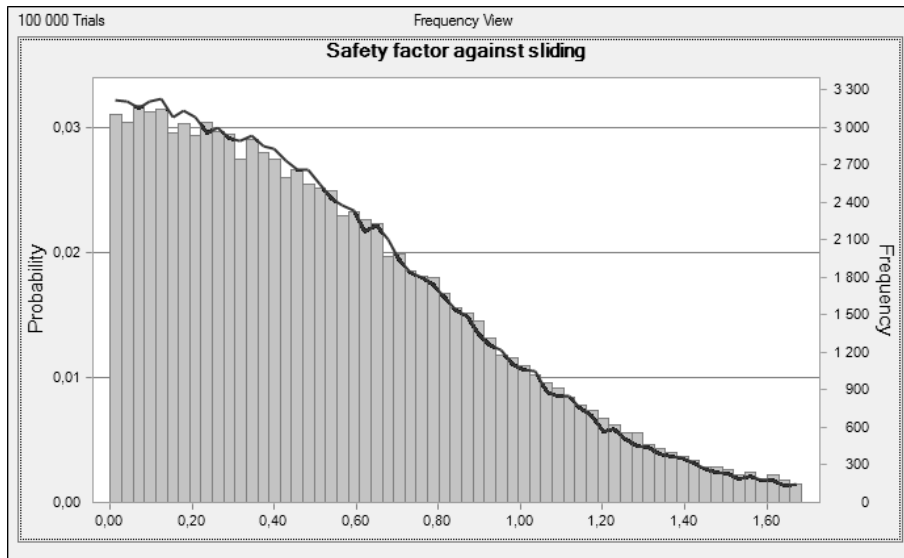
Figure 82 Comparison between the distribution of the safety factor against sliding in Calculation 1_1, line, and Calculation 2_5, column

Calculation 2_6

In this calculation the depth dependency of the horizontal stress equation is halved compared to Calculation 1_1, see Equation 4 and Figure 83, all other input are the same.

$$\sigma_h = 1 + 0.011B$$ **Equation 4**

Figure 83 Distribution for the horizontal stress in Calculation 2_6

Input

$\varphi = 63.21°$

$\varphi_{5\%} = 19.41°$

$\varphi_{95\%} = 84.70°$

$\phi = 33.81°$

$\phi_{5\%} = 20.55°$

$\phi_{95\%} = 71.72°$

$L = 13.7m$

$L_{5\%} 13.4m$

$L_{95\%} = 14.2m$

$B = 3.5m$

$B_{5\%} = 3.0m$

$B_{95\%} = 4.0m$

$g = 9.82m/s^2$

$D_{soil} = 10m$

$D_{soil,5\%} = 9.5m$

$D_{soil,95\%} = 10.5m$

$q_{ext} = 50kN/m^2$

$\rho = 2650kg/m^3$

$\rho_{5\%} = 2600kg/m^3$

$\rho_{95\%} = 2700kg/m^3$

$\gamma = 18.5kN/m^3$

$\gamma_{5\%} = 17.0kN/m^3$

$\gamma_{95\%} = 20.0kN/m^3$

$\sigma_h = 1 + 0.011B$

$\sigma_{h,std} = 0.12 \cdot \sigma_h$

Output

$f = 2.70m$

$f_{5\%} = 2.47m$

$f_{95\%} = 3.07m$

$\alpha = 38.19°$

$\alpha_{5\%} = 35.74°$

$\alpha_{95\%} = 41.62°$

$\phi' = 8.81°$

$\phi'_{5\%} = 1.66°$

$\phi'_{95\%} = 48.82°$

$p(f < B) = 0.99$

$p(\alpha < \phi') = 0.12$

$FS_{rot} = 1.27$

$FS_{rot,5\%} = 1.07$

$FS_{rot,95\%} = 1.49$

$FS_{slide} = 0.23$

$FS_{slide,5\%} = 0.04$

$FS_{slide,95\%} = 1.27$

Results Calculation 2_6

Calculation 2_6 shows that the most probable value for the arch height is 2.70 m. This is 0.05 m more than in Calculation 1_1. The 5-percentile increases with 0.05 m to 2.47 m and the 95-percentile increases with 0.06 m to 3.07 m, see Figure 84. For the

angle of the pressure line the most probable value is 38.19 degrees, which is 0.50 degrees more than in Calculation 1_1. The 5-percentile increases with 0.47 degrees to 35.74 degrees and the 95-percentile increases with 0.54 degrees to 41.62 degrees, see Figure 85. Most probable equivalent friction angle is 8.81 degrees, which is 0.02 degrees less than in Calculation 1_1. The 5-percentile increases with 0.01 degrees to 1.66 degrees and the 95-percentile increases with 0.17 degrees to 48.82 degrees, see Figure 86. The probability that the arch height is less than the bedding plane is 0.99, which is the same as in Calculation 1_1. Most probable value for the factor of safety against rotation is 1.27, which is 0.03 less than in Calculation 1_1. The 5-percentile decreases with 0.02 to 1.07 and the 95-percentile decreases with 0.03 to 1.49, see Figure 87. The probability that the angle of the pressure line is lower than the equivalent friction angle is 0.12, which is 0.01 less than in Calculation 1_1. Most probable value for the factor of safety against sliding is 0.23, which is the same as in Calculation 1_1. The 5-percentile is the same, 0.04, and the 95-percentile decreases with 0.01 to 1.27, see Figure 88.
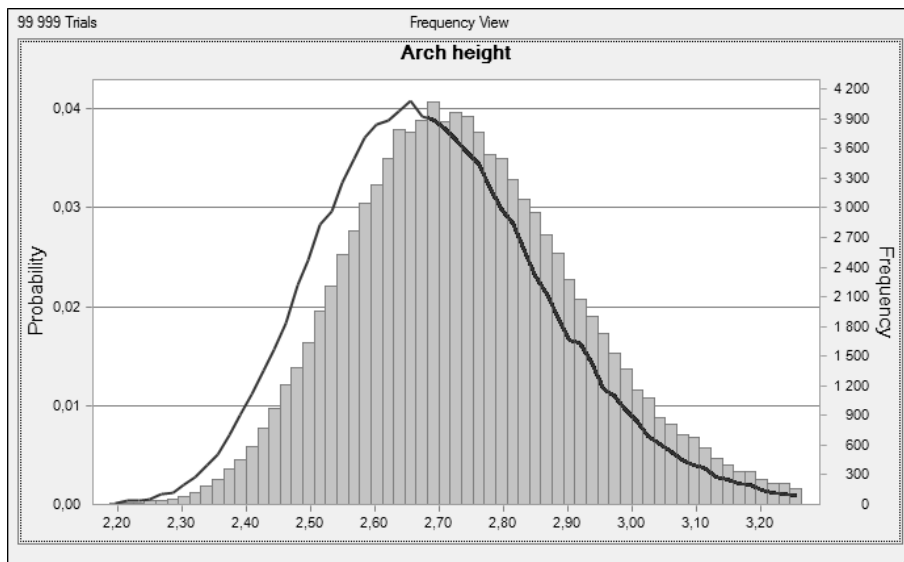
Figure 84 Comparison between the distribution of the arch height in Calculation 1_1, line, and Calculation 2_6, column
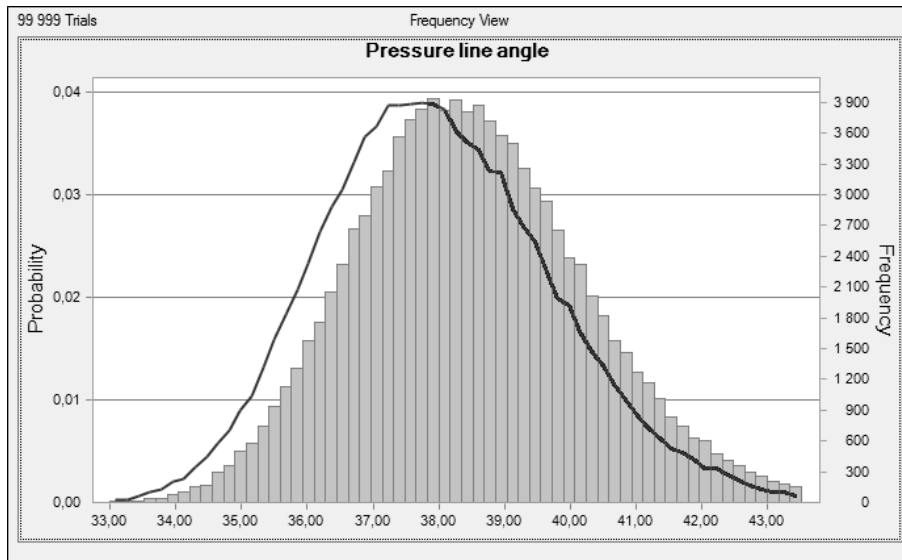
Figure 85 Comparison between the distribution of the pressure line angle in Calculation 1_1, line, and Calculation 2_6, column
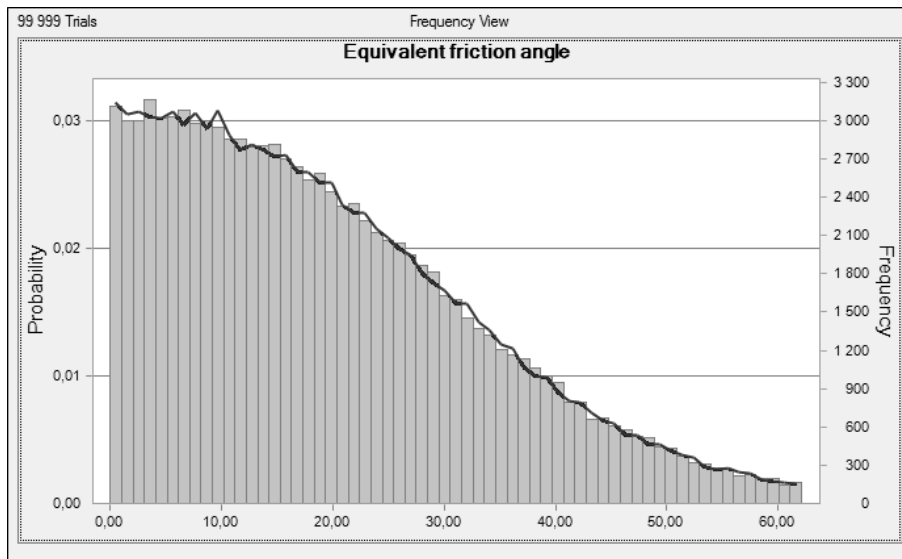
Figure 86 Comparison between the distribution of the equivalent friction angle in Calculation 1_1, line, and Calculation 2_6, column
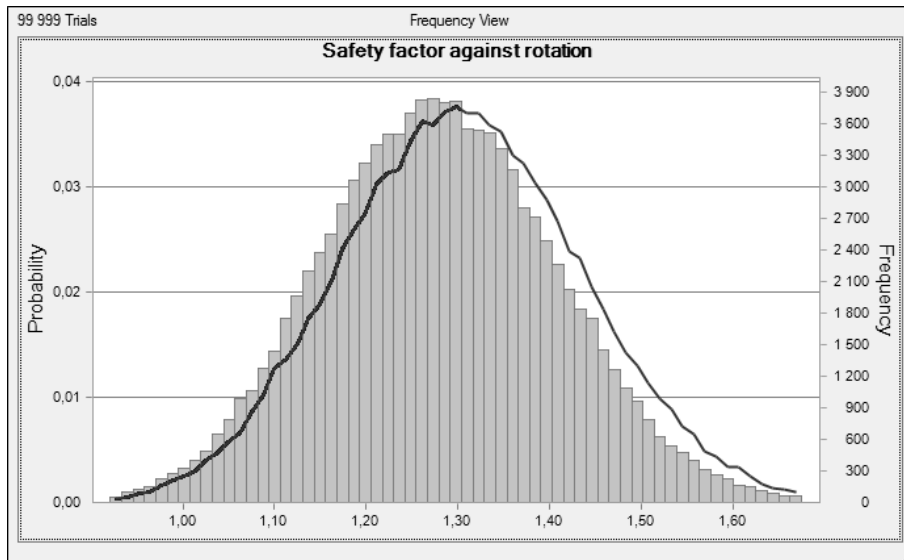
Figure 87 Comparison between the distribution of the safety factor against rotation in Calculation 1_1, line, and Calculation 2_6, column
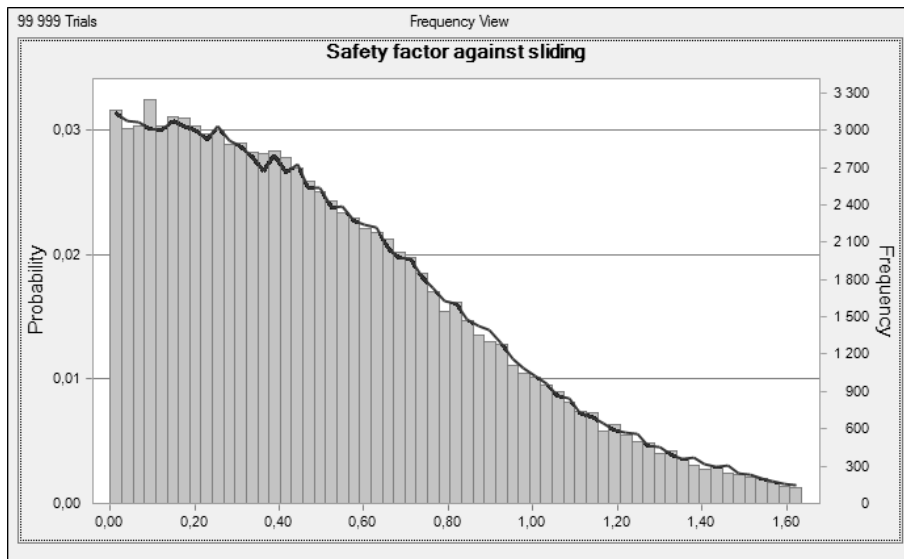
Figure 88 Comparison between the distribution of the safety factor against sliding in Calculation 1_1, line, and Calculation 2_6, column

Calculation 2_7

In this calculation the difference from Calculation 1_1 is that the standard deviation for the horizontal stress is doubled, see Figure 89.

Figure 89 Distribution for the horizontal stress in Calculation 2_7

Input

$\varphi = 63.21°$

$\varphi_{5\%} = 19.41°$

$\varphi_{95\%} = 84.70°$

$\phi = 33.81°$

$\phi_{5\%} = 20.55°$

$\phi_{95\%} = 71.72°$

$L = 13.7m$

$L_{5\%} 13.4m$

$L_{95\%} = 14.2m$

$B = 3.5m$

$B_{5\%} = 3.0m$

$B_{95\%} = 4.0m$

$g = 9.82m / s^2$

$D_{soil} = 10m$

$D_{soil,5\%} = 9.5m$

$D_{soil,95\%} = 10.5m$

$q_{ext} = 50kN / m^2$

$\rho = 2650kg / m^3$

$\rho_{5\%} = 2600kg / m^3$

$\rho_{95\%} = 2700kg / m^3$

$\gamma = 18.5kN / m^3$

$\gamma_{5\%} = 17.0kN / m^3$

$\gamma_{95\%} = 20.0kN / m^3$

$\sigma_h = 1 + 0.022B$

$\sigma_{h,std} = 0.24 \cdot \sigma_h$

Output

$$f = 2.58m$$
$$f_{5\%} = 2.26m$$
$$f_{95\%} = 3.46m$$
$$\alpha = 36.99°$$
$$\alpha_{5\%} = 33.28°$$
$$\alpha_{95\%} = 45.11°$$
$$\phi' = 8.75°$$
$$\phi'_{5\%} = 1.63°$$
$$\phi'_{95\%} = 48.88°$$
$$p(f < B) = 0.94$$
$$p(\alpha < \phi') = 0.13$$
$$FS_{rot} = 1.30$$
$$FS_{rot,5\%} = 0.98$$
$$FS_{rot,95\%} = 1.61$$
$$FS_{slide} = 0.15$$
$$FS_{slide,5\%} = 0.04$$
$$FS_{slide,95\%} = 1.30$$

Results Calculation 2_7

Calculation 2_7 shows that the most probable value for the arch height is 2.58 m. This is 0.07 m less than in Calculation 1_1. The 5-percentile decreases with 0.16 m to 2.26 m and the 95-percentile increases with 0.45 m to 3.46 m, see Figure 90. For the angle of the pressure line the most probable value is 36.99 degrees, which is 0.70 degrees less than in Calculation 1_1. The 5-percentile decreases with 1.99 degrees to 33.28 degrees and the 95-percentile increases with 4.03 degrees to 45.11 degrees, see Figure 91. Most probable equivalent friction angle is 8.75 degrees, which is 0.08 degrees less than in Calculation 1_1. The 5-percentile decreases with 0.02 degrees to 1.63 degrees and the 95-percentile increases with 0.23 degrees to 48.88 degrees, see Figure 92. The probability that the arch height is less than the bedding plane is 0.94, which is 0.05 less than in Calculation 1_1. Most probable value for the factor of safety against rotation is 1.30, which is the same as in Calculation 1_1. The 5-percentile decreases with 0.11 to 0.98 and the 95-percentile increases with 0.09 to 1.61, see Figure 93. The probability that the angle of the pressure line is lower than the equivalent friction angle is 0.13, which is the same as in Calculation 1_1. Most probable value for the factor of safety against sliding is 0.15, which is 0.08 less than in Calculation 1_1. The 5-percentile is the same, 0.04, and the 95-percentile increases with 0.02 to 1.30, see Figure 94.
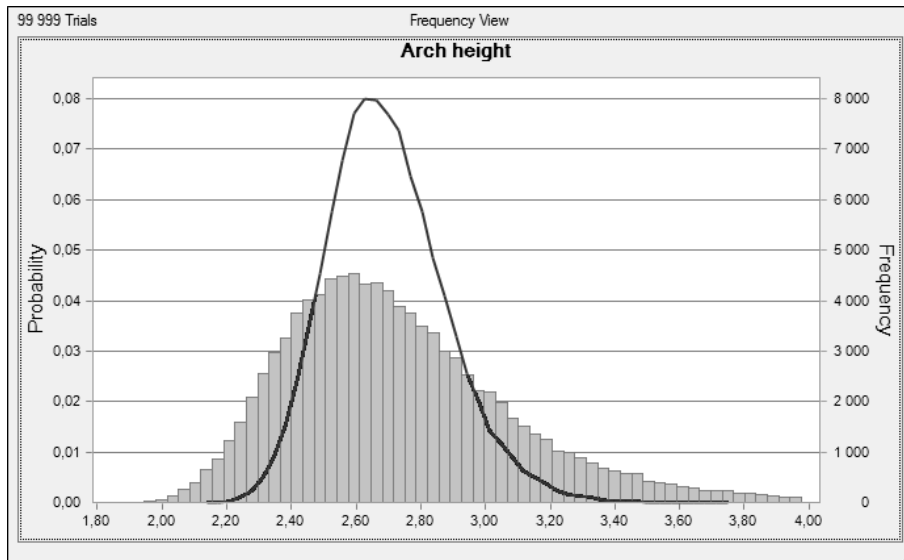
Figure 90 Comparison between the distribution of the arch height in Calculation 1_1, line, and Calculation 2_7, column
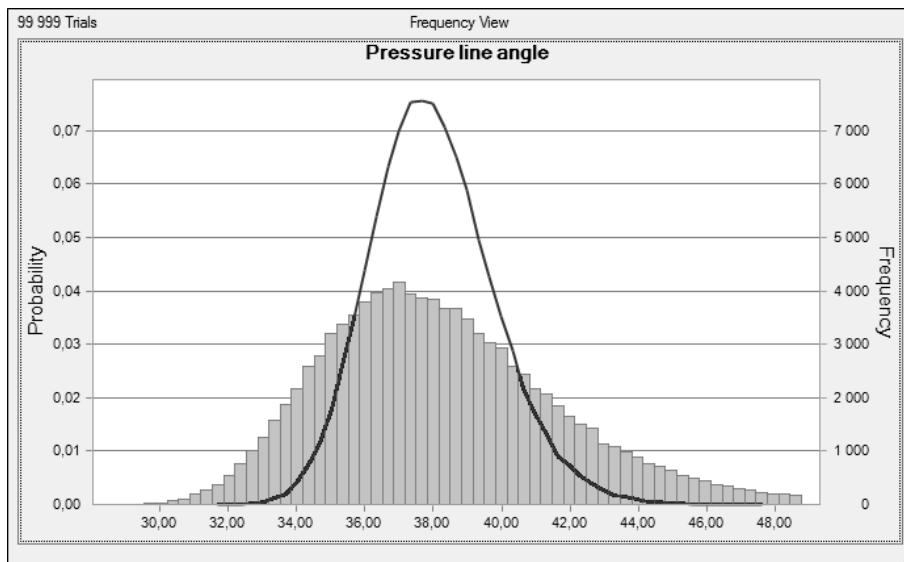
Figure 91 Comparison between the distribution of the pressure line angle in Calculation 1_1, line, and Calculation 2_7, column
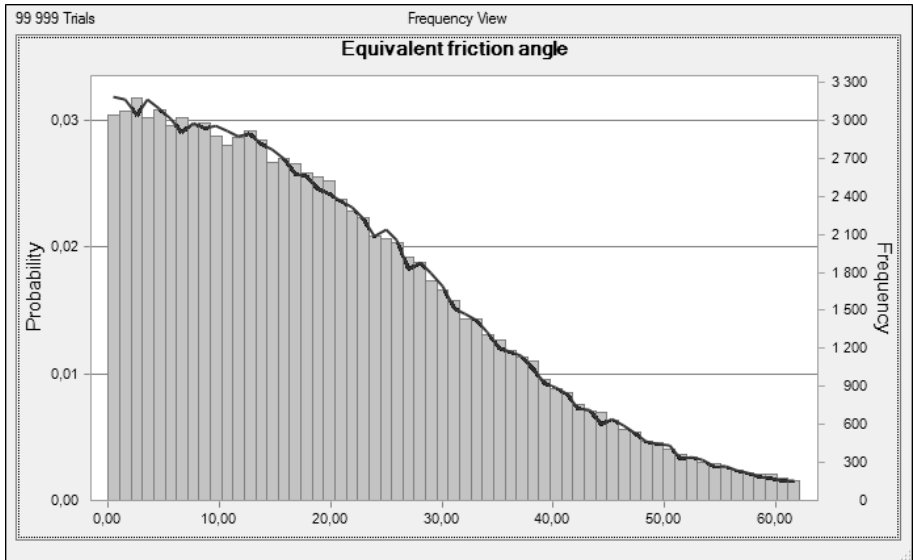
Figure 92 Comparison between the distribution of the equivalent friction angle in Calculation 1_1, line, and Calculation 2_7, column
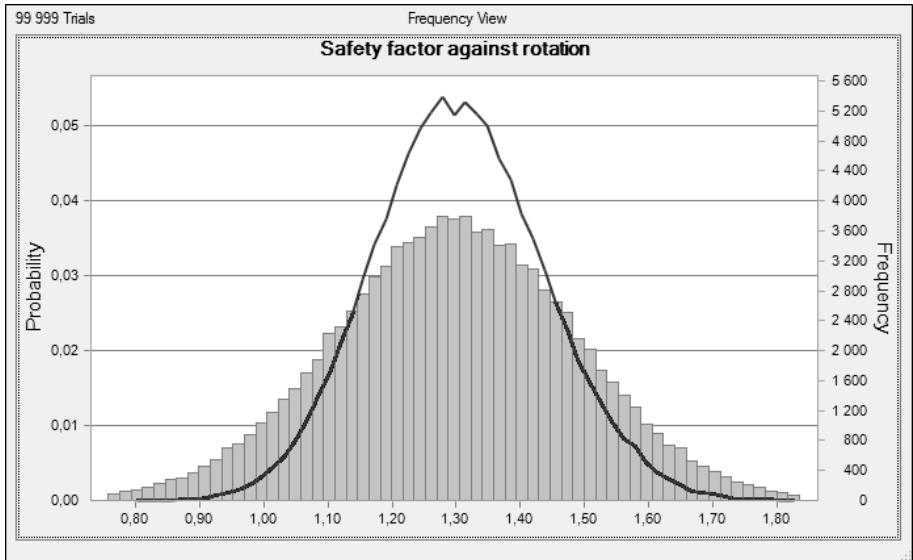
Figure 93 Comparison between the distribution of the safety factor against rotation in Calculation 1_1, line, and Calculation 2_7, column

99 999 Trials   Frequency View

Safety factor against sliding
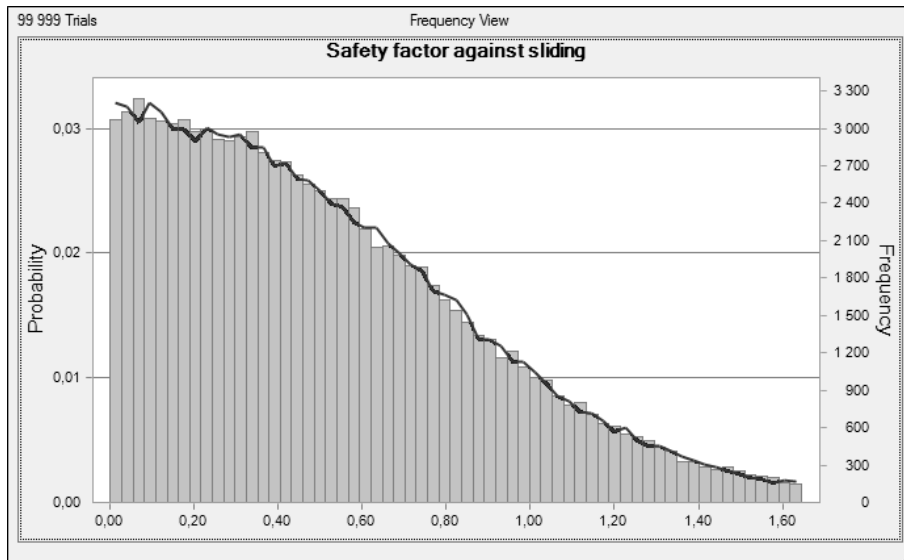
Figure 94 Comparison between the distribution of the safety factor against sliding in Calculation 1_1, line, and Calculation 2_7, column

Calculation 2_8

In this calculation the uncertainties for all factors except the horizontal stress are doubled, see Figure 95 to Figure 101. Some of the values for the dip and friction angle get outside of their range and in these cases the 5 % and/or 95 % are set to the limit value.

Φ
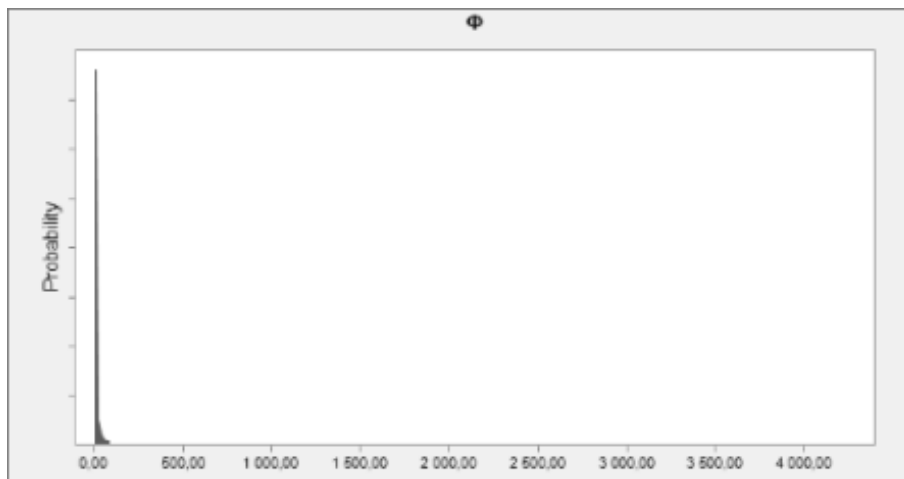
Figure 95 Distribution for the friction angle of the fractures in Calculation 2_8
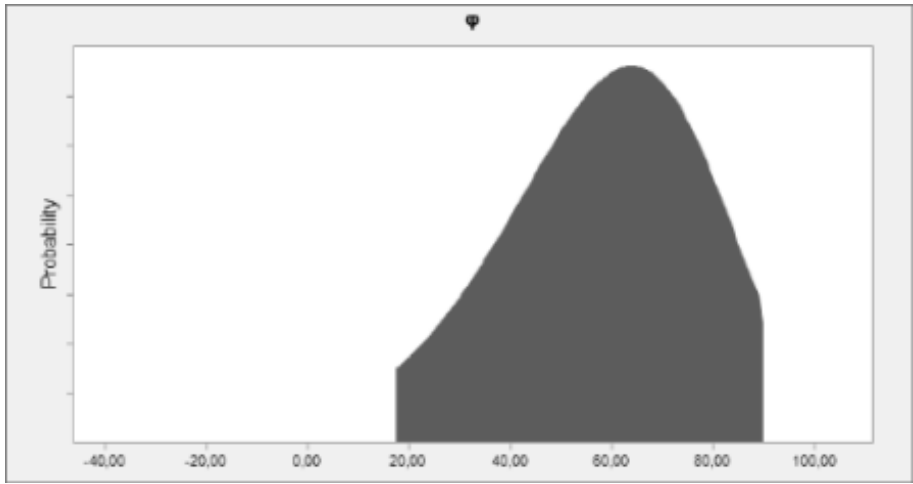
Figure 96 Distribution for the fracture dip in Calculation 2_8
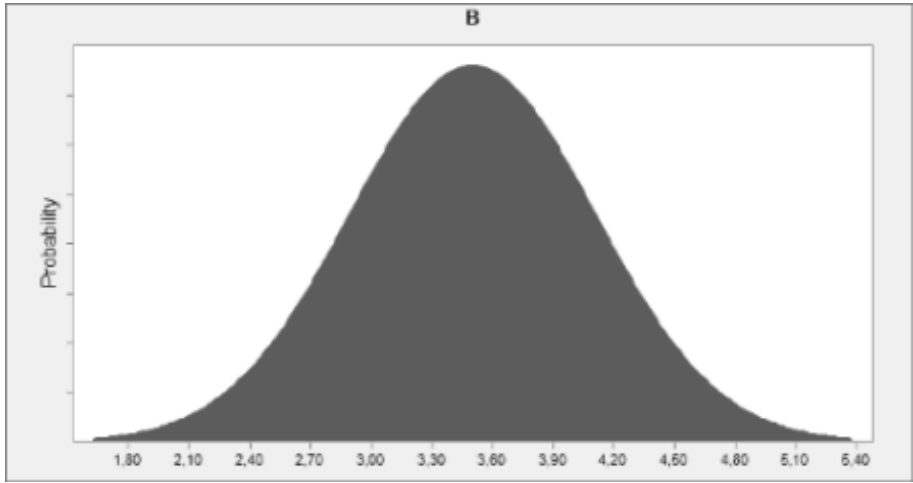
Figure 97 Distribution for the rock cover and the height of the bedding plane in Calculation 2_8
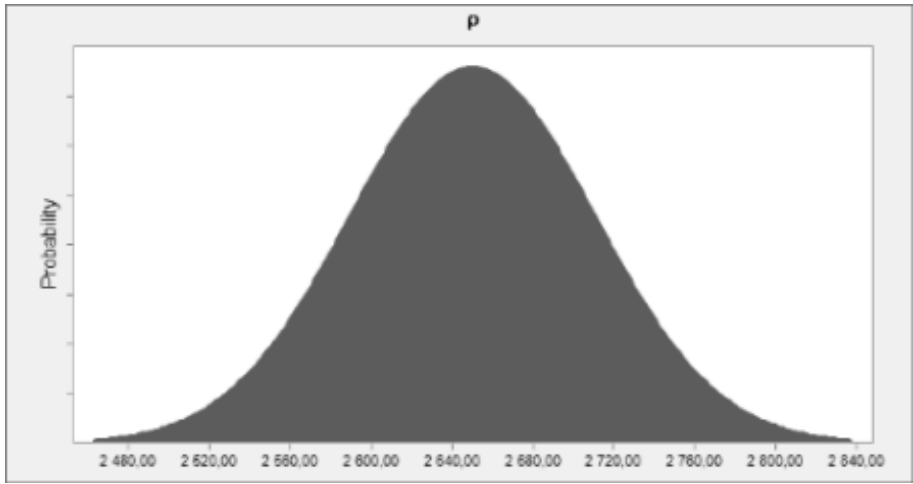
Figure 98 Distribution for the rock density in Calculation 2_8
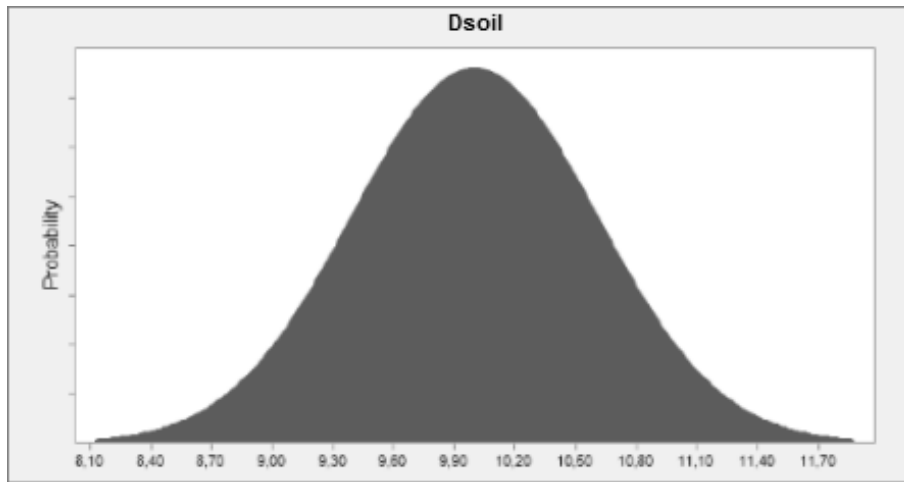
Figure 99 Distribution for the soil depth in Calculation 2_8
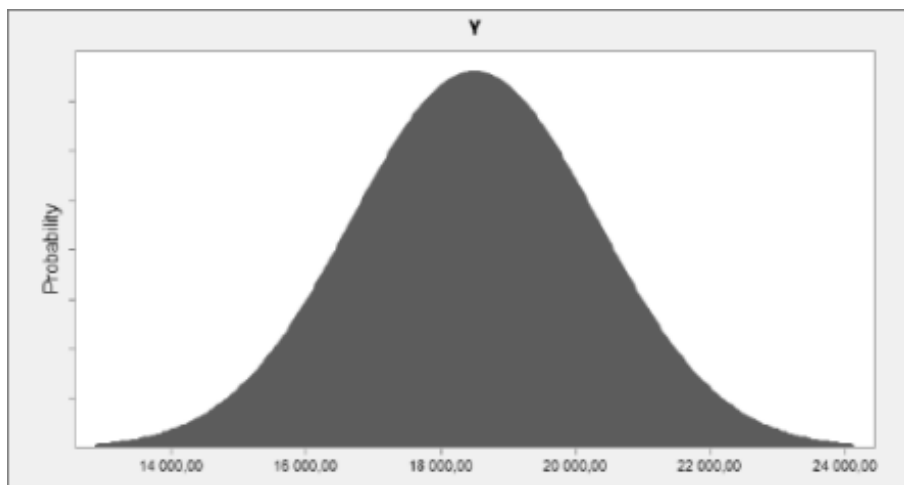
Figure 100 Distribution for the heaviness of the soil in Calculation 2_8
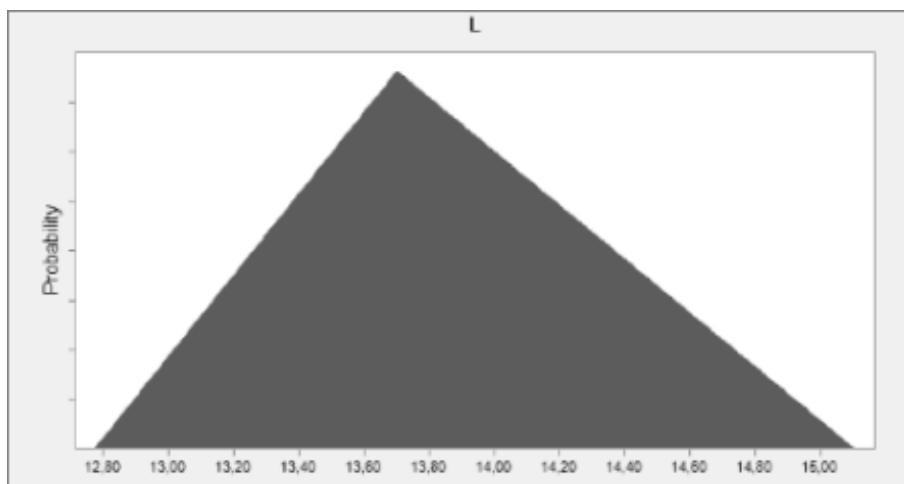
Figure 101 Distribution for the tunnel width in Calculation 2_8

Input

$\varphi = 63.21°$

$\varphi_{5\%} = 17°$

$\varphi_{95\%} = 90°$

$\phi = 33.81°$

$\phi_{5\%} = 7.29°$

$\phi_{95\%} = 90°$

$L = 13.7m$

$L_{5\%} 13.1m$

$L_{95\%} = 14.7m$

$B = 3.5m$

$B_{5\%} = 2.5m$

$B_{95\%} = 4.5m$

$g = 9.82m/s^2$

$D_{soil} = 10m$

$D_{soil,5\%} = 9m$

$D_{soil,95\%} = 11m$

$q_{ext} = 50kN/m^2$

$\rho = 2650kg/m^3$

$\rho_{5\%} = 2550kg/m^3$

$\rho_{95\%} = 2750kg/m^3$

$\gamma = 18.5kN/m^3$

$\gamma_{5\%} = 15.5kN/m^3$

$\gamma_{95\%} = 21.5kN/m^3$

$\sigma_h = 1 + 0.022B$

$\sigma_{h,std} = 0.24 \cdot \sigma_h$

Output

$f = 2.67m$

$f_{5\%} = 2.38m$

$f_{95\%} = 3.09m$

$\alpha = 37.72°$

$\alpha_{5\%} = 34.82°$

$\alpha_{95\%} = 41.36°$

$\phi' = 11.95°$

$\phi'_{5\%} = 0.71°$

$\phi'_{95\%} = 57.65°$

$p(f < B) = 0.91$

$p(\alpha < \phi') = 0.25$

$FS_{rot} = 1.28$

$FS_{rot,5\%} = 0.93$

$FS_{rot,95\%} = 1.67$

$FS_{slide} = 0.33$

$FS_{slide,5\%} = 0.05$

$FS_{slide,95\%} = 1.53$

Results Calculation 2_8

Calculation 2_8 shows that the most probable value for the arch height is 2.67 m. This is 0.02 m more than in Calculation 1_1. The 5-percentile decreases with 0.04 m to 2.38 m and the 95-percentile increases with 0.08 m to 3.09 m, see Figure 102. For the

angle of the pressure line the most probable value is 37.72 degrees, which is 0.03 degrees more than in Calculation 1_1. The 5-percentile decreases with 0.45 degrees to 34.82 degrees and the 95-percentile increases with 0.28 degrees to 41.36 degrees, see Figure 103. Most probable equivalent friction angle is 11.95 degrees, which is 3.12 degrees more than in Calculation 1_1. The 5-percentile decreases with 0.94 degrees to 0.71 degrees and the 95-percentile increases with 9.00 degrees to 57.65 degrees, see Figure 104. The probability that the arch height is less than the bedding plane is 0.91, which is 0.08 less than in Calculation 1_1. Most probable value for the factor of safety against rotation is 1.28, which is 0.02 less than in Calculation 1_1. The 5-percentile decreases with 0.16 to 0.93 and the 95-percentile increases with 0.15 to 1.67, see Figure 105. The probability that the angle of the pressure line is lower than the equivalent friction angle is 0.25, which is 0.12 more than in Calculation 1_1. Most probable value for the factor of safety against sliding is 0.33, which is 0.10 more than in Calculation 1_1. The 5-percentile increases with 0.01 to 0.05 and the 95-percentile increases with 0.25 to 1.53, see Figure 106.
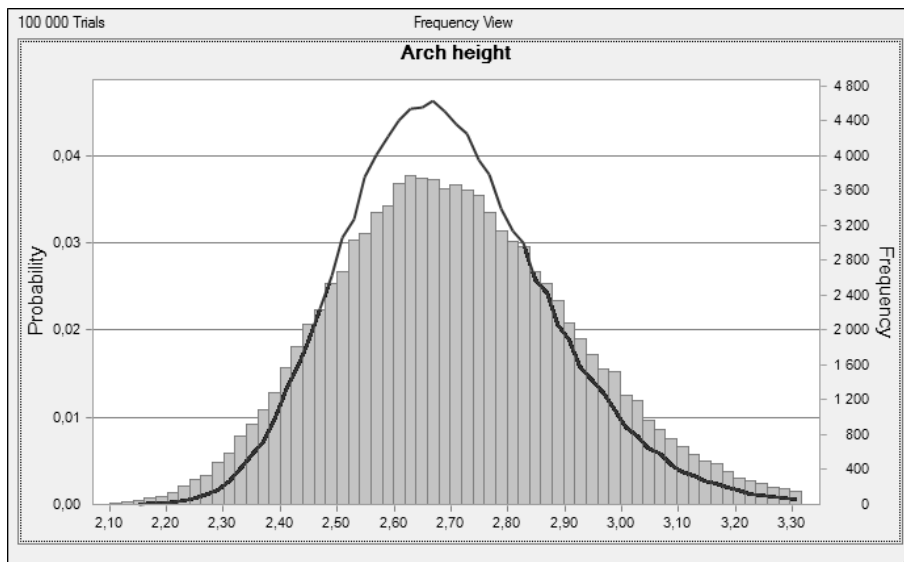
Figure 102 Comparison between the distribution of the arch height in Calculation 1_1, line, and Calculation 2_8, column
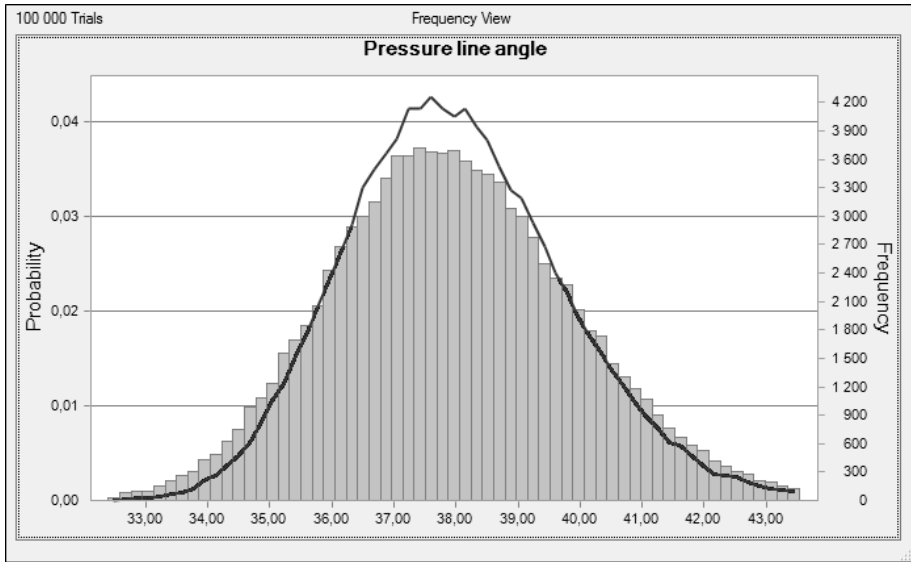
Figure 103 Comparison between the distribution of the pressure line angle in Calculation 1_1, line, and Calculation 2_8, column
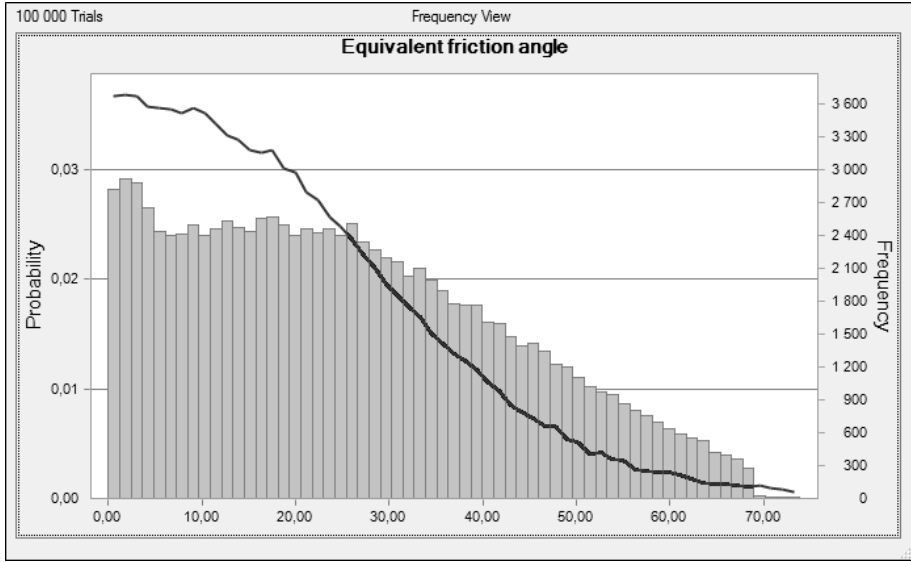
Figure 104 Comparison between the distribution of the equivalent friction angle in Calculation 1_1, line, and Calculation 2_8, column
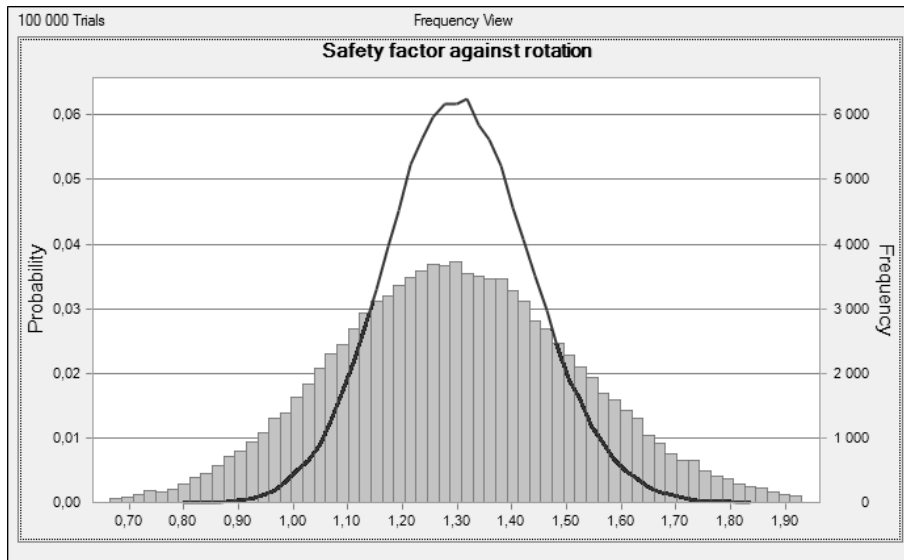
Figure 105 Comparison between the distribution of the safety factor against rotation in Calculation 1_1, line, and Calculation 2_8, column
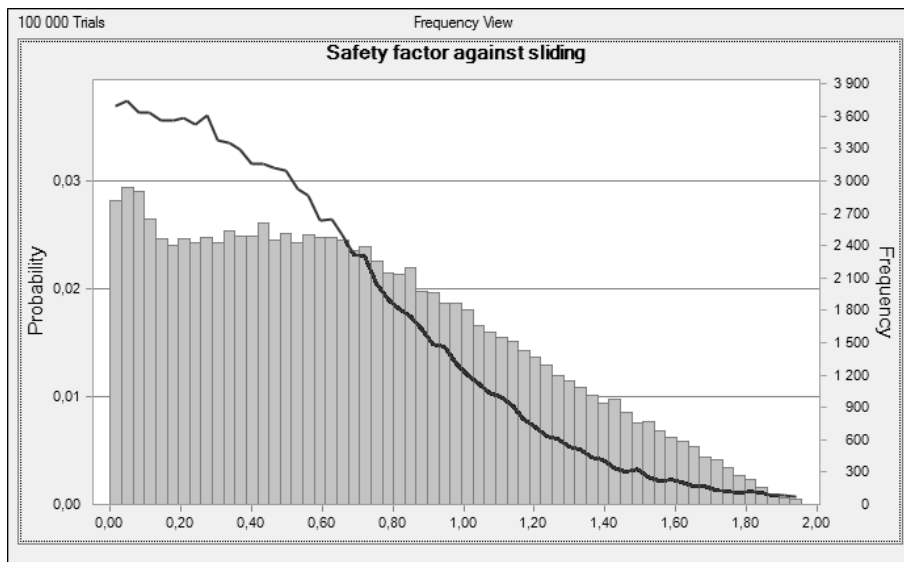
Figure 106 Comparison between the distribution of the safety factor against sliding in Calculation 1_1, line, and Calculation 2_8, column

Results Model 2

Table 4 Calculation results from Model 2

Parameter		Calculation							
		2_1	2_2	2_3	2_4	2_5	2_6	2_7	2_8
5%		2.51	2.44	1.72	3.43	2.34	2.47	2.26	2.38
f	m	2.66	2.65	1.88	3.75	2.56	2.70	2.58	2.67
95%		2.86	2.99	2.13	4.26	2.91	3.07	3.46	3.09
5%		36.32	35.38	26.57	44.99	34.35	35.74	33.28	34.82
α	degrees	37.85	37.89	28.63	47.55	36.71	38.19	36.99	37.72
95%		39.56	41,00	31.65	50.98	40.09	41.62	45.11	41.36
5%		1.64	0.71	1.63	1.61	1.64	1.66	1.63	0.71
Φ'	degrees	8.24	1.56	8.60	9.07	8.59	8.81	8.75	11.95
95%		49.22	25.70	49.04	48.48	48.81	48.82	48.88	57.65
p(f<B)	-	1.00	1.00	1.00	0.20	1.00	0.99	0.94	0.91
5%		1.12	1.15	1.54	0.77	1.12	1.07	0.98	0.93
FS_{rot}	-	1.31	1.31	1.84	0.92	1.34	1.27	1.30	1.28
95%		1.50	1.46	2.16	1.08	1.58	1.49	1.61	1.67
p(α<Φ')	-	0.13	0.01	0.25	0.05	0.14	0.12	0.13	0.25
5%		0.04	0.02	0.06	0.03	0.04	0.04	0.04	0.05
FS_{slide}	-	0.22	0.04	0.30	0.19	0.23	0.23	0.15	0.33
95%		1.30	0.68	1.70	1.01	1.33	1.27	1.30	1.53

The results from all calculations made in Model 2, presented in Table 4, show that by halving the uncertainties for the horizontal stress, Calculation 2_1, the difference between the 5-percentile and the 95-percentile lowers with a little bit more than 40 % compared to Calculation 1_1. This is much more than if the uncertainties for all parameters except the horizontal stress are halved, Calculation 2_2, here the difference between the 5-percentile and the 95-percentile is less than 10 %. For the safety factor against rotation the difference between the 5-percentile and the 95-percentile is lower for the case with a lowered uncertainty for the horizontal stress than it is when all parameters except the horizontal stress is has its uncertainties halved. For Calculation 2_1 it is lowered 12 % and for Calculation 2_2 it is lowered 18 %. Small changes in the safety factor against sliding are seen when the uncertainties in the horizontal pressure are halved, but they are so small that they can be ignored. When all other parameters have their uncertainties halved, the difference is much larger. In Calculation 2_1 the change is just a few percent and in Calculation 2_2 the change is almost 50 %.

If the uncertainty of the horizontal stress is doubled, Calculation 2_7, the difference between the 5-percentile and the 95-percentile is increased a little more than 100 %. This is compared to when the uncertainty of all parameters except the horizontal stress are doubled, Calculation 2_8, where the difference is increased a little more than 20 %. Just as when the uncertainty was halved the change in safety factor against rotation is larger when the uncertainties for all parameters except the horizontal stress are doubled than it is when the uncertainty for the horizontal stress is doubled. In Calculation 2_7 the difference between the 5-percentile and the 95-percentile is

increased with 47 % and in Calculation 2_8 it is increased 72 %. For the safety factor against sliding block Calculation 2_7 show an increased uncertainty of 2 %. The change in Calculation 2_8 is larger, almost 20 %.

In Calculation 2_3 the horizontal stress has been doubled and as a result the height of the arch has been lowered. The most probable value for the arch height is 29 % lower than in Calculation 1_1, the same change applies to the 5-percentile that also has been lowered 29 %. The difference between the 5-percentile and the 95-percentile has decreased 30 % which is almost the same as the decrease in the most probable value. In Calculation 2_4 where the horizontal stress has been halved the most probable arch height is increased 42 %. Just as in Calculation 2_3 the 5-percentile has the same increase as the most probable value and the difference between the 5-percentile and the 95-percentile has almost the same change has the most probable value. The change in the difference between the 5-percentile and the 95-percentile is 41 %. The safety factor against rotation, most probable value, increases 42 % in Calculation 2_3, the 5-percentile increases 41 % and the difference between the 5-percentile and the 95-percentile increases 44 %. In Calculation 2_4 the most probable value for the safety factor against rotation decreases 29 % just like the 5-percentile also does and the difference between the 5-percentile and the 95-percentile decreases 28 %. The most probable value for the safety factor against sliding is increased 30 % in Calculation 2_3 compared to Calculation 1_1. For Calculation 2_4 the most probable value for the safety factor against rotation has decreased 17 % instead. The change in 5-percentile is plus 50 % and minus 25 % respectively, and the difference between the 5-percentile and the 95-percentile has changed with plus 32 % and minus 21 % respectively in Calculation 2_3 and 2_4.

Calculation 2_5 and 2_6 show the same type of behaviour as Calculation 2_3 and 2_4 but since the change in horizontal stress is smaller, in 2_5 it is increased 7 % and in 2_6 it is decreased 4 % compared to 1_1, the changes in arch height, safety factor against rotation and safety factor against sliding are smaller. In Calculation 2_5 the most probable value for the arch height is 3 % lower than in Calculation 1_1, the same change is seen in the 5-percentile and the difference between the 5-percentile and the 95-percentile. For Calculation 2_6 the most probable value for the arch height, the 5-percentile and the difference between the 5-percentile and the 95-percentile has increased 2 %. The most probable value and the 5-percentile for the safety factor against rotation is in Calculation 2_5 increased 3 % and in Calculation 2_6 they are decreased 2 %. The difference between the 5-percentile and the 95-percentile is in Calculation 2_5 increased 7 % and in Calculation 2_6 it is decreased 2 %. In the safety factor against sliding both Calculation 2_5 and 2_6 show no change in the most probable value and 5-percentile compared to Calculation 1_1. Small changes are seen in the 95-percentile which make small change in the difference between the 5-percentile and 95-percentile. In Calculation 2_5 the difference has increased 4 % and in Calculation 2_6 the difference has decreased 1 %.

Analysis Model 2

The uncertainty for the horizontal stress influence the uncertainty for the height of the arch more than the uncertainties for all the other parameters combined. In Calculation 2_1 and 2_7 the uncertainty of the horizontal stress is changed and both these calculations show larger changes in the uncertainty of the arch height than the results from Calculation 2_2 and 2_8, where the uncertainties for all other parameters

are changed. When all parameters except the horizontal stress have their uncertainties doubled or halved the safety factor against rotation show larger changes in the uncertainty than if only the horizontal stress has changed. This due to that the changes in the uncertainty of the rock cover that occur when all parameters except the horizontal stress are changed are larger than the changes that occur in the uncertainty of the arch height when the uncertainty of the horizontal stress is changed. The uncertainty in the horizontal stress has a minor role in the uncertainty of the safety factor against sliding.

When the most probable value for the horizontal stress is changed the most probable value for the arch height is changed. This change also affects the uncertainty of the arch height with the same amount. The same thing happens with the safety factor against rotation. Calculation 2_3 to 2_6 shows that the size of the horizontal pressure is important to estimate size of the safety factor against sliding.

The results from Model 2 shows that it is more important to have a good estimation on how large the most probable value for the horizontal stress is than it is to have a low spread in the measured data.